

University of Windsor

Scholarship at UWindor

Electronic Theses and Dissertations

Theses, Dissertations, and Major Papers

1978

PHOTOCHEMICAL PROCESSES OF RHODIUM(III)-AMINE COMPLEXES.

CYNTHIA MARY. OWENS

University of Windsor

Follow this and additional works at: <https://scholar.uwindsor.ca/etd>

Recommended Citation

OWENS, CYNTHIA MARY., "PHOTOCHEMICAL PROCESSES OF RHODIUM(III)-AMINE COMPLEXES." (1978). *Electronic Theses and Dissertations*. 3089.

<https://scholar.uwindsor.ca/etd/3089>

This online database contains the full-text of PhD dissertations and Masters' theses of University of Windsor students from 1954 forward. These documents are made available for personal study and research purposes only, in accordance with the Canadian Copyright Act and the Creative Commons license—CC BY-NC-ND (Attribution, Non-Commercial, No Derivative Works). Under this license, works must always be attributed to the copyright holder (original author), cannot be used for any commercial purposes, and may not be altered. Any other use would require the permission of the copyright holder. Students may inquire about withdrawing their dissertation and/or thesis from this database. For additional inquiries, please contact the repository administrator via email (scholarship@uwindsor.ca) or by telephone at 519-253-3000ext. 3208.



National Library of Canada

Cataloguing Branch
Canadian Theses Division

Ottawa, Canada
K1A 0N4

Bibliothèque nationale du Canada

Direction du catalogage
Division des thèses canadiennes

NOTICE

The quality of this microfiche is heavily dependent upon the quality of the original thesis submitted for microfilming. Every effort has been made to ensure the highest quality of reproduction possible.

If pages are missing, contact the university which granted the degree.

Some pages may have indistinct print especially if the original pages were typed with a poor typewriter ribbon or if the university sent us a poor photocopy.

Previously copyrighted materials (journal articles, published tests, etc.) are not filmed.

Reproduction in full or in part of this film is governed by the Canadian Copyright Act, R.S.C. 1970, c. C-30. Please read the authorization forms which accompany this thesis.

**THIS DISSERTATION
HAS BEEN MICROFILMED
EXACTLY AS RECEIVED**

AVIS

La qualité de cette microfiche dépend grandement de la qualité de la thèse soumise au microfilmage. Nous avons tout fait pour assurer une qualité supérieure de reproduction.

S'il manque des pages, veuillez communiquer avec l'université qui a conféré le grade.

La qualité d'impression de certaines pages peut laisser à désirer, surtout si les pages originales ont été dactylographiées à l'aide d'un ruban usé ou si l'université nous a fait parvenir une photocopie de mauvaise qualité.

Les documents qui font déjà l'objet d'un droit d'auteur (articles de revue, examens publiés, etc.) ne sont pas microfilmés.

La reproduction, même partielle, de ce microfilm est soumise à la Loi canadienne sur le droit d'auteur, SRC 1970, c. C-30. Veuillez prendre connaissance des formules d'autorisation qui accompagnent cette thèse.

**LA THÈSE A ÉTÉ
MICROFILMÉE TELLE QUE
NOUS L'AVONS REÇUE**

PHOTOCHEMICAL PROCESSES OF
RHODIUM(III)-AMINE COMPLEXES

by

Cynthia Mary Owens

A Dissertation
submitted to the Faculty of Graduate Studies,
through the Department of Chemistry
in Partial Fulfillment of the requirements for
the Degree of Doctor of Philosophy at
The University of Windsor

Windsor, Ontario, Canada

1978

● Cynthia Mary Owens

To Brian,
whose continuing interest and encouragement
helped make a dream become a reality.

ACKNOWLEDGEMENTS

I wish to express my sincere gratitude to my research advisor, Dr. R. C. Rumfeldt, whose patience, encouragement, and example helped me mature not only as a scientist but also as an individual. I would also like to thank the members of my immediate committee, Dr. D. McKenney, Dr. B. McGarvey, and Dr. M. Schlesinger for their interest and ready assistance during the course of this work.

To my Mom and Dad I am eternally thankful for the guidance, faith, and encouragement given to me from my first day of school. Without them, this dissertation would have been nonexistent in more ways than one.

A warm thank you is extended to the technical staff, the secretaries, and Dr. W. Holland of the Department of Chemistry whose competent assistance and sense of humour helped make memorable my years at the University of Windsor.

Finally, I am very grateful to the National Research Council of Canada for the postgraduate scholarship awarded to me during my graduate studies.

ABSTRACT

A series of Rh(III)-amine complexes were photolysed in both the LF and CT manifolds to gain insight into the intrinsic electronic properties that dictate the product distribution(s) following absorption of a photon. In all cases, the weak field axis was found to be the axis of labilization. A model based on the degree of localization of antibonding character within the excited state has been used to interpret the specificity of a particular ligand or ligands aquated. The photochemistry of the trans-[Ir(en)₂X₂]⁺ (X = Cl, Br, I) series was also studied and was observed to parallel the qualitative trends of the analogous Rh(III) series.

The possibility of redox processes occurring in the CT photochemistry of Rh(III)-amines was investigated by comparison of the products obtained from direct photolysis with those incurred from redox processes initiated by reaction with hydrated electrons. These latter studies revealed interesting features and characteristics of the relatively unknown monomeric Rh(II) species.

The effects of pH, temperature, and solvent medium on various photolytic systems were studied. The observed sensitivity of the yields to the reaction environment

has been interpreted as evidence of the relative importance of mechanistic pathway on the sensitivity of the photochemical systems. A diffusion model is proposed as the dominant mechanistic pathway involved in these systems.

TABLE OF CONTENTS

	<u>Page</u>
Dedication.....	ii
Acknowledgements.....	iii
Abstract.....	iv
List of Tables.....	x
List of Figures.....	xii
I. Introduction.....	1
II. Experimental.....	32
1. Materials.....	32
2. Preparation of Complexes.....	32
2.1. Cyclam Complexes of Rh(III).....	32
2.2. Bisethylenediamine Complexes of Rh(III) and Ir(III).....	33
2.3. Halopentaamine Complexes of Rh(III).....	33
2.3.1. $\text{Rh}(\text{NH}_3)_5\text{X}^{2+}$ Series.....	33
2.3.2. $\text{Rh}(\text{N}(\text{CH}_3)_3)_5\text{X}^{2+}$ Series.....	34
2.4. Tetraamine Complexes of Rh(III).....	34
3. Actinometer Complexes.....	35
4. Spectral Measurements.....	36
5. Photolyses.....	36
III. Results.....	40

2

	<u>Page</u>
1. Electronic Spectra and Band Assignments.....	40
2. Photolysis of Rh(III)-Amines Under Standard Conditions.....	40
2.1. $\text{Rh}(\text{NH}_3)_5\text{X}^{2+}$ and $\text{Rh}(\text{NMe}_3)_5\text{X}^{2+}$: Photolyses.....	47
2.1.1. Irradiation of $\text{Rh}(\text{NH}_3)_5\text{X}^{2+}$	47
2.1.2. Irradiation of $\text{Rh}(\text{NMe}_3)_5\text{X}^{2+}$	49
2.2. <u>trans</u> - $[\text{Rh}(\text{A}_4)\text{X}_2]^+$ (A = NH_3 , en, cyclam): Photolysis.....	51
2.3. <u>trans</u> - $[\text{Rh}(\text{A}_4)\text{XY}]^+$ (A = en, cyclam): Photolysis.....	54
2.4. <u>cis</u> - $[\text{Rh}(\text{cyclam})\text{X}_2]^+$: Photolysis.....	58
2.5. pH Effects on the Photolysis of $\text{Rh}(\text{NR}_3)_5\text{X}^{2+}$	58
3. Photolysis of <u>trans</u> - $[\text{Ir}(\text{en})_2\text{X}_2]^+$ Under Standard Conditions.....	62
4. Photolysis of Iodide Solutions Containing Rh(III)-Amine Complexes.....	65
4.1. Photolysis of Aqueous Iodide Solutions...	65
4.2. Solutions Containing $[\text{Rh}(\text{en})_2\text{Cl}_2]^+$ Complexes.....	67
4.2.1. Aerated Conditions.....	67
4.2.2. Deaerated Conditions.....	69

	<u>Page</u>
4.3. Solutions Containing $[\text{Rh}(\text{cyclam})\text{Cl}_2]^+$	
Complexes.....	69
4.3.1. Aerated Conditions.....	69
4.3.2. Deaerated Conditions.....	73
4.4. Solutions Containing $[\text{Rh}(\text{cyclam})\text{I}_2]^+$	
Complexes.....	73
4.5. Solutions Containing $\text{Rh}(\text{NR}_3)_5\text{I}^{2+}$	74
4.6. Solutions Containing Nonabsorbing	
Concentrations of Iodide in the Presence	
of Rh(III)-Amines.....	76
5. Temperature Dependence Studies.....	76
6. Solvent Dependence Studies.....	77
IV. Discussion.....	82
1. General.....	82
2. Photochemistry of Rh(III)-Amines Under Standard	
Conditions.....	82
3. Charge Transfer Photochemistry of Rh(III)-	
Amines.....	93
4. Effect of Temperature on the Photochemistry	
of Rh(III)-Amines.....	104
5. Effect of pH on the Photochemistry of	
$\text{Rh}(\text{NR}_3)_5\text{X}^{2+}$	114
6. Solvent Effects on the Photochemistry of	
Rh(III)-Amines.....	117

	<u>Page</u>
Epilogue.....	124
Appendix I.....	126
Appendix II.....	127
References.....	128
Vita Auctoris.....	134

LIST OF TABLES

<u>Table</u>	<u>Title</u>	<u>Page</u>
1	Electronic Spectra of Some Rh(III)-Amine Complexes.....	41
2	Quantum Yields from the Photolysis of Rh(NR ₃) ₅ X ²⁺	50
3	Quantum Yields from the Photolysis of <u>trans</u> -[Rh(A ₄)X ₂] ⁺	55
4	Quantum Yields from the Photolysis of <u>trans</u> -[Rh(A ₄)XY] ⁺	57
5	Quantum Yields from the Photolysis of <u>cis</u> -[Rh(cyclam)X ₂] ⁺	59
6	Quantum Yields of Rh(III)-Amines as a Function of pH at 254 nm.....	64
7	Quantum Yields from the Photolysis of <u>trans</u> -[Ir(en) ₂ X ₂].....	66
8	Quantum Yields from the Photolysis of Aqueous Iodide Solutions Containing Rh(III)-Amine Complexes.....	72
9	Quantum Yields from the Photolysis of Aqueous Iodide Solutions Containing Rh(III)-Amine Complexes.....	75

<u>Table</u>	<u>Title</u>	<u>Page</u>
10	Quantum Yields for the Photoaquation of Various Rh(III)-Amines as a Function of Temperature.....	78
11	Quantum Yields of Rh(III)- and Ir(III)-Amines as a Function of Medium.....	80
11A	Quantum Yields of Rh(III)- and Ir(III)-Amines as a Function of Medium.....	81
12	Apparent Activation Energies for Some Rh(III)-Amines.....	109

LIST OF FIGURES

<u>Figure</u>	<u>Title</u>	<u>Page</u>
1	Photophysical and Photochemical Processes of a d^6 Ion with O_h Symmetry.....	4
2	Energy Level Diagram for d^6 Complexes of O_h and D_{4h} Symmetries.....	11
3	Strong and Weak Coupling Deactivation Limits.....	13
4	Qualitative Energy Level Scheme for the Photochemistry of $Rh(NH_3)_5X^{2+}$ Complexes.....	18
5	Approximate MO Diagram for σ Interactions Along the Unique Axis.....	27
6	Electronic Spectrum of $Rh(NMe_3)_5Cl^{2+}$ in H_2O	42
7	Electronic Spectrum of $Rh(NMe_3)_5Br^{2+}$ in H_2O	43
8	Electronic Spectrum of $Rh(NMe_3)_5I^{2+}$ in H_2O	44
9	Product Yield versus Irradiation Time Plot from the Photolysis of $Rh(NMe_3)_5I^{2+}$ at 254 nm.....	48
10	Product Yield versus Irradiation Time Plot from the Photolysis of $Rh(NH_3)_5Cl^{2+}$ at 254 nm in a Medium of pH 5.75.....	61
11	Product Yield versus Irradiation Time Plots from the Photolysis of $Rh(NH_3)_5I^{2+}$ at 254 nm in the Media pH 3.0, 5.5, and 8.7.....	63

<u>Figure</u>	<u>Title</u>	<u>Page</u>
12	Electronic Spectrum of the Product from the Photolysis of Aqueous Iodide Solutions of <u>trans</u> -[Rh(en) ₂ Cl ₂] ⁺ at 254 nm.....	68
13	Electronic Spectrum of the Product from the Photolysis of Aqueous Iodide Solutions of <u>cis</u> -[Rh(cyclam)Cl ₂] ⁺ at 254 nm.....	70
14	Relative Energy Level Diagram for <u>Trans</u> Ligands of Mixed-Ligand Rh(III)-Amine Complexes.....	86
15	Reaction Scheme for Direct Photolysis and Photolysis of Aqueous Iodide Solutions of <u>trans</u> -[Rh(en) ₂ Cl ₂] ⁺ at 254 nm.....	98
16	LF*, CT*, and Rh(II) d Electron Configurations...	99
17	"Activation Energy" Plot of the Temperature Dependent Quantum Yield for Photoaquation of <u>cis</u> -[Rh(cyclam)Br ₂] ⁺ at 254 nm.....	108

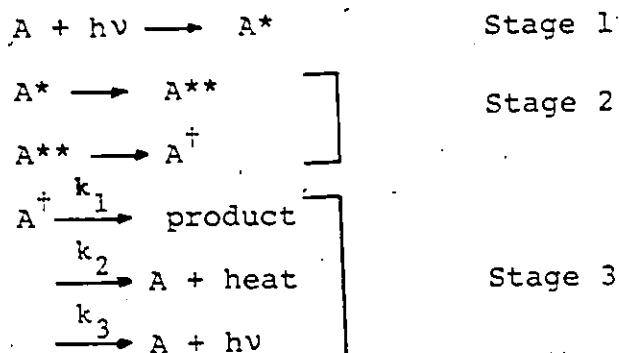
I. INTRODUCTION

In the past decade, the photochemistry of transition metal coordination compounds has received considerable attention from both a fundamental and applied point of view. Much progress has been made in the elucidation and identification of excited states and reaction pathways.

In essence, a photochemical reaction may be regarded as a bimolecular process in which one reactant is a photon and the other is the absorbing molecule. However, the overall response of a system after the absorption of a photon is rarely simple and usually involves a series of intramolecular events some of which are sequential whilst others are competitive. Because of the potential complexities inherent in photochemistry, it is convenient to define three separate stages which together combine to represent a primary photochemical reaction. The first stage is termed the primary act and is merely the absorption of a photon. The resultant state, however transitory, can be identified as a spectroscopic state of the molecule and where the incident radiation is sufficiently energetic (i.e. visible or ultraviolet), this state will be an electronically excited state. Apart from the obvious significance as the initiating step, the

primary act defines the manifold of excited states which may be activated in subsequent stages.

It has been well established in numerous cases that the initial state produced in the primary act is not the state which undergoes reaction. This conversion from the initial excited state to the ultimate reacting state constitutes the second stage and the events comprising this stage are termed the primary photophysical processes. The three stages can be represented by the following scheme:



It should be noted that in some instances Stage 2 could be totally absent (i.e. $A^\dagger = A^*$) or could involve a very large number of steps.

As was mentioned, the reactive species may be in the same state as was initially populated or it may be in some other state brought about by intermolecular or intramolecular conversion (A^{**}). Thus, in addition to producing chemical reaction, they may also dissipate their energy

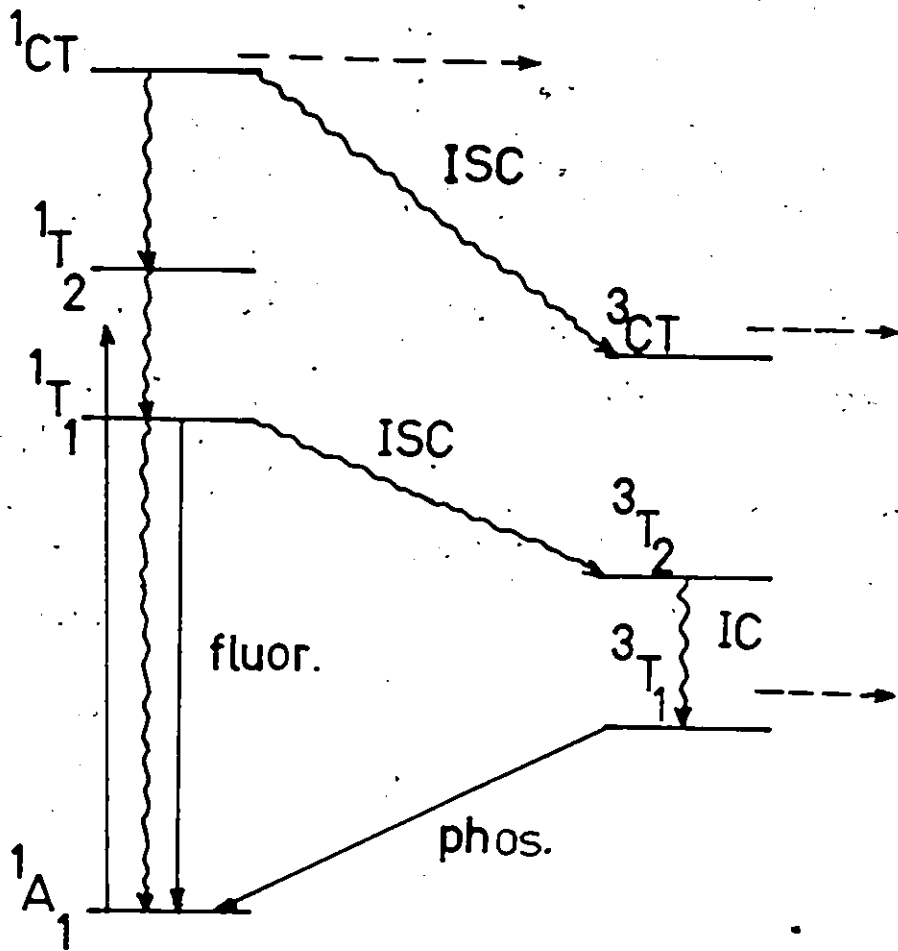
by means of radiative and nonradiative processes to the surrounding medium. These processes may also convert the excited states of the same or differing spin multiplicities. A radiative transition to a lower excited state of the same multiplicity is termed "fluorescence" while one to a lower state of differing multiplicity is "phosphorescence". Nonradiative transitions between states of the same multiplicity are designated as "internal conversions" (IC) while those between states of different multiplicity are termed "intersystem crossing" (ISC).

From luminescence and photochemical studies on transition metal complexes, it is generally inferred that the nonradiative transitions between excited states of the same multiplicity are very fast and first order in kinetics ($k=10^{11} \text{ sec}^{-1}$). Intersystem crossing between excited states are very rapid even though they are nominally forbidden (1,2). It has also been found that the radiative and nonradiative transitions from the lowest excited states to the ground state are relatively slow (2). That particular excited state from which reaction occurs is frequently denoted as the "photoactive state". The above possible photophysical and photochemical processes upon irradiation of a d^6 ion with octahedral microsymmetry are illustrated in Figure 1. For a more detailed discussion of these

Figure 1

W

Figure 1. Photophysical and Photochemical Processes
of a d^6 Ion with O_h Symmetry (Ref. 1).



—————→ Radiative
 ~~~~~→ Nonradiative  
 - - - - -→ Chemical Rxn.

processes, the reader is referred to the comprehensive texts of Adamson (1) and Balzani (3)†

In addition to characterizing photoevents in terms of the associated rate constants, it is more common to describe the efficiency of such events relative to the amount of absorbed light because these are usually more readily obtainable experimentally (2). The efficiency for a particular photochemical or physical process such as those shown in Figure 1, is expressed in terms of the quantum yield,  $\phi$ , equation [1].

$$\phi = \frac{\text{rate of change of the process of interest}}{\text{rate of absorption of light quanta of a specified wavelength}} \quad [1]$$

The totality of all such events, excluding possible secondary thermal ones, must be unity. This may be expressed as in equation [2]:

$$\phi_T = \phi_f + \phi_p + \phi_{Rx} + \phi_{NR} \quad [2]$$

where:

$\phi_T$  = total quantum yield

$\phi_f$  = quantum yield for fluorescence

$\phi_p$  = quantum yield for phosphorescence



$\phi_{Rx}$  = quantum yield for chemical reaction

$\phi_{NR}$  = quantum yield for nonradiative transitions.

In general, the quantum yields for photochemical reactions of transition metal complexes are less than unity and in many instances much less. This indicates that to understand the chemistry of the excited states, not only must the photochemical aspects be investigated, but also the competing photophysical ones.

Based on the steady state approximation, the quantum yield for disappearance of A or formation of products may be expressed as:

$$\phi = \frac{k_1[A^*]}{(k_1 + k_2)[A^*]} \quad [3a]$$

or

$$\phi = \frac{k_1[A^*]}{\sum_i k_i[A^*]} = \frac{k_1}{\sum_i k_i} \quad [3b]$$

where  $\sum_i k_i$  = sum of all rate constants deactivating A\*.

When the reacting state is not populated by direct absorption of light but is reached indirectly through interconversion processes, the efficiency of formation of A\* (IC) must also be considered.

$$\phi = \phi_{IC} \frac{k_1}{\sum_i k_i} \quad [4]$$

In the event that emission occurs:

$$\phi_e = \phi \frac{k_3}{k_2 + k_3} \quad [5]$$

The reaction of the excited state going to products, as in the case of ground state thermal reactions, has an activation energy such that the rate constant,  $k_1$ , can be expressed in terms of an Arrhenius equation.

$$k_1 = A e^{-E_a/RT} \quad [6]$$

Combining equations [3a] and [6], the following expression is derived:

$$\phi = \frac{A e^{-E_a/RT}}{A e^{-E_a/RT} + k_2} \quad [7a]$$

or

$$\ln \phi = -E_a/RT - (\ln(e^{-E_a/RT} + k_2/A)) \quad [7b]$$

The above process assumes that the  $k_2$  process is temperature independent. In the limiting case where  $k_2 \gg e^{-E_a/RT}$  (i.e.  $\phi < 0.1$ ),  $\ln(e^{-E_a/RT} + k_2/A)$  should be nearly temperature independent (3). Plots of  $\ln \phi$  vs.  $\frac{1}{T}$  in this case would be linear with a slope of  $-E_a/R$ . Normally, plots of this type are not linear because  $\phi > 0.1$  or  $k_2$  (nonradiative processes) are temperature dependent. Thus, over any temperature range  $T_1$  to  $T_2$ , an apparent activation energy ( $E_{app}$ ) can be calculated

$$E_{app} = R \frac{\ln \phi_{T_1} - \ln \phi_{T_2}}{\frac{1}{T_2} - \frac{1}{T_1}} \quad [8]$$

and this will be less than or equal to the activation energy  $E_a$  of  $k_1$  (3).

Electronic transitions may occur through electric dipole, magnetic dipole, or electric quadrupole mechanisms (4). Electric dipole is the only important mechanism for the absorption of light in solutions of complex ions (5). An energy level diagram, such as the one shown in Figure 1, provides a convenient representation of possible excited state events, but does not adequately convey one very important aspect, that is, the change in electron density upon excitation. Such a change is not only the source

of the nonequilibrium condition of the excited state but also determines the nature of the excited state and thus has a strong bearing on the subsequent course of events (2).

From quantum mechanical descriptions and from spectral properties of absorption and emission bands, there has arisen an oversimplified, but nevertheless useful, classification of electronic transitions in transition metal complexes as d-d or charge transfer (CT) (3,6). Transitions of the d-d or ligand field (LF) type are essentially localized on the central metal and represent an angular redistribution of electronic charge. For a  $d^6$  metal system, this involves promotion of a  $t_{2g}$  electron ( $\pi$ -symmetry with respect to M-L bond axes) to an  $e_g$  orbital ( $\sigma$ -antibonding with respect to M-L bond axes). This angular redistribution of charge does not modify the electron density on the metal or the ligands substantially and seldom leads to oxidation-reduction reactions. The energy required to promote an electron from the  $t_{2g}$  to the  $e_g$  set of orbitals depends on the ligand field strength,  $\Delta$ , or  $10 Dq$ , which is a property of both the metal and the ligand. For centrosymmetric complexes such as octahedral ones, ligand field transitions are frequently symmetry forbidden (Laporte forbidden). This results in low values for the molar extinction coefficients ( $1-150 \text{ dm}^3 \text{ mol}^{-1} \text{ cm}^{-1}$ ) for  $O_h$  complexes and

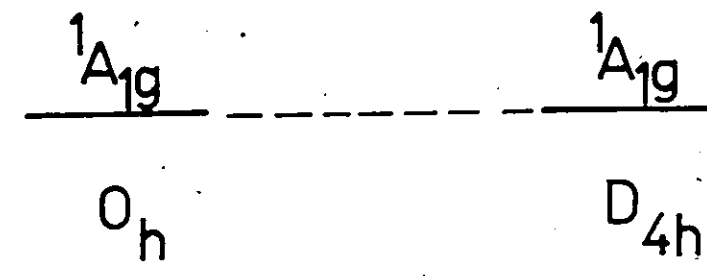
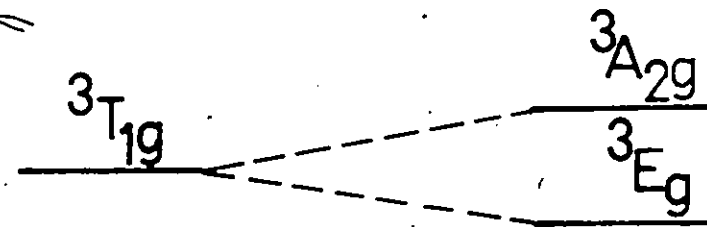
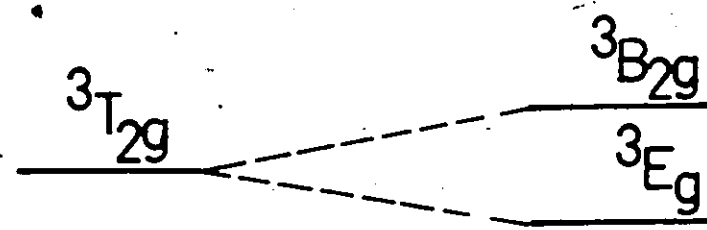
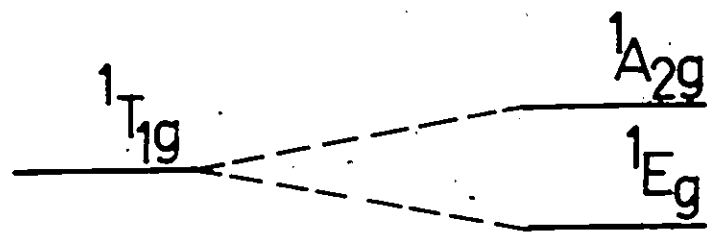
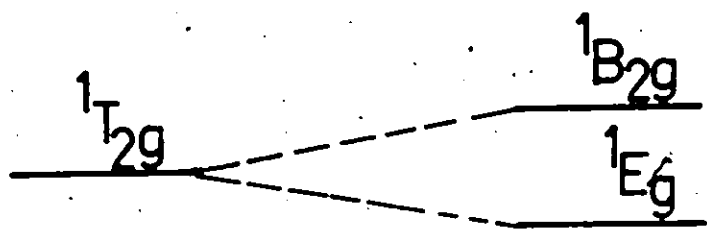
smaller if the transitions are also spin-forbidden. The energy level diagram for  $d^6$  complexes of  $O_h$  and  $D_{4h}$  symmetry is illustrated in Figure 2.

Charge transfer transitions, on the other hand, are frequently both orbitally and spin-allowed and consequently exhibit extinction coefficients of considerable magnitude ( $10^4 \text{ dm}^3 \text{ mol}^{-1} \text{ cm}^{-1}$ ). They represent a much more extensive redistribution of electron density and one of a more radial nature. They are generally observed at higher energies (but, not always) than those for d-d transitions and may mask the higher-energy ligand field bands. CT transitions may be further subdivided into those involving movement of charge from the metal to ligand(s) (CTML), from the ligand(s) to the metal (CTLM), or from one ligand-centred orbital to another one (L-L). Frequently, CT transitions are associated with redox processes.

Recently, a number of authors have attached a considerable significance with respect to the nonradiative deactivation processes being competitive with photochemical reaction. Therefore, it would be appropriate to briefly discuss the current models employed to describe nonradiative transitions. For large molecules, vibronic coupling between an excited state and the ground state has been analysed in terms of two limiting models (7,8), "strong

Figure 2

Figure 2. Energy Level Diagram for  $d^6$  Complexes of  $O_h$  and  $D_{4h}$  Symmetries (in  $C_{4v}$  symmetry, the g subscript should be omitted. Only the lowest energy levels are shown. Diagram not drawn to scale.) (Ref. 1).





coupling" and "weak coupling".

The "strong coupling limit" (Figure 3a) has a non-radiative decay probability that depends on the mean vibrational frequency of the molecule. This limit is usually encountered when the relative displacements ( $\Delta_s$ ), at least along one normal mode of the two electronic potential energy surfaces, are large such that an intersection of these surfaces will occur reasonably close to the minimum point of the excited state potential surface. With respect to the above treatment, the strong coupling deactivation limit should be relatively insensitive to isotopic changes (e.g. deuteration) and display a temperature dependence similar in appearance to a conventional rate equation where  $\Delta E$  functions as the activation energy (9).

The "weak coupling limit" (Figure 3b), normally associated with a small displacement of the potential energy surfaces ( $\Delta_w$ ), has a transition probability dominated by the frequency corresponding to the normal vibration of maximum frequency (7). The transition probability is determined by two opposing factors, the density of acceptor states, and the overlap integral between donor and acceptor states. The more dominant term is the overlap integral which is maximized for the highest frequency vibration of the molecule. Weak coupling deactivation would not be

Figure 3

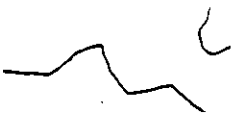


Figure 3. Strong and Weak Coupling Deactivation Limits.

(a) Strong Coupling Limit

$\Delta_s$  is the Stokes shift.

$\Delta E + E_m$  corresponds to the energy of the absorption maximum.

$\Delta E$  is the 0-0 transition energy.

$\Delta E'$  represents the activation energy for strong coupling deactivation.

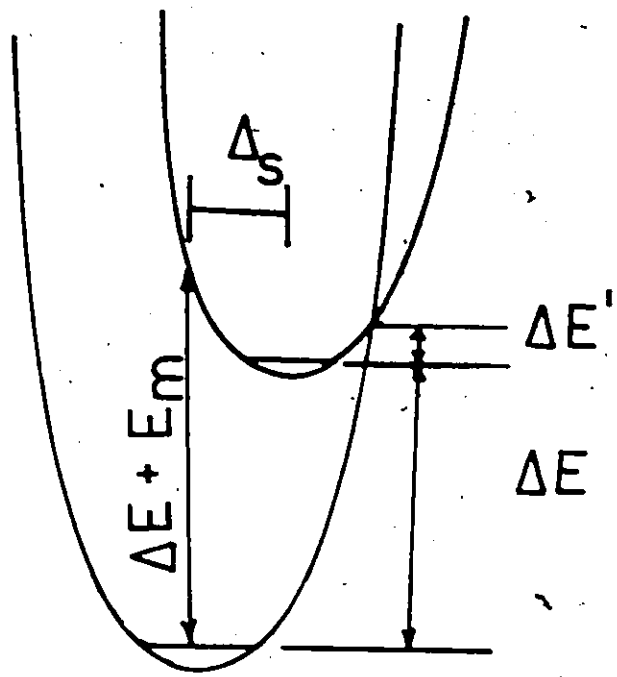
(b) Weak Coupling Limit

$\Delta_w$  is the Stokes shift.

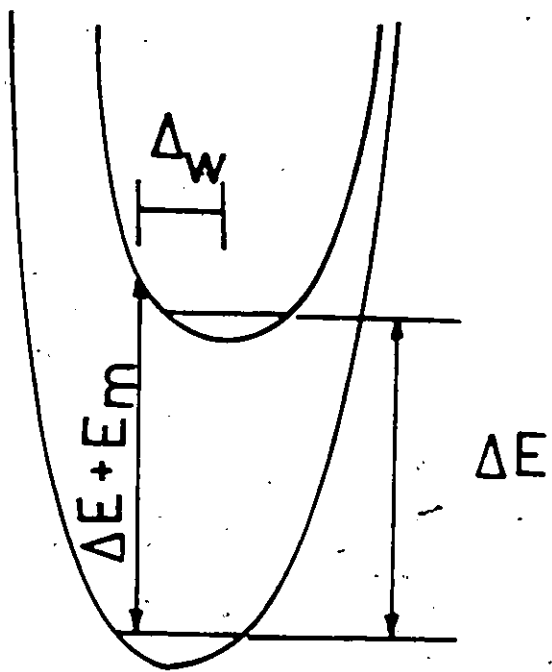
$\Delta E + E_m$  corresponds to the energy of the absorption maximum.

$\Delta E$  is the 0-0 transition energy.

(a)



(b)



expected to depend on medium temperature since the energy of the promoting and accepting modes are not a function of temperature. However, temperature changes may indirectly change the nonradiative deactivation rate by changing the Boltzmann population of promoting modes in the electronically excited state. Such a perturbation should be minor in comparison to isotopic changes in the acceptor modes.

At the present stage of development, it is difficult to fully assess the relationship between possible coupling modes and the overall photochemical activity. In particular, the effect of vibronic coupling on the nonradiative deactivation processes in the photochemistry of  $d^6$  complexes remains very much open to question and is the subject of further discussion in this thesis (pages 111-113).

To acquire an appreciation and understanding for a physical process, it is desirable to establish qualitative and quantitative trends exhibited by a series of molecules. Such a categorization was first initiated in 1967 by Arthur Adamson (10) who proposed two semiempirical rules in an attempt to predict the photoaquation behavior of nonoctahedral Cr(III) complexes. The principal statements are as follows:

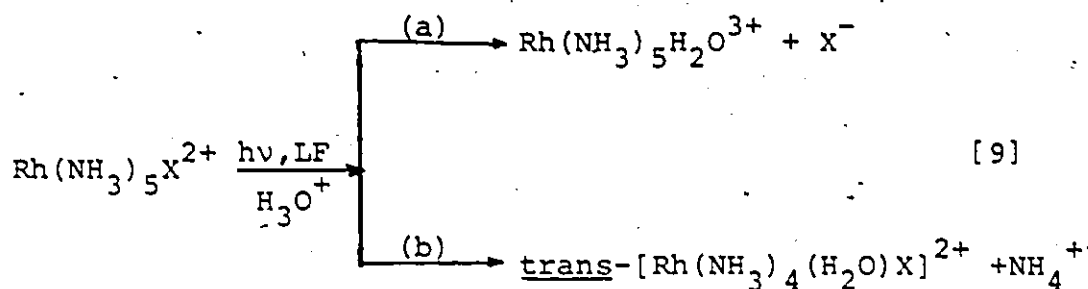
- "(i) Consider the six ligands to lie in pairs at the ends of three mutually perpendicular axes. That axis

having the weakest average crystal field will be the one labilized, and the total quantum yield will be about that for an  $O_h$  complex of the same average field.

(ii) If the labilized axis contains two different ligands, then the ligand of greater field strength preferentially aquates."

The applicability of these rules has met considerable success not only for Cr(III) systems but also for the majority of Co(III) and Rh(III) complexes thus far studied. The predictive utility of the rules can be seen with the complex  $Cr(NH_3)_5Cl^{2+}$ . Chloride has a spectrochemical position lower than  $NH_3$  and hence the axis of weakest average field strength is along the  $NH_3$ -Cr-Cl molecular axis. Ammonia is predicted and found (11) to be the ligand preferentially aquated.

The photochemical behavior of rhodium(III)-amine complexes is of interest both for its uniqueness and for its similarities to the behavior of other  $nd^6$  complexes. The halopentaammines were first studied by Moggi (12) and then in more detail by Kelly and Endicott (13-17). The latter authors found that irradiation of the ligand field bands of  $Rh(NH_3)_5X^{2+}$  led to two different reactions depending on the nature of X, equation[9].



When X = Cl, only path (a) was observed, while path (b) was the only pathway involved when X = I. For X = Br, intermediate behavior was found with both  $\text{Rh(NH}_3)_5\text{H}_2\text{O}^{3+}$  and  $\text{trans-[Rh(NH}_3)_4(\text{H}_2\text{O)Br]}^{2+}$  being formed. The quantum yields were observed to increase in the following order:  $\text{Rh(NH}_3)_5\text{Cl}^{2+} < \text{Rh(NH}_3)_5\text{Br}^{2+} < \text{Rh(NH}_3)_5\text{I}^{2+}$ .

$\text{Rh(NH}_3)_5\text{X}^{2+}$  complexes have been reported to quench the phosphorescence of biacetyl (14). Concurrent with phosphorescence quenching was the formation of the same products through direct excitation of  $\text{Rh(NH}_3)_5\text{X}^{2+}$ . On the basis of these data and limiting quantum yields from the Stern-Volmer plots, it was suggested that the reactive excited state has triplet spin multiplicity and internal conversion/intersystem crossing occurs with unit efficiency ( $\phi_{\text{ISC}} = 1$ ).

In conjunction with these studies, low temperature (77-110°K) emissions and lifetimes have been recorded for a series of Rh(III)-amine complexes (18-20). These emissions have been assigned as spin-forbidden d-d phosphorescence

( $(^3T_{1g} \leftarrow ^1A_{1g})$  for  $O_h$  symmetry and ( $^3E$  or  $^3A \leftarrow ^1A_1$ ) for  $C_{4v}$  symmetry) since the relative energy of the emission band follows the same ordering as the relative energy of the lowest d-d absorption band. Also, the energy difference between the absorption and emission bands is too large to assign the emission as fluorescence (18). Whereas these studies are strongly indicative that the photoactive state is the first excited  $^3E$ , it cannot be immediately assumed that the same state will act as the photoactive state in aqueous media at room temperature. However, there is a relative abundance of evidence drawn from sensitization studies (14) and wavelength dependencies (14,40) that offers rather convincing support for the contention that the  $^3E$  is the photoactive state.

To account for the relative product distributions resulting from the photochemistry of  $Rh(NH_3)_5X^{2+}$  complexes (equation[9]), Endicott and Kelly (16) have proposed the energy level diagram pictured in Figure 4. In the case where  $X = Cl$  (i.e.  $Rh(NH_3)_5Cl^{2+}$ ), the  $^3X$  state is proposed to be  $10^3 \text{ cm}^{-1}$  higher than  $^3Y$  (only  $Cl^-$  aquation observed). For  $Rh(NH_3)_5Br^{2+}$ , this energy is approximated as 300 to  $900 \text{ cm}^{-1}$  (14,16), with thermal back population of  $^3X$  being responsible for  $NH_3$  aquation. The high quantum yield for aquation of  $NH_3$  ( $\phi = 0.83$ ) for  $Rh(NH_3)_5I^{2+}$  suggests that





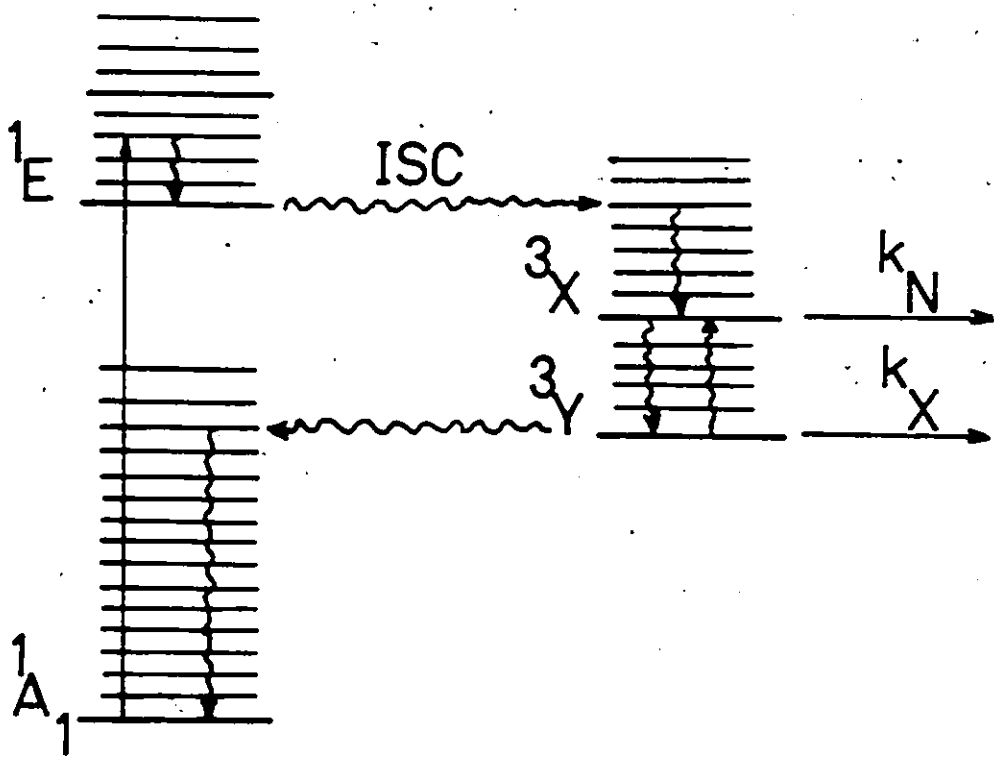
Figure 4

Figure 4. Qualitative Energy Level Scheme for the  
Photochemistry of  $\text{Rh}(\text{NH}_3)_5\text{X}^{2+}$  Complexes.

ISC refers to intersystem crossing. The first order rate constants  $k_N$  and  $k_X$  are indicated for product formation from loss of  $\text{NH}_3$  and  $\text{X}^-$  respectively (Ref. 16).

${}^1\text{CTTM}$  \_\_\_\_\_

${}^1\text{B}_2$   ${}^1\text{E}$  \_\_\_\_\_  
\_\_\_\_\_



the  $^3x$  is very close or lower in energy than the  $^3y$  state.

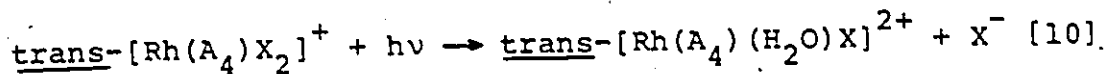
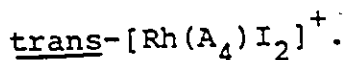
Quantum yields have also been measured for ligand field excitation of pentaamminerhodium(III) complexes of the uncharged ligands  $\text{NH}_3$ , pyridine, acetonitrile, and benzonitrile (21,22). Like the chloro complex, these predominantly undergo photoaquation of the sixth ligand. A simple spectrochemical series for these Rh(III) complexes, based upon the energy of the first LF band, gives the following order for the various halide and uncharged ligands:  $\text{I}^- < \text{Br}^- < \text{Cl}^- < \text{NH}_3 = \text{py} = \text{CH}_3\text{CN} = \text{C}_6\text{H}_5\text{CN}$  (23,24). This series suggests that unlike the iodo and bromo complexes, the electronic distortion of the various  $\text{Rh}(\text{NH}_3)_5\text{L}^{3+}$  complexes away from the octahedral microsymmetry of the hexammine is small (21). The magnitude of the photoaquation yields follow the order  $\text{NH}_3 < \text{py} < \text{C}_6\text{H}_5\text{CN} = \text{CH}_3\text{CN}$ , which is the approximate inverse of the Brønsted basicities of the free ligands:  $\text{NH}_3 > \text{py} \gg \text{CH}_3\text{CN} = \text{C}_6\text{H}_5\text{CN}$ . The relatively high ligand field strength of the nitriles has been attributed to their polarizability (24).

The lowest Rh(III) LF excited state will derive from the  $t_{2g}^5 e_g^1$  configuration. Not only should this be dissociation labile owing to population of the  $e_g$  orbital, which is  $\sigma^*$  in character, but also the excited state might be considerably less polarizable (harder) owing to the

angular redistribution of charge, thus reducing the bonding interaction relative to the ground state more for the unsaturated organic base than for  $\text{NH}_3$  (24). This explanation not only rationalizes the relative values of  $\phi(L)$ , but also the essentially exclusive aquation of the sixth ligand from the pentaammine complexes.

Ligand field irradiation of  $\text{Rh}(\text{NH}_3)_5(\text{H}_2\text{O})^{3+}$  has been reported to lead to photoexchange of solvent and coordinated water with a quantum yield of 0.43 (25). Similar excitation in the presence of added chloride or bromide results in photoanation to form the halopentaammine complexes  $\text{Rh}(\text{NH}_3)_5\text{X}^{2+}$  with the quantum yields dependent on the concentration of added halide. The mechanism for photoexchange and photoanation has been postulated to occur via a dissociative pathway since the photoanation quantum yields in bromide solution were not dramatically different from those in chloride solution.

The visible and u.v. photolysis of trans- $[\text{Rh}(\text{A}_4)\text{X}_2]^+$  molecules (where  $\text{A} = 4\text{NH}_3, 2\text{en},$  and cyclam;  $\text{X} = \text{Cl}, \text{Br},$  or  $\text{I}$ ) has been studied (13,26,27,28). All photoreactions were found to proceed via halide aquation with complete isomeric retention for both ligand field and charge transfer excitations (equation [10]). The quantum yields followed the order: trans- $[\text{Rh}(\text{A}_4)\text{Cl}_2]^+ < \text{trans-}[\text{Rh}(\text{A}_4)\text{Br}_2]^+ <$



Sellan and Rumfeldt have shown the yields to be sensitive to the degree of chelation of the amine system (28). For example, whilst the electronic spectra of trans- $[\text{Rh}(\text{NH}_3)_4\text{Cl}_2]^+$  and trans- $[\text{Rh}(\text{cyclam})\text{Cl}_2]^+$  are very similar, the quantum yield of chloride aquation for the cyclam complex is much lower. These authors have suggested that this chelation effect is more likely to be mechanistic rather than electronic in origin.

The u.v. irradiation of both  $\text{Rh}(\text{NH}_3)_5\text{I}^{2+}$  and trans- $[\text{Rh}(\text{NH}_3)_4\text{I}_2]^+$  leads to formation of trans- $[\text{Rh}(\text{NH}_3)_4(\text{H}_2\text{O})\text{I}]^{2+}$  as a primary photoproduct (13). Product yields were found to be lower for irradiation of charge-transfer-to-metal (CTTM) bands than for irradiation of d-d bands. Hence, Kelly and Endicott (13) have concluded that the decreased yields at higher excitation energy signify that efficiency of the interconversion from CTLM states to the lowest LF state is less than unity. Consequently, direct radiationless deactivation from the CTLM states is competitive with intersystem crossing. The opposite trend was observed for irradiations of trans- $[\text{Rh}(\text{A}_4)\text{X}_2]^+$  ( $\text{A} = \text{en}, \text{cyclam}$ ) complexes whereby yields resulting from charge transfer excitation are

greater (28). An explanation for this difference in trends is still outstanding.

Rumfeldt and Sellan have also studied the photochemistry of  $\text{cis-}[\text{Rh}(\text{cyclam})\text{X}_2]^+$  (where  $\text{X} = \text{Cl}, \text{Br}, \text{I}$ ) and  $\text{cis-}[\text{Rh}(\text{en})_2\text{Cl}_2]^+$  (29). Although only halide aquation with complete isomeric retention was observed for the cyclam complexes, amine aquation is the principal reaction mode for the ethylenediamine complex with evidence for cis to trans isomerization. In each case, the photosensitivity was greater for CT excitation than LF excitation. The results for the  $\text{cis-}[\text{Rh}(\text{cyclam})\text{X}_2]^+$  complexes were interesting since the dependence on the leaving group is completely reversed from the corresponding trans complexes (i.e.  $\phi(\text{Cl}^-) > \phi(\text{Br}^-) > \phi(\text{I}^-)$ ) with the diiodo complex basically photo-inert.

The  $\text{cis-}[\text{Rh}(\text{cyclam})\text{X}_2]^+$  series appear to be an exception to Adamson's second rule. The anticipated reaction would have been dissociation of a Rh-N bond as is found for  $\text{cis-}[\text{Rh}(\text{en})_2\text{Cl}_2]^+$ . Rather than constituting an exception to the rule,  $\text{cis-}[\text{Rh}(\text{cyclam})\text{X}_2]^+$  (where  $\text{X} = \text{Cl}, \text{Br}$ ) demonstrates the potential inadequacy of any semiempirical rules that lack sound theoretical justification. The  $\text{Cl}^-$  and  $\text{Br}^-$  yields have been attributed as deriving from a process of specific labilization which is determined by some factors

unique to these complexes (29). From a comparison of the spectra of cis-[Rh(en)<sub>2</sub>Cl<sub>2</sub>]<sup>+</sup> and cis-[Rh(cyclam)Cl<sub>2</sub>]<sup>+</sup>, the change from amine to halide aquation appears to be related to a structural distortion in the complex (29).

A tetragonal pyramidal intermediate has been proposed for both the cis- and trans-Rh(III) cyclam complexes. Such an intermediate not only satisfies the demand for stereomobility but also isomeric retention (28,29). It has also been suggested that the mechanism for photochemical reaction for complexes of the type trans- and cis-[Rh(A<sub>4</sub>)X<sub>2</sub>]<sup>+</sup> (A = en, cyclam) proceeds via a dissociative pathway (40).

Amine complexes of iridium(III) have also been shown to be photoreactive but so far have been the subject of relatively little quantitative study. Broad band irradiation of the complexes trans-[Ir(en)<sub>2</sub>X<sub>2</sub>]<sup>+</sup> (X = Cl, Br, I) in aqueous solution leads to stereospecific aquation (30, 31,32). Since the haloquo product reacts stereospecifically with excess ligand Y<sup>-</sup>, the photoreaction provides a useful route for preparation of mixed diacidobis(ethylene-diamine) complexes. For the above complexes, only trans-[Ir(en)<sub>2</sub>Cl<sub>2</sub>]<sup>+</sup> has been studied quantitatively where for 350 nm excitation, the quantum yield of chloride was found to be approximately 0.10 (32).

To provide a theoretical basis to Adamson's empirical



rules, Zink has presented a molecular orbital model (33, 34,35) for the photoreactions of  $d^6$  complexes and applied this to rationalize the product distributions resulting from the photolysis of the halopentaamminerhodium(III) complexes. The fundamental assumption in the model is that the lowest excited state will be the dominant photoactive state (33a). The model consists of three interrelated parts (33b): (a) first, crystal field theory is used to determine the symmetry wave functions, the relative energies of the states, and hence the directionality of the photoreactions, (b) second, molecular orbital theory is included in the analysis to determine the distribution of the excitation energy along the labilized axis in order to understand which ligand on the axis will be preferentially labilized, and (c) thirdly, a crystal field determination of the fractional d-orbital composition of the photoactive excited state is used to determine the relative quantum yields of the photoreactions. Since direct reference will be made to the model, it would be appropriate to present a brief resumé of its more pertinent points.

When an electronic transition occurs, the population of the electronic ground state decreases and that of the excited states increases. Since the two states in a ligand field transition involve metal d orbitals which participate

in the metal-ligand bonding, shifts of electron density will change the metal-ligand bond strength. In a  $d^6$  system the orbital to which an electron is promoted in the low-energy ligand field transitions always involves the unoccupied  $d_{x^2-y^2}$  and/or  $d_z^2$  orbitals which in the molecular orbital picture are  $\sigma$ -antibonding molecular orbitals. If the acceptor orbital is primarily  $d_{x^2-y^2}$  (or  $d_z^2$ ) in character,  $\sigma$  bonding in the xy plane (or z axis) will be weakened and if the axial ligand has filled  $\pi$ -orbitals, the loss of electron density from the ( $\pi$ -antibonding)  $d_{xz}, d_{yz}$  pair will concomitantly result in a strengthening of the  $\pi$  bonding in the z direction (34a).

As an example of the analysis of the total bonding changes caused by a particular excitation, consider the  ${}^1A_1 \rightarrow {}^1E({}^1T_1)$  transition. From the wavefunctions for  ${}^1A_1$  and  ${}^1E({}^1T_1)$  below, the transition results from promotion of an electron from the degenerate  $d_{xz}, d_{yz}$  set to primarily the  $d_z^2$  orbital.

$$A_1 \quad (d_{xy}^2)(d_{xz}^2)(d_{yz}^2)$$

$$E(T_{1g}) \quad -\sqrt{3}/2(d_{xy}^2 d_{xz}^2 d_{yz}^1 d_z^1) - 1/2(d_{xy}^2 d_{xz}^2 d_{yz}^1 d_{x^2-y^2}^1) \\ +\sqrt{3}/2(d_{xy}^2 d_{xz}^1 d_{yz}^2 d_z^1) - 1/2(d_{xy}^2 d_{xz}^1 d_{yz}^1 d_{x^2-y^2}^1)$$

In this case, the Slater determinant representing the  ${}^1E({}^1T_1)$

eigenstate does not contain the pure one-electron  $d_z^2$  orbital but instead contains a linear combination of  $d_z^2$  and  $d_{x^2-y^2}$  and the relative probability of finding the electron in the  $d_z^2$  orbital compared to that of finding it in the  $d_{x^2-y^2}$  orbital is  $3/4:1/4 = 3:1$  (34a). The model predicts that the larger the percent  $d_z^2$  character in the excited state, the more antibonding the metal-ligand bonds on the axis become, thereby increasing the probability of photolabilization of the z-axis ligands (35b). The approximate trends in percent  $d_z^2$  character can be obtained from the trends in the ligand field theory parameter  $Dt$  (i.e., the greater  $Dt$  the more distortion along the z axis).

When the ligands in the labilized direction are different, different degrees of labilization are expected for each of them which will depend on the metal-ligand antibonding properties of each ligand in the excited state (35a). Zink has proposed a model problem in which the four ligands in the horizontal plane are neglected so that the system may be regarded as an effective linear triatomic array. The molecular orbital treatment of the  $\sigma$ -system was based on a simple three-center, three-orbital problem. The MO diagram for atoms along the labilized axis is shown in Figure 5.

In the model problem, the  $\psi_3$  molecular orbital corr-

Figure 5





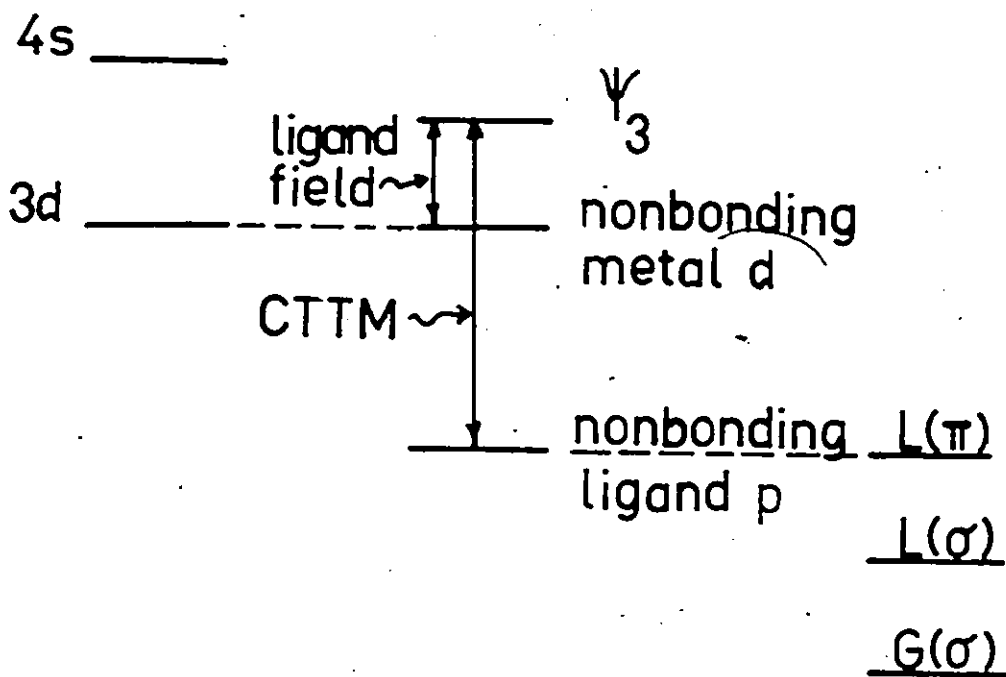
Figure 5. Approximate MO Diagram for  $\sigma$  Interactions  
Along the Unique Axis ( $G(\sigma)$  and  $L(\sigma)$  are  
ligand  $\sigma$ -donor orbitals of appropriate  
symmetry.  $L(\pi)$  represents a nonbonding  
ligand p orbital of  $\pi$  symmetry) (Ref: 34a).



Metal A.O.

M.O.'s

Ligand A.O.



esponded to the metal  $d_{z^2}$  orbital of crystal field theory and  $\phi_L$  and  $\phi_G$  are the respective ligands. The energy of the lowest unoccupied MO,  $E(\psi_3)$ , is always greater than the energy of the most stable ligand donor orbital,  $E(\phi_L)$  (34a). The degree to which one ligand is preferentially labilized over the other depends upon two related factors: (i) the difference in energy between the two ligand donor orbitals and (ii) the difference in energy between  $E(\psi_3)$  and the ligand energies  $E(\phi_L)$  and  $E(\phi_G)$ . When  $E(\phi_L) = E(\phi_G)$ , for example, both ligands will be labilized identically. The greater the energy difference between  $E(\phi_L)$  and  $E(\phi_G)$ , the greater the degree to which the bond between the metal and the lowest is preferentially labilized (34a).

Using the model, Zink has recently reported MO calculations for mixed-ligand cobalt(III)- and chromium(III)-amine complexes (35a). The results revealed that the ligand with the larger metal-ligand overlap or the smallest valence orbital ionization potential (VOIP) the greater the  $\sigma$  labilization of that particular ligand. In other words, of the two ligands on the labilized axis, the one with the smallest VOIP will gain the greatest antibonding character in the excited state and thus will be the one preferentially aquated. As the VOIP of the metal increases, the energy of the  $\psi_3$  orbital decreases. As  $\psi_3$

approaches the energy of the L donor orbital, the difference in antibonding character of the two ligands rapidly increases. The maximum difference in the overlap population occurs when the energy of the  $\psi_3$  orbital equals that of the L or G donor orbitals. When  $\psi_3$  lies between L and G in energy, the overlap population between the metal and the ligand with the smallest VOIP represents metal-ligand stability in the  $\psi_3$  orbital (35a).

The ligand field model (LFM) has met fair success in qualitatively predicting the ligand which will be aquated. However, Ford has presented a critical evaluation concerning its use for quantitative prediction of quantum yields (36). By placing the responsibility for changes in the quantum yields for a homologous series,  $ML_5X^{n+}$ , principally on the substitution reactivity changes in the excited states, the LFM automatically assumes that other pathways for depletion of energy of the excited state differ little over the series considered. Over a homologous series such as  $ML_4L'X^{n+}$ , where either X or L' is being varied, it is felt (36) that it is a dangerous assumption to conclude that nonradiative deactivation will remain uniformly constant. Since significant differences in  $k_n$  (nonradiative deactivation rate constant) have been measured at 77°K for the  $Rh(NH_3)_5X^{2+}$  series (19), it is not inconceivable that



comparable or greater differences will carry over to the photochemical conditions (36).

Another criticism of the LFM voiced by Adamson et al. (37), is that this model employs absorption spectral data (therefore Franck-Condon states) in the calculations used to predict relative quantum yields. For a series such as  $\text{Rh}(\text{NH}_3)_5\text{X}^{2+}$  where X or  $\text{X}^-$  is the leaving group, predictions of photochemical liabilities are based on the ground-state configurations (not those of the thermally equilibrated excited states) and ignore possible mechanistic differences in the steps leading to substitution.

The major liability of the model proposed by Zink rests with its potential for abuse. If the model is interpreted as an absolute dictum of the photochemistry of transition metal complexes, then its failures would demand its immediate demise. On the other hand, if it is accepted merely as a model by which selected electronic features can be hypothetically isolated from the myriad influences of real environments, then it becomes a useful tool in providing both insights and directions into the elucidation of photochemical mechanisms. It seems that the primary need in the maturation of transition metal photochemistry is not so much in the evolution of models, but the acquisition of reliable data which can sensibly act as a precursor to

any substantial model.

Significantly, the findings of Sellan and Rumfeldt (28,29) may be taken to indicate a separation of the qualitative and quantitative aspects of the photoreactions of rhodium(III)-amines. They suggested that whereas the type of photoreaction was principally determined by electronic properties, the quantitative features were strongly influenced by mechanistic factors. In order to more fully assess the role of mechanistic participation in determining the overall efficiency of photochemical reactions, it was deemed that a more systematic and critical investigation of both structural and environmental influences was warranted. Accordingly, for this reason, the effects of pH, temperature, and solvent medium were studied for a series of Rh(III)-amines in an attempt to determine if these parameters were in any way responsible for the photoreactivity of a molecule. Also, by synthesizing and studying the photochemistry of a series of mixed-ligand complexes, it was hoped that they would provide a greater insight into the specificity of the reactions of an excited state molecule. The ultimate goal in the project was to utilize the data obtained from the above investigations and determine those mechanistic features that differentiate the photochemistry of one molecule from another.

## II. EXPERIMENTAL

### 1. Materials

Chemicals used in the preparation of complexes were reagent grade.  $\text{RhCl}_3 \cdot 3\text{H}_2\text{O}$  and  $\text{IrCl}_3 \cdot 3\text{H}_2\text{O}$  (Matthey-Bishop, Inc.) were used without further purification. Since no difference could be detected between using ion exchanged distilled water and distilled water, the latter was used for convenience. Reagent grade methanol and ethanol were also used as solvents.

Spectrophotometric and photolytic solutions were prepared with distilled water for the same reason noted above. Other solvents used were reagent grade.

### 2. Preparation of Complexes

#### 2.1. Cyclam Complexes of Rh(III)

The cyclam complexes and cyclam itself were prepared according to the procedure of Bounsall and Koprach (38). The trans-dibromo, diiodo, chloriodo, and bromiodo complexes were prepared by the revised procedure of Koprach (39). The cis- and trans-dihalo complexes were first isolated as the respective halide salts and then converted to the perchlorate salt by dissolving the complex in a minimum amount of water and adding cold conc.  $\text{HClO}_4$  to precipitate the perchlorate salt. The product was filtered,

washed with ethanol and ether, and dried under vacuum.

The purity of these complexes was determined by comparison of extinction coefficients and peak positions of their electronic spectra to literature data.

## 2.2. Bisethylenediamine Complexes of Rh(III) and Ir(III)

Ethylenediamine dihydrochloride was prepared in accordance with that described by Sellan (40). The trans- and cis-dihalo-bisethylenediamine complexes were prepared using procedures outlined by Basolo (41) with slight modifications as described by Sellan (40). The mixed-dihalo complex trans-[Rh(en)<sub>2</sub>ClBr]ClO<sub>4</sub> was prepared according to the procedure of Bott and Poe (42) and the trans-[Rh(en)<sub>2</sub>-ClI] to that of Bounsall and Poe (43).

The dihalo-bisethylenediamine complexes of iridium (III) were synthesized using the procedures of Bauer and Basolo (44) and converted to the perchlorate salts as described above. The purity of these complexes was determined by comparison of their absorption spectra with literature data.

## 2.3. Halopentaamine Complexes of Rh(III)

### 2.3.1. Rh(NH<sub>3</sub>)<sub>5</sub>X<sup>2+</sup> Series

Chloropentaamminerhodium(III) chloride was prepared following the procedure of Johnson and Basolo (45). A by-product of this reaction is the trans-[Rh(NH<sub>3</sub>)<sub>4</sub>Cl<sub>2</sub>]Cl

complex.

The  $[\text{Rh}(\text{NH}_3)_5\text{Cl}]\text{Cl}_2$  complex was converted to the perchlorate salt by dissolving it in the minimum amount of water and adding cold conc.  $\text{HClO}_4$  to precipitate the perchlorate salt. The product was filtered, washed with ethanol and ether and dried under vacuum.

The bromo- and iodopentaamminerhodium(III) complexes were prepared as described by Bushnell et al. (46) and then converted to their respective perchlorate salts.

The purity of the complexes was determined by comparison of their electronic spectra with literature data.

#### 2.3.2. $\text{Rh}(\text{N}(\text{CH}_3)_3)_5\text{X}^{2+}$ Series

The methylated halopentaamminerhodium(III) series was prepared using identical procedures as outlined above (45,46) with the exception that trimethylamine hydrochloride rather than ammonium chloride was used as the amine source. To avoid confusion, these complexes will be abbreviated as  $\text{Rh}(\text{NMe}_3)_5\text{X}^{2+}$ .

The purity of these complexes was determined by comparison of their absorption spectra with the similar  $\text{Rh}(\text{NH}_3)_5\text{X}^{2+}$  spectra.

#### 2.4. Tetraamine Complexes of Rh(III)

The by-product trans- $[\text{Rh}(\text{NH}_3)_4\text{Cl}_2]\text{Cl}$  from the synthesis of Basolo and Johnson (45) was recrystallized by

extracting it into 100 cm<sup>3</sup> 2:1 boiling HCl. Upon standing, yellow crystals were formed which were filtered, washed with ethanol and ether, and dried under vacuum. Using the dichloro complex as the starting material, the dibromo and diiodo complexes were synthesized in an analogous fashion as the corresponding ethylenediamine complexes (40,41). All complexes were converted to their perchlorate salts prior to use. Trans-[Rh(NMe<sub>3</sub>)<sub>4</sub>I<sub>2</sub>]ClO<sub>4</sub> was synthesized from trans-[Rh(NMe<sub>3</sub>)<sub>4</sub>Cl<sub>2</sub>]ClO<sub>4</sub> as outlined directly above.

The purity of the complexes was determined by comparison of extinction coefficients and peak positions of their electronic spectra to literature data.

### 3. Actinometer Complexes

K<sub>3</sub>Fe(C<sub>2</sub>O<sub>4</sub>)<sub>3</sub> was prepared as described by Hatchard and Parker (47) with the complex being dried over low heat in a current of dry air.

KCr(NH<sub>3</sub>)<sub>2</sub>(NCS)<sub>4</sub> was prepared according to the procedure of Adamson and Wegner (48) with the complex being filtered to remove insoluble matter before the addition of KNO<sub>3</sub>. The complex was recrystallized by repeating the procedure.

#### 4. Spectral Measurements

A Beckman Model DK-1A ratio recording spectrophotometer was used to obtain electronic spectra in the region 650 nm to 180 nm.

Spectral measurements were carried out at room temperature (20-25°C) using sample and reagent blank solutions. Sample solutions of different concentrations were made up for different regions of the spectrum so that optimum values of absorbance could be obtained.

Quartz cells with a pathlength of 1.000 cm were obtained from Hellma.

#### 5. Photolyses

The perchlorate salt of each complex was used since the corresponding halide salt would involve (a) the necessity of a large blank correction in the yield analyses, (b) the occurrence of anion photolysis in the case of 254 nm irradiation of the iodide complexes, (c) the possibility of homogeneous anation reactions, and (d) the possibility of undetectable heterogeneous anation reactions if any of the various complexes employed were susceptible to ion-pairing. Due to the sparing solubility of the cyclam complexes in water, a 10%  $\text{CH}_3\text{CN}$  - 90%  $\text{H}_2\text{O}$  solvent system was used (40) for both spectral and photolytic experiments.

An Oriel model C-13-62 low pressure Hg lamp operated with a stabilized power supply in conjunction with a 22 mm H<sub>2</sub>O filter (to remove 185 nm light) was used as the source for 254 nm irradiations. The reaction cell employed was a 1 cm spectrophotometer cell. Light intensities were measured using the differential technique with the ferrioxalate actinometer (47).

For irradiations in the 320-500 nm region, an Oriel model 611 system employing a 150 W high pressure Xenon lamp in conjunction with an Oriel model 7240 filter monochromator (approximate bandpass 20 nm at half peak) was used. A thermostated 10.0 cm pathlength quartz cell was employed for irradiations with this system. Light intensities were determined using either ferrioxalate (47) or the Reineckate ion (48) as the actinometer. The former was used for calibration in the wavelength region 320-420 nm whilst the latter was employed for wavelengths greater than 420 nm.

The concentrations of both the photolytic and actinometer solutions were adjusted so as to give an optical density of 2 (for the total pathlength of the cell) for the various wavelengths employed. In the event that such an optical density could not be achieved (e.g., low solubility), the actinometer solution was prepared in accordance with the maximum attainable optical density of the



photolytic sample. For purposes of reference, photolysis of a complex in an aqueous medium at 25°C with an optical density of 2 at the excitation wavelength, will be defined as "standard conditions".

To ensure constant light intensity, actinometry was repeated both before and after each run. Absorbances of the actinometer solutions were consistently taken with a Hitachi Perkin-Elmer 139 spectrophotometer.

Halide ion analyses were performed using appropriate Orion selective ion electrodes with a double junction reference electrode and Orion model 801 meter. Calibration curves were prepared according to the procedure of Ingram (49) after measurements on standard solutions with reagent blanks typical of those used in the various experiments. Ingram's method proved to be the most sensitive means for electrode measurements as it minimized uncertainties with respect to electrode stabilization and thermal reactions.

After each photolysis run, the visible-uv spectrum was recorded with a Beckman DK-1A spectrophotometer in order to observe other products (photoaquated complex and any possible photoisomerization). Spectrophotometric and ion analyses of thermal blanks prepared with each series of photochemical runs revealed negligible effects due to dark reactions.

The determination of pH was made by a Sigma pH combination electrode with a model E510 Brinkmann Instruments meter. The electrode was calibrated before each measurement using a commercial standard buffer solution.

### III. RESULTS

#### 1. Electronic Spectra and Band Assignments

For a detailed compilation and interpretation of the electronic spectra of the bisethylenediamine and cyclam complexes of rhodium(III) used in this work, the reader is referred to the Ph.D. dissertation of James Sellan (40). For the tetraamine complexes, the spectra were compared to those reported by Basolo (45) and Endicott (13,14). In all cases good agreement was found with literature data.

The electronic spectra of the series  $\text{Rh}(\text{NMe}_3)_5\text{X}^{2+}$  used in this work were found to closely resemble those of the analogous  $\text{Rh}(\text{NH}_3)_5\text{X}^{2+}$  series (50). The spectra of the  $\text{Rh}(\text{NMe}_3)_5\text{X}^{2+}$  series are presented in Figures 6, 7, and 8. For purposes of comparison, Table 1 presents the absorption spectra of the two series and due to insufficient data, the bands are only assigned as LF or CT.

#### 2. Photolysis of Rh(III)-Amines Under Standard Conditions

A series of rhodium(III)-amines were photolysed in both the ligand field and charge transfer wavelength regions using the "standard conditions" previously outlined. In order to minimize potential difficulties due to secondary

Table 1

## Electronic Spectra of Some Rh(III)-Amine Complexes

| Complex                     | $\lambda_{\text{max}}$ (nm) | Band Assignment | $\epsilon_{\text{max}}$ ( $M^{-1}cm^{-1}$ ) |
|-----------------------------|-----------------------------|-----------------|---------------------------------------------|
| $Rh(NH_3)_5Cl^{2+}$         | 348                         | LF <sub>1</sub> | 108                                         |
|                             | 277                         | LF <sub>2</sub> | 110                                         |
| $Rh(NMe_3)_5Cl^{2+}$        | 348                         | LF <sub>1</sub> | 141                                         |
|                             | 277                         | LF <sub>2</sub> | 162                                         |
| $Rh(NH_3)_5Br^{2+}$         | 420 (sh)                    | LF <sub>1</sub> | 30                                          |
|                             | 360                         | LF <sub>2</sub> | 137                                         |
| $Rh(NMe_3)_5Br^{2+}$        | 420 (sh)                    | LF <sub>1</sub> | 40                                          |
|                             | 360                         | LF <sub>2</sub> | 130                                         |
| $Rh(NH_3)_5I^{2+}$          | 415                         | LF <sub>1</sub> | 305                                         |
|                             | 277                         | CT              | 3,162                                       |
|                             | 224                         | CT              | 31,620                                      |
| $Rh(NMe_3)_5I^{2+}$         | 415                         | LF <sub>1</sub> | 160                                         |
|                             | 277                         | CT              | 1,900                                       |
|                             | 226                         | CT              | 22,000                                      |
| trans- $[Rh(NMe_3)_4I_2]^+$ | 470                         | LF <sub>1</sub> | 480                                         |
|                             | 340                         | CT              | 18,330                                      |
|                             | 270                         | CT              | 36,670                                      |

Figure 6

Figure 6. Electronic Spectrum of  $\text{Rh}(\text{NMe}_3)_5\text{Cl}^{2+}$  in  $\text{H}_2\text{O}$ .

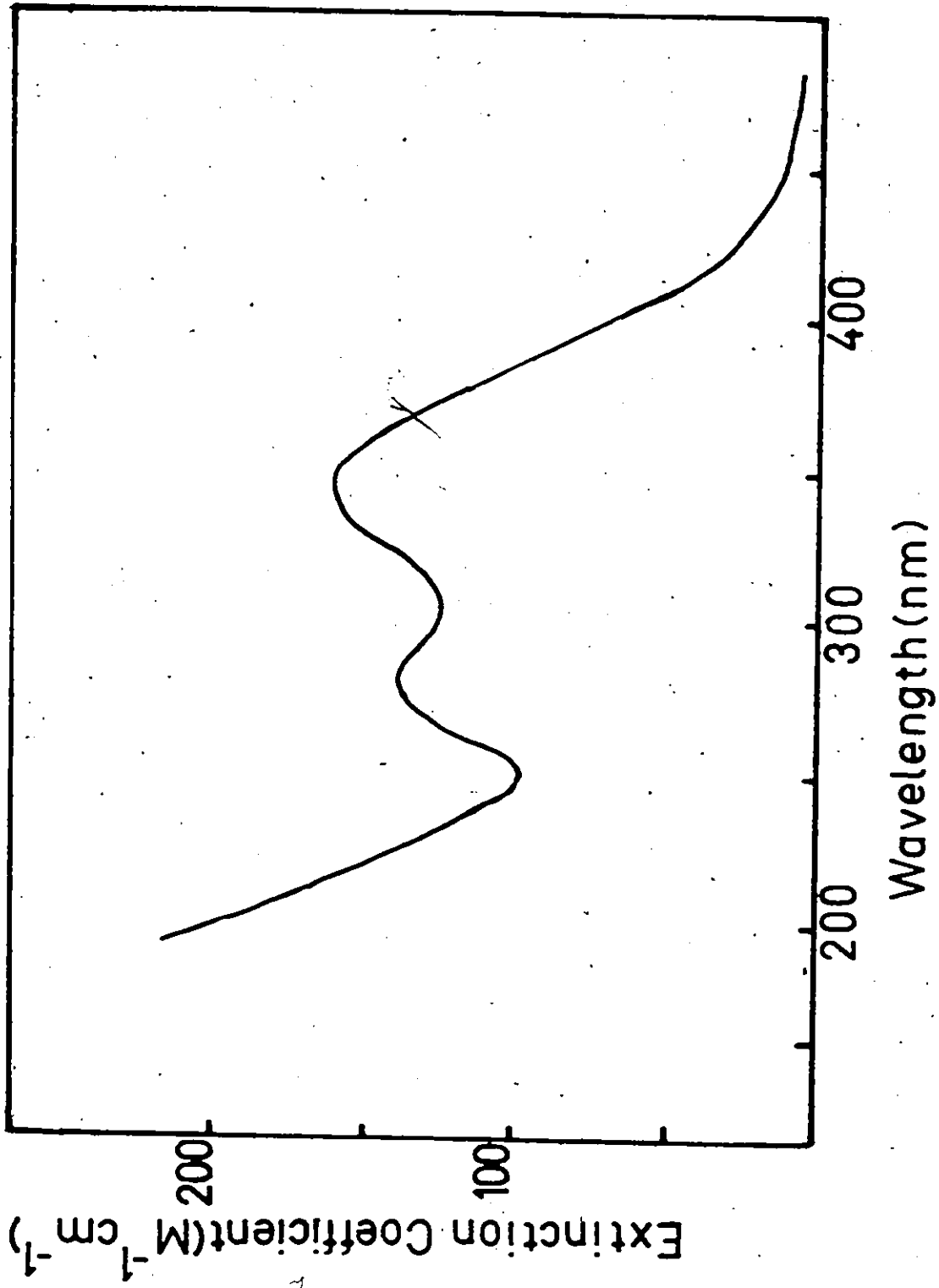


Figure 7





Figure 7. Electronic Spectrum of  $\text{Rh}(\text{NMe}_3)_5\text{Br}^{2+}$  in  $\text{H}_2\text{O}$ .

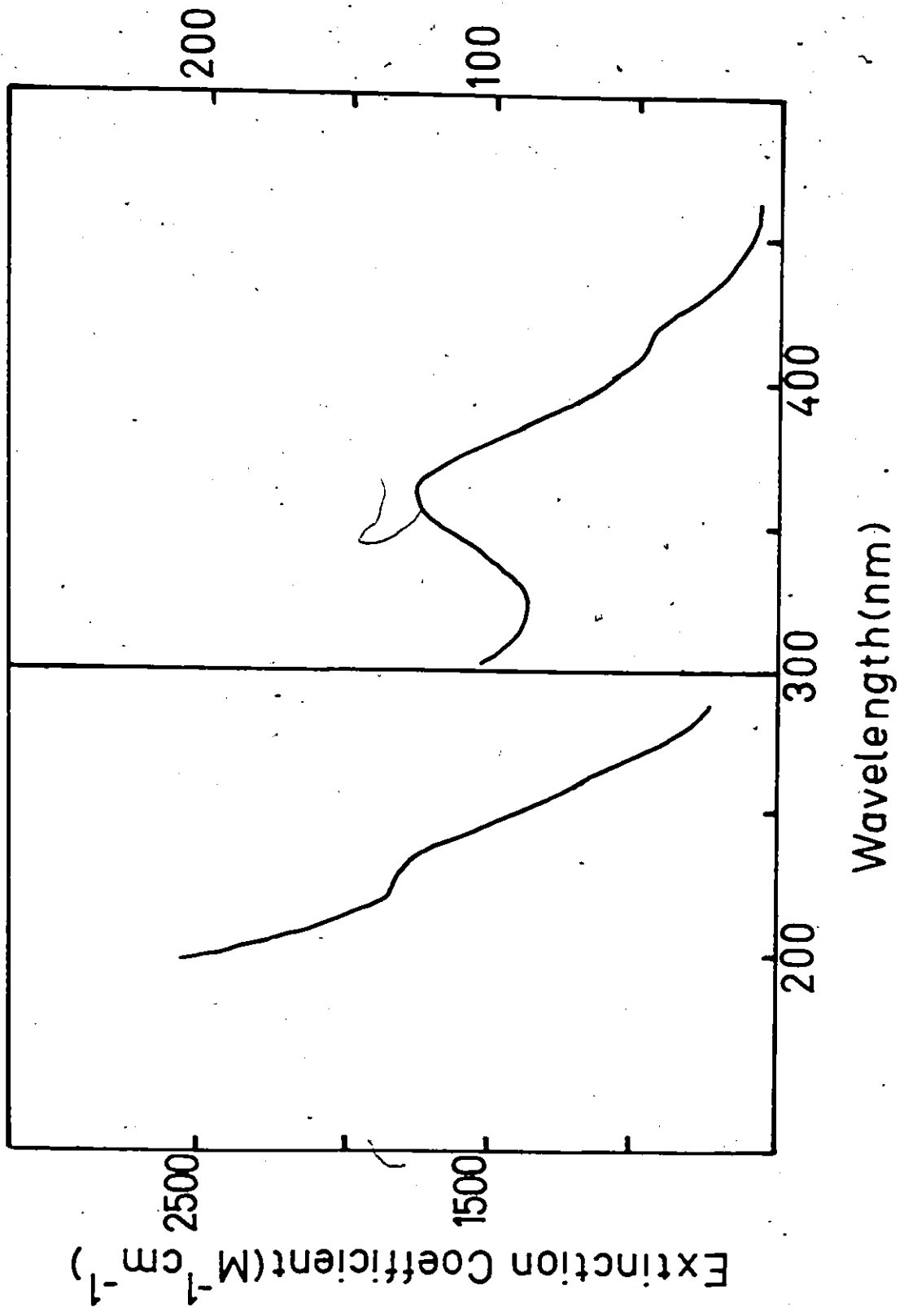
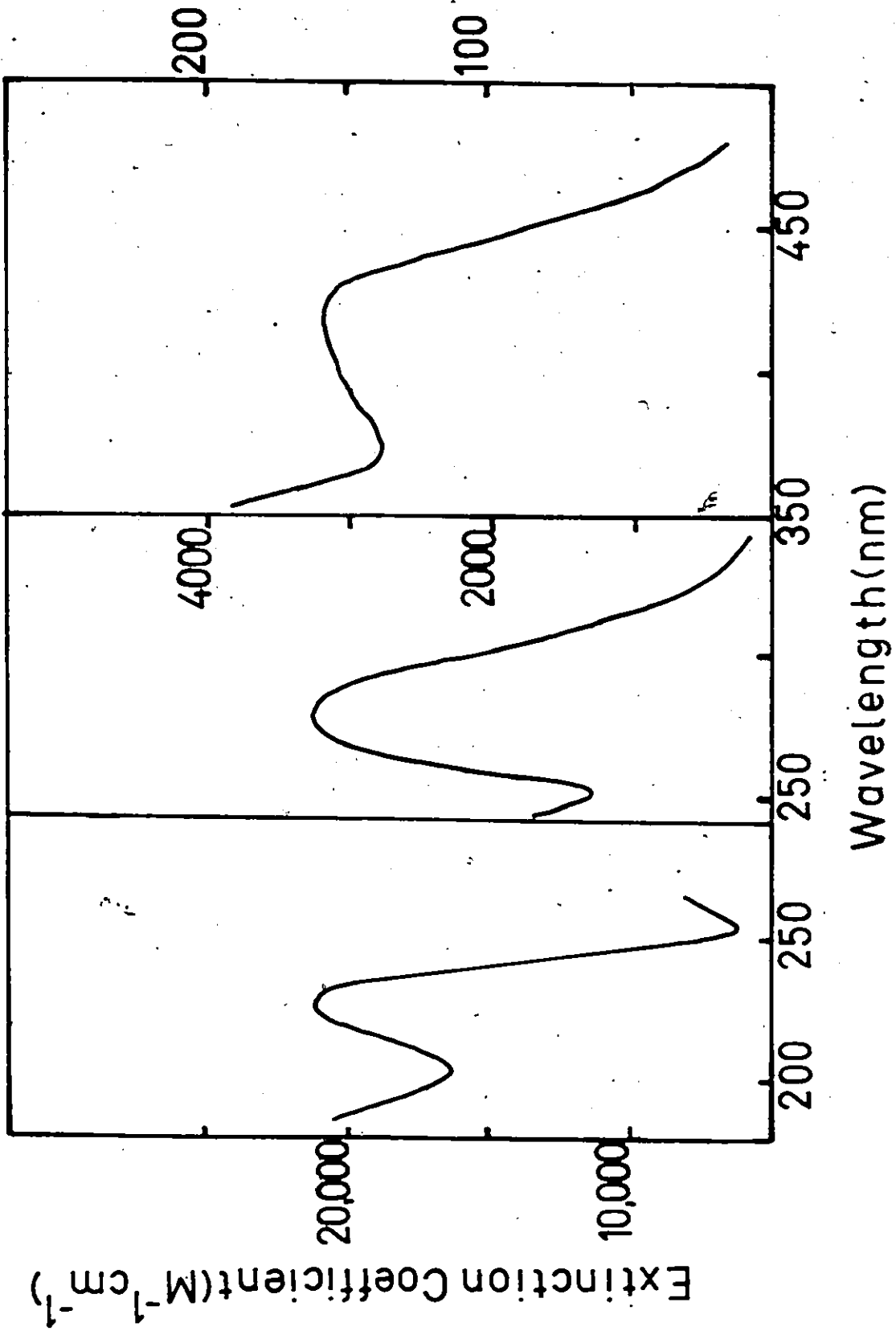


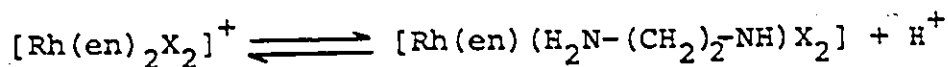
Figure 8

Figure 8. Electronic Spectrum of  $\text{Rh}(\text{NMe}_3)_5\text{I}^{2+}$  in  $\text{H}_2\text{O}$ .



photolysis or backreactions, photolysis was restricted in the majority of cases to less than 20% conversion.

Prior to irradiation, the pentaamine and tetraamine complexes were acidified with  $\text{HClO}_4$  to a pH of 3.0. Since the perchlorate salts of the cyclam and bisethylenediamine complexes tended to precipitate upon addition of perchloric acid, all solutions of these complexes were irradiated at their "natural pH". As a consequence, each complex would exist in equilibrium with its conjugate base, e.g.,



For the most acidic of the complexes, trans- $[\text{Rh}(\text{en})_2\text{Cl}_2]^+$ , a typical value of natural pH for a  $2.2 \times 10^{-3}$  M solution was pH = 3.53. Adamson and Kutal (26) have photolysed the chloride salt of trans- $[\text{Rh}(\text{en})_2\text{Cl}_2]^+$  acidified to pH = 3.0 with nitric acid and their results are essentially the same as those reported both in this study and by Sellan (40). A summary of approximate acid dissociation constants are given in Appendix I.

In each case a thermal blank was prepared to estimate possible background yields due to dark reactions. Although it was found for the majority of molecules studied that thermal yields were negligible, this practice was continued with all samples as a precaution against acci-

dental contamination.

The concentrations of halide ion released during photolysis were measured using the appropriate specific ion electrode. All amine yields, with the exception of the iodopentaamine complexes, were calculated from the difference in the pH of the systems prior to and after irradiation. To ensure accuracy, the solutions were adjusted prior to irradiation to an ionic strength of 0.10 with  $\text{NaClO}_4$  when pH measurements were taken. For the iodopentaamine complexes, the rate of formation of tetraammine-rhodium(III) product was an equivalent measure of the rate of amine aquation. This method was feasible because trans- $[\text{Rh}(\text{NR}_3)_4(\text{H}_2\text{O})\text{I}]^{2+}$  ( $\text{R} = \text{H}, \text{CH}_3$ ) aquated very rapidly in 0.20 M NaI. This procedure proved to be the most sensitive measure of amine aquation due to the distinct and intense absorption spectrum of trans- $[\text{Rh}(\text{NR}_3)_4\text{I}_2]^+$ . Product yields were calculated from absorbance measurements at 270 nm.

For each sample, the yields were measured for various irradiation times and product yield versus time plots were constructed. All systems exhibited an initial linear region in these plots followed ultimately by a region of curvature. The onset of curvature depended upon the complex used. For example, linearity was preserved beyond 60% conversion with  $\text{Rh}(\text{NH}_3)_5\text{Cl}^{2+}$  whereas trans- $[\text{Rh}(\text{en})_2\text{I}_2]^+$  could not tolerate more than 10% conversion. In

any event, all yields were computed from the initial linear portion of the respective curves using the relationship

$$\phi(\text{product}) = \frac{\text{slope (M/min)}}{\text{intensity (einsteins/l-min)}}$$

A typical plot is illustrated in Figure 9.

### 2.1. Rh(NH<sub>3</sub>)<sub>5</sub>X<sup>2+</sup> and Rh(NMe<sub>3</sub>)<sub>5</sub>X<sup>2+</sup>: Photolyses

The photolysing wavelengths in the LF region were normally chosen to coincide with the first and/or second LF bands. In the case of the fixed 254 nm radiation, absorption occurred along the leading edge of the first CT band for the bromo complexes whereas with the iodo complexes, absorption would be about equally distributed between the overlapping first and second CT bands. For the chloro complexes, 254 nm radiation resulted in the second LF band being excited with some CT absorption.

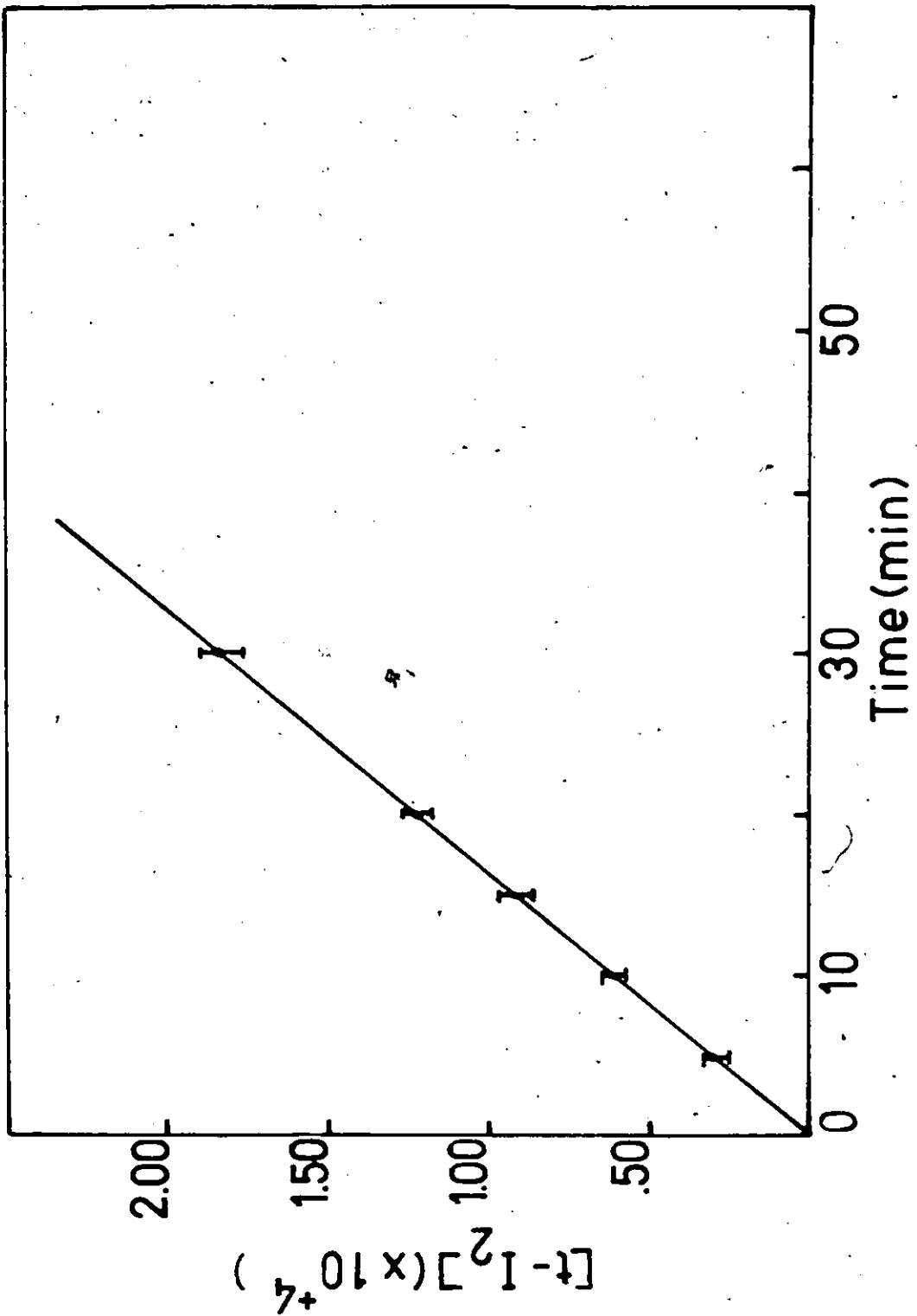
#### 2.1.1. Irradiation of Rh(NH<sub>3</sub>)<sub>5</sub>X<sup>2+</sup>.

For Rh(NH<sub>3</sub>)<sub>5</sub>Cl<sup>2+</sup>, Cl<sup>-</sup> was the only detectable aquation product. Attempts to detect NH<sub>3</sub> aquation by measuring changes in pH showed that  $\phi(\text{NH}_3) < 10^{-3}$ . These results are in agreement with those reported by Moggi (12) and Endicott (14). The chloride yield was observed to be slightly sensitive to the wavelength of irradiation with



Figure 9

Figure 9. Product Yield versus Irradiation Time Plot  
from the Photolysis of  $\text{Rh}(\text{NMe}_3)_5\text{I}^{2+}$  at  
254 nm.



the yield decreasing with increasing excitation energy.

The photolysis of  $\text{Rh}(\text{NH}_3)_5\text{Br}^{2+}$  resulted in the liberation of both  $\text{NH}_3$  and  $\text{Br}^-$  with  $\text{NH}_3$  appearing as the major product. It is noteworthy that  $\text{Br}^-$  aquation was independent of irradiation time up to at least 25% decomposition of  $\text{Rh}(\text{NH}_3)_5\text{Br}^{2+}$  thereby indicating that it should be regarded as a primary product and not a consequence of either secondary thermal or photochemical processes. The bromide yields were found to exhibit a modest wavelength dependence. In contrast, ammine yields were significantly reduced from irradiation at 254 nm.

Ammine aquation was the sole photolysis product from irradiations of  $\text{Rh}(\text{NH}_3)_5\text{I}^{2+}$ . A marked wavelength dependence was observed whereby product yields increased with increasing wavelength.

In all cases, good agreement was obtained with the previously reported results of Endicott and Kelly (13,14, 16) and are presented in Table 2.

#### 2.1.2. Irradiation of $\text{Rh}(\text{NMe}_3)_5\text{X}^{2+}$

In contrast to  $\text{Rh}(\text{NH}_3)_5\text{Cl}^{2+}$ , irradiation of  $\text{Rh}(\text{NMe}_3)_5\text{Cl}^{2+}$  resulted in both  $\text{Cl}^-$  and  $\text{NMe}_3$  formation with the former being the principal aquation product. Whereas the amine yield appeared to be wavelength independent over the region studied, the quantum yield of chloride increased

Table 2

Quantum Yields from the Photolysis of  $\text{Rh}(\text{NR}_3)_5\text{X}^{2+}$ 

| Complex                                   | Absorption Band | $\lambda$ nm | $\phi(\text{X}^-)$ | $\phi(\text{amine})$ | Ref. |
|-------------------------------------------|-----------------|--------------|--------------------|----------------------|------|
| $\text{Rh}(\text{NH}_3)_5\text{Cl}^{2+}$  | LF+CITM         | 254          | 0.11±0.01          | $10^{-3}$            | a,b  |
|                                           | LF              | 280          | 0.12±0.01          | $10^{-3}$            | b    |
|                                           | LF              | 350          | 0.16±0.01          | $10^{-3}$            | a,b  |
|                                           | LF              | 380          | 0.14±0.01          | $10^{-3}$            | b    |
| $\text{Rh}(\text{NMe}_3)_5\text{Cl}^{2+}$ | LF+CITM         | 254          | 0.085±0.005        | 0.030±0.002          | a    |
|                                           | LF              | 354          | 0.13±0.01          | 0.030±0.002          | a    |
| $\text{Rh}(\text{NH}_3)_5\text{Br}^{2+}$  | CITM            | 254          | 0.019±0.001        | 0.027±0.003          | a    |
|                                           | LF              | 360          | 0.019±0.001        | 0.18±0.02            | b    |
|                                           | LF              | 360          | 0.015±0.001        | 0.14±0.02            | a    |
|                                           | LF              | 420          | 0.019±0.001        | 0.17±0.02            | b    |
| $\text{Rh}(\text{NMe}_3)_5\text{Br}^{2+}$ | CITM            | 254          | 0.035±0.005        | 0.14±0.02            | a    |
|                                           | LF              | 360          | 0.015±0.003        | 0.12±0.02            | a    |
|                                           | LF              | 420          | 0.032±0.002        | 0.20±0.02            | a    |
| $\text{Rh}(\text{NH}_3)_5\text{I}^{2+}$   | CITM            | 254          | —                  | 0.43±0.04            | a,c  |
|                                           | CITM+LM         | 350          | —                  | 0.58±0.03            | b    |
|                                           | LF              | 420          | —                  | 0.87±0.07            | a,b  |
| $\text{Rh}(\text{NMe}_3)_5\text{I}^{2+}$  | CITM            | 254          | —                  | 0.55±0.03            | a    |
|                                           | LF              | 412          | —                  | 0.58±0.03            | a    |

<sup>a</sup>This work.<sup>b</sup>References 14 and 16.<sup>c</sup>Reference 13.

with increasing wavelength.

As with the above, irradiations of  $\text{Rh}(\text{NMe}_3)_5\text{Br}^{2+}$  produced both amine and bromide as products with the former being greater. Whilst the quantum yields of amine released were similar to those of  $\text{Rh}(\text{NH}_3)_5\text{Br}^{2+}$ , the bromide yields were generally larger. Wavelength dependence studies revealed product yields to be of the same magnitude from irradiations either in the first LF or CT band. However, excitation into the second LF band showed a notable decrease in the bromide yields.

Photolysis of  $\text{Rh}(\text{NMe}_3)_5\text{I}^{2+}$  produced only amine and within the limits of the experimental error, no wavelength dependence was observed. Such results are in contrast with those observed for the nonmethylated analog. The quantum yields are summarized in Table 2.

## 2.2. $\text{trans-}[\text{Rh}(\text{A}_4)\text{X}_2]^+$ (A = $\text{NH}_3$ , en, cyclam): Photolysis

For irradiations in the LF region, the wavelength employed was chosen to correspond to the frequency at the band maximum of the first spin-allowed LF band of each complex. Illuminations with 254 nm radiation resulted in absorption by the first CT band in the dichloro complexes, while for the dibromo complexes absorption occurs at the leading edge of the second CT band. For the diiodo complexes, the main absorption is by the second CT band

although some excitation of the third band should also occur.

The principal product in all cases was the halide ion. Analysis of the spectra of the photolyte solutions confirmed the presence of the respective trans-monoquo complexes, and since at no time could any evidence of a cis isomer be detected, it was concluded that the photo-aquation proceeded with complete isomeric retention. The very slight decrease of 0.01 - 0.02 units observed in the pH of the photolysed solutions corresponds to the higher acidity of aquo complexes compared to amine complexes.

It was particularly necessary to use short irradiation times (<10% decomposition) for all of the diiodo complexes at 254 nm because longer times allowed for an accumulation of  $I^-$  which, in turn, created an inner filter effect. Determination of  $I^-$  concentrations could not be performed by electrode measurement for trans- $[Rh(NH_3)_4I_2]^+$  since no free iodide could be detected in either the thermal blanks or photolysed solutions. In addition, the absorption spectrum of the irradiated sample showed no decay. This strongly suggested a highly efficient back reaction and for this reason  $AgNO_3$  was introduced into the system to serve as a scavenger for free  $I^-$ . The concentration of  $AgNO_3$  used was low enough ( $2.10 \times$

$10^{-3}$  M) so as not to cause a catalytic decomposition. Using this technique and measuring the disappearance of complex at 270 nm, a quantum yield of  $0.90 \pm 0.10$  for iodide release was obtained. On the other hand, determination of free  $I^-$  by specific ion electrode was possible for trans- $[Rh(en)_2I_2]^+$ . For the tetraammine and bisethylene-diamine complexes studied, the quantum yields are considerably larger than those previously reported (13,28). It is the opinion of this author that the quantum yields reported earlier (13,28) have been significantly reduced due to a highly efficient anation via a redox mechanism initiated by reaction with hydrated electrons generated from the photolysis of the liberated iodide. This opinion derives from experience obtained with the photolysis of aqueous  $I^-$  solutions containing nonabsorbing quantities of complex. These systems are discussed in detail in Section 4.

The analysis of bromide release from the photolysis of trans- $[Rh(NH_3)_4Br_2]^+$  using a specific ion electrode proved unreliable due to extremely erratic results. The reason for the failure of this otherwise standard technique still remains uncertain. The only method that proved to be appropriate was spectrophotometric monitoring of the decay of the second LF band (275 nm). The overall



quantum yield of hydrolysis was calculated from linear plots of absorbance versus irradiation time. No evidence for wavelength dependence of the yields could be detected. However, owing to the lesser degree of sensitivity with spectrophotometric techniques such as that outlined above, the possibility of undetected wavelength dependence cannot be excluded.

The quantum yields from the respective complexes are summarized in Table 3.

2.3.  $\text{trans-}[\text{Rh}(\text{A}_4)\text{XY}]^+$  (A = en, cyclam): Photolysis

The choice of the wavelength of excitation for the LF region was complicated by the fact that the apparent first band was split. Hence, the wavelengths were selected to correspond to the maximum of the band. Using 254 nm radiation results in absorption by both the first and second CT bands in the chlorobromo complexes whereas for both the chloroiodo and bromoiodo cases, absorption would be exclusively by the second band.

Halide ion analyses using specific ion electrodes are complicated with complexes of this type since  $\text{I}^-$  interferes with  $\text{Br}^-$  or  $\text{Cl}^-$  and  $\text{Br}^-$  interferes with  $\text{Cl}^-$ . Accurate determinations of  $\text{I}^-$  and  $\text{Br}^-$  in the presence of  $\text{Cl}^-$  were made; however, in agreement with Sellan (40),  $\text{Cl}^-$  yields were badly scattered and were of only qualita-

Table 3

Quantum Yields from the Photolysis of  $\text{trans-}[\text{Rh}(\text{A}_4)\text{X}_2]^+$ 

| Complex                                                | Absorption Band | $\lambda$ nm | $\phi(X^-)$ | Ref.  |
|--------------------------------------------------------|-----------------|--------------|-------------|-------|
| $\text{trans-}[\text{Rh}(\text{NH}_3)_4\text{Cl}_2]^+$ | CTTM            | 254          | 0.11±0.02   | a,b   |
|                                                        | LF              | 412          | 0.13±0.02   | b     |
| $\text{trans-}[\text{Rh}(\text{en})_2\text{Cl}_2]^+$   | CTTM            | 254          | 0.12±0.02   | a,b,c |
|                                                        | LF              | 408          | 0.08±0.01   |       |
| $\text{trans-}[\text{Rh}(\text{cyclam})\text{Cl}_2]^+$ | CTTM            | 254          | 0.035±0.002 | a,c   |
|                                                        | LF              | 401          | 0.008±0.001 | c     |
| $\text{trans-}[\text{Rh}(\text{NH}_3)_4\text{Br}_2]^+$ | CTTM            | 254          | 0.17±0.04   | a     |
|                                                        | LF              | 438          | 0.17±0.04   | a     |
| $\text{trans-}[\text{Rh}(\text{en})_2\text{Br}_2]^+$   | CTTM            | 254          | 0.09±0.02   | a,c   |
|                                                        | LF              | 430          | 0.07±0.01   | c     |
| $\text{trans-}[\text{Rh}(\text{cyclam})\text{Br}_2]^+$ | CTTM            | 254          | 0.10±0.01   | a,c   |
|                                                        | LF              | 400          | 0.030±0.003 | c     |
|                                                        | LF              | 400          | 0.023±0.003 | a     |
| $\text{trans-}[\text{Rh}(\text{NH}_3)_4\text{I}_2]^+$  | CTTM            | 254          | 0.20±0.02   | d     |
|                                                        | CTTM            | 254          | 0.90±0.10   | a     |
|                                                        | LF              | 470          | 0.48±0.10   | d     |
| $\text{trans-}[\text{Rh}(\text{en})_2\text{I}_2]^+$    | CTTM            | 254          | 0.20±0.02   | c     |
|                                                        | CTTM            | 254          | 0.86±0.01   | a     |
|                                                        | LF              | 460          | 0.20±0.02   | c     |
| $\text{trans-}[\text{Rh}(\text{cyclam})\text{I}_2]^+$  | CTTM            | 254          | 0.18±0.01   | c     |
|                                                        | LF              | 460          | 0.14±0.01   | c     |

a This work.

b Reference 26.

c Reference 28.

d References 13 and 14.

tive value.

Fortunately, the photohydrolysis of the chloriodo complexes was accompanied by a spectrophotometric decay of the first CT band with a well defined isobestic point. The overall quantum yield of hydrolysis was calculated from linear plots of absorbance versus irradiation time. The presence of this isobestic point was indicative of a single major product, and since the  $I^-$  yields were measured directly and found to be very small by comparison with the overall yield, the principal ligand aquated was therefore  $Cl^-$ .

It was presupposed that from Adamson's rules (10),  $Cl^-$  should be the major product for the chlorobromo-bis-ethylenediamine complex. However, it was discovered that bromide rather than chloride is the principal ligand aquated. To ensure qualitatively that only bromide was being released,  $CCl_4$  and  $Cl_2$  were added to the photolyte sample to oxidize  $Br^-$  to  $Br_2$ . The sample was then extracted with 15 mls  $CCl_4$  with the resultant organic layer evaporated to approximately  $3\text{ cm}^3$ . With  $CCl_4$  as the reference, the absorption spectrum of the sample was recorded and found to correspond to that for  $Br_2$  and  $BrCl$  (52).

All of the quantum yields are reported in Table 4 with some adopted from Sellan (40) for purposes of comple-

- Table 4.  
Quantum Yields from the Photolysis of trans-[Rh(A<sub>4</sub>)XY]<sup>+</sup>

| Complex                                               | Absorption Band | λ nm | φ(X <sup>-</sup> ) | φ(Y <sup>-</sup> ) | Ref. |
|-------------------------------------------------------|-----------------|------|--------------------|--------------------|------|
| <u>trans</u> -[Rh(en) <sub>2</sub> ClBr] <sup>+</sup> | CITM            | 254  | -                  | 0.07±0.01          | a    |
|                                                       | LF              | 418  | -                  | 0.03±0.005         | a    |
| <u>trans</u> -[Rh(en) <sub>2</sub> ClI] <sup>+</sup>  | CITM            | 254  | 0.35±0.02          | 0.04               | a,b  |
|                                                       | LF              | 430  | -                  | 0.003              | b    |
| <u>trans</u> -[Rh(cyclam)ClI] <sup>+</sup>            | CITM            | 254  | 0.32±0.02          | 0.01               | a,b  |
|                                                       | LF              | 433  | -                  | 0.001              | b    |
| <u>trans</u> -[Rh(en) <sub>2</sub> BrI] <sup>+</sup>  | CITM            | 254  | 0.29±0.02          | 0.02               | b    |
|                                                       | LF              | 450  | -                  | 0.003              | b    |
| <u>trans</u> -[Rh(cyclam)BrI] <sup>+</sup>            | CITM            | 254  | 0.32±0.02          | 0.01               | b    |
|                                                       | LF              | 497  | 0.28±0.02          | 0.001              | b    |

<sup>a</sup>This work.

<sup>b</sup>Reference 40.

tion of the series.

#### 2.4. $\text{cis-}[\text{Rh}(\text{cyclam})\text{X}_2]^+$ : Photolysis

For excitation in the LF region, the wavelengths were chosen to coincide with the first spin-allowed ligand field band. Absorption resulting from 254 nm radiation occurred along the leading edge of the first CT band in the dichloro and dibromo complexes whereas with the diiodo complexes, absorption would be about equally distributed between the strongly overlapping first and second CT bands.

Photolysis of all of the complexes resulted in halide release with the cis geometry being retained by the complex. Analysis of the spectra of the photolyte solutions showed no evidence for the formation of the trans-mono-aquo complexes. With the exception of the bromide yield, the quantum yields listed in Table 5 were calculated from the usual yield versus irradiation time plots. However, due to the large extinction coefficient of cis-}[\text{Rh}(\text{cyclam})-\text{Br}\_2]^+ at 254 nm, it was necessary to use solutions adjusted to an absorbance of 4.2 to avoid rapid solute depletion that occurred with the dilute solutions (i.e. absorbance = 2:10) (40).

#### 2.5. pH Effects on the Photolysis of $\text{Rh}(\text{NR}_3)_5\text{X}^{2+}$

The role played by  $\text{H}^+$  in the photolyses of the penta-

Table 5

Quantum Yields from the Photolysis of  $\text{cis-}[\text{Rh}(\text{cyclam})\text{X}_2]^+$ 

| Complex                                              | Absorption Band | $\lambda_{\text{nm}}$ | $\phi(\text{X}^-)$        | Ref. |
|------------------------------------------------------|-----------------|-----------------------|---------------------------|------|
| $\text{cis-}[\text{Rh}(\text{cyclam})\text{Cl}_2]^+$ | CITM            | 254                   | $0.47 \pm 0.02$           | a    |
|                                                      | CITM            | 254                   | $0.45 \pm 0.02$           | b    |
|                                                      | LF              | 400                   | $0.37 \pm 0.02$           | a    |
|                                                      | LF              | 400                   | $0.36 \pm 0.02$           | b    |
| $\text{cis-}[\text{Rh}(\text{cyclam})\text{Br}_2]^+$ | CITM            | 254                   | $0.34 \pm 0.02$           | a    |
|                                                      | CITM            | 254                   | $0.22 \pm 0.02$           | b    |
|                                                      | LF              | 400                   | $0.32 \pm 0.02$           | a    |
| $\text{cis-}[\text{Rh}(\text{cyclam})\text{I}_2]^+$  | CITM            | 254                   | $0.050 \pm 0.001$         | a    |
|                                                      | LF              | 402                   | $0.030 \pm 0.001$         | a    |
| $\text{cis-}[\text{Rh}(\text{en})_2\text{Cl}_2]^+$   | CITM            | 254                   | 0.1                       | c    |
|                                                      |                 |                       | $\phi(-\text{H}^+) = 0.4$ | a    |

<sup>a</sup>Reference 29.<sup>b</sup>This work.<sup>c</sup>Reference 27.

amine complexes of rhodium(III) was investigated by 254 nm irradiation of selected complexes at various acidities. The molecules chosen were  $\text{Rh}(\text{NH}_3)_5\text{Cl}^{2+}$ ,  $\text{Rh}(\text{NMe}_3)_5\text{Cl}^{2+}$ , trans- $[\text{Rh}(\text{NH}_3)_4\text{Cl}_2]^+$  and  $\text{Rh}(\text{NH}_3)_5\text{I}^{2+}$ . It was necessary to closely monitor the thermal blank at concentrations of  $\text{H}^+ < 10^{-3}$  M for the chloro complexes since chloride is the ligand aquated in the "antithermal" reactions of these complexes. For  $\text{Rh}(\text{NH}_3)_5\text{I}^{2+}$ , the amine group is not a product of thermal reactions thereby not creating any interferences at the higher pH values.

In the case of  $\text{Rh}(\text{NH}_3)_5\text{Cl}^{2+}$ , irradiations were performed employing a pH range of 4.0 - 5.75 where 4.0 corresponds to the "natural" pH for this complex. Lower acidities were accomplished by using a  $\text{KH}_2\text{PO}_4$ -KOH buffer system. A significant increase in  $\phi(\text{Cl}^-)$  was found for pH media greater than 3.0. However, the yields of chloride were found to be independent of pH in the range 4.0 - 5.75. The reproducibility in the yields and the linearity of yield versus time plots strongly suggested that the enhanced yields were not a consequence of thermal reactions. Figure 10 is illustrative of typical yield versus irradiation time plots.

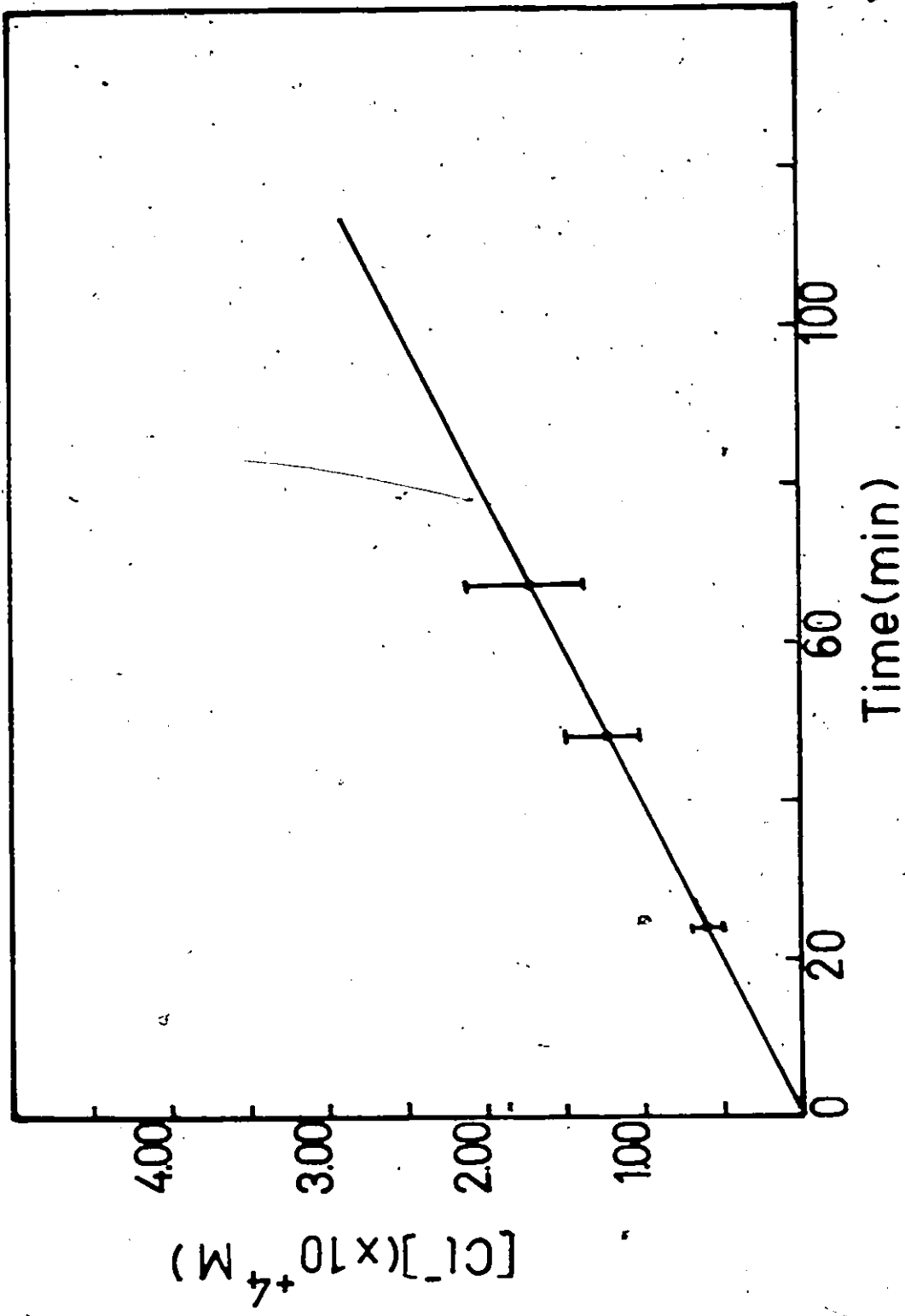
When trans- $[\text{Rh}(\text{NH}_3)_4\text{Cl}_2]^+$  was irradiated at natural pH (4.2), the yield was  $\phi(\text{Cl}^-) = 0.23 \pm 0.03$  which is in

Figure 10

✓



Figure 10. Product Yield versus Irradiation Time Plot  
from the Photolysis of  $\text{Rh}(\text{NH}_3)_5\text{Cl}^{2+}$  at  
254 nm in a Medium of pH 5.75.



contrast to a value of  $\phi(\text{Cl}^-) = 0.11 \pm 0.02$  obtained at pH = 3.0.

Irradiating  $\text{Rh}(\text{NMe}_3)_5\text{Cl}^{2+}$  under natural pH conditions (pH = 5.0) resulted in identical chloride yields as those found at pH 3.0. However, the amine yield was found to decrease by a factor of 3 (i.e. 0.03  $\rightarrow$  0.01).

The illumination of  $\text{Rh}(\text{NH}_3)_5\text{I}^{2+}$  resulted in yield versus time plots which were invariant over the pH range 4.4 - 8.7. However, for this range, the quantum yield of ammine was lower than that found from irradiations in a medium of pH 3.0. This effect is demonstrated in Figure 11.

Table 6 presents the yields as a function of pH for the various complexes. To eliminate any possibility of an inner filter effect from photolysis of  $\text{I}^-$ , yields were calculated from initial irradiation times for pH ranges higher than 3.0 for  $\text{Rh}(\text{NH}_3)_5\text{I}^{2+}$ .

### 3. Photolysis of $\text{trans-}[\text{Ir}(\text{en})_2\text{X}_2]^+$ Under Standard Conditions

Due to the low extinction coefficients of the first spin-allowed LF bands, it was more practical to irradiate into the second spin-allowed LF bands. Illuminations with 254 nm radiation resulted in the first CT band being excited in the dichloro complex, the leading edge of the sec-

3

Figure 11

Figure 11. Product Yield versus Irradiation Time Plots  
from the Photolysis of  $\text{Rh}(\text{NH}_3)_5\text{I}^{2+}$  at 254  
nm in the Media pH 3.0 (●), pH 5.5 (○),  
and pH 8.7 (▲).

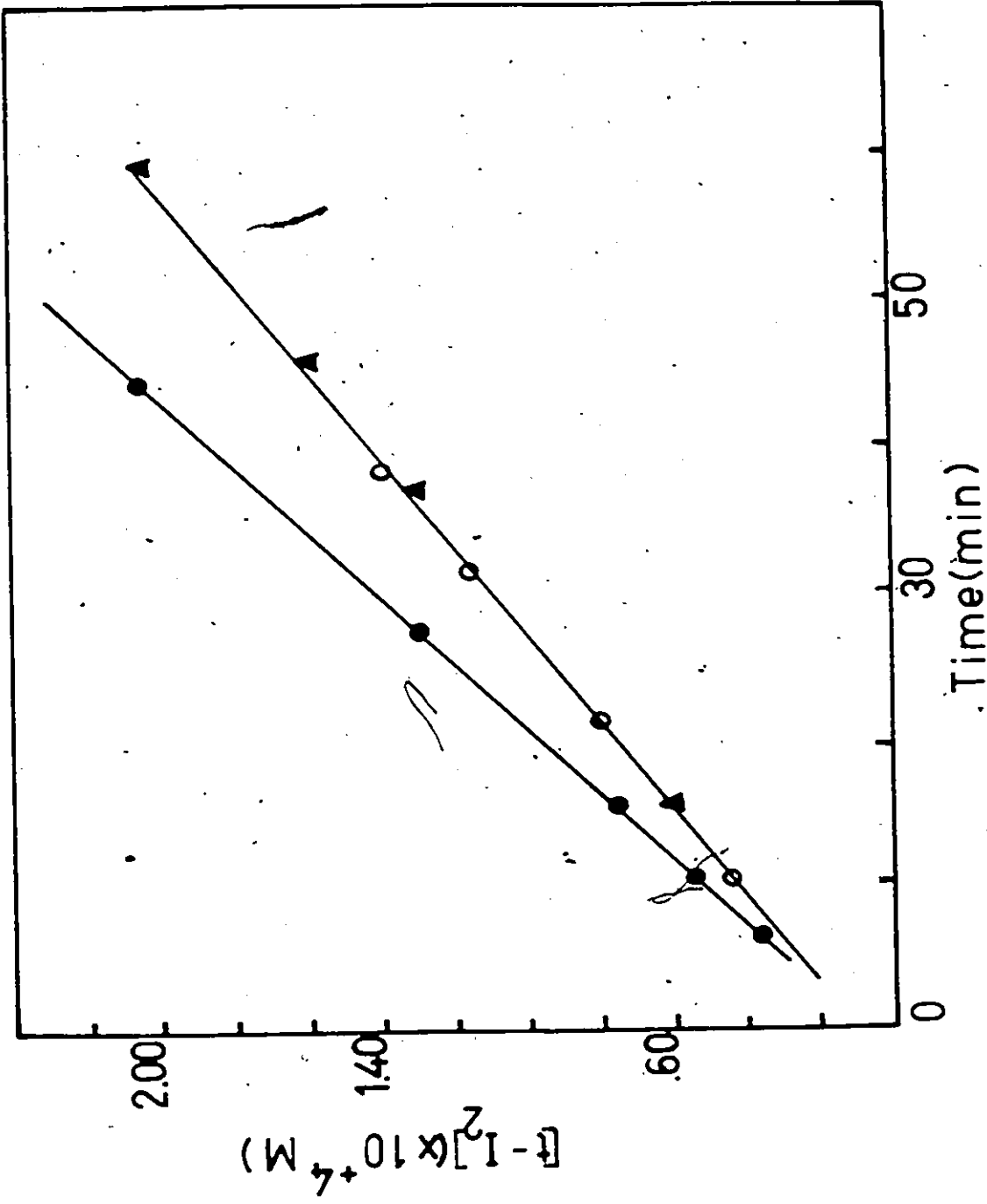


Table 6

Quantum Yields of Rh(III)-Amines as a Function of pH at 254 nm

| Complex                                                  | pH   | $\phi$ (amine) | $\phi$ ( $X^-$ ) |
|----------------------------------------------------------|------|----------------|------------------|
| $\text{Rh}(\text{NH}_3)_5\text{Cl}^{2+}$                 | 3.0  | —              | 0.11±0.01        |
|                                                          | 4.0  | —              | 0.23±0.03        |
|                                                          | 5.75 | —              | 0.23±0.03        |
| $\text{Rh}(\text{NMe}_3)_5\text{Cl}^{2+}$                | 3.0  | 0.030±0.002    | 0.085±0.005      |
|                                                          | 5.0  | 0.010±0.002    | 0.090±0.005      |
| $\text{Rh}(\text{NH}_3)_5\text{I}^{2+}$                  | 3.0  | 0.43±0.04      | —                |
|                                                          | 5.5  | 0.33±0.04      | —                |
|                                                          | 6.9  | 0.33±0.04      | —                |
|                                                          | 8.7  | 0.33±0.04      | —                |
| <u>trans</u> - $[\text{Rh}(\text{NH}_3)_4\text{Cl}_2]^+$ | 3.0  | —              | 0.11±0.02        |
|                                                          | 4.2  | —              | 0.23±0.03        |

ond CT band in the dibromo molecule and principally the second CT band with possible excitation into the third CT band in the diiodo complex.

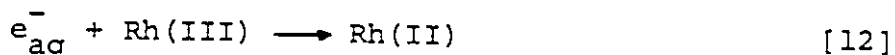
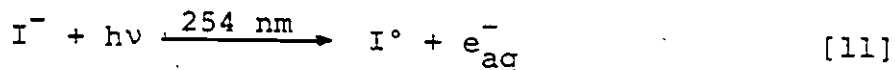
As with their Rh(III) analogs, the photoproduct in each case was the halide ion with complete isomeric retention as indicated by the spectral analyses of the photolysed solutions. Table 7 presents the quantum yields from the respective complexes.

#### 4. Photolysis of Iodide Solutions Containing

##### Rh(III)-Amine Complexes

##### 4.1. Photolysis of Aqueous Iodide Solutions

Initiation of a redox substitution reaction involving selected Rh(III)-amine complexes was achieved by employing the simple technique of photolysing aqueous iodide solutions in the presence of nonabsorbing concentrations of complex.



The criteria imposed on the solution composition were dictated by the following considerations: (a) essentially all the incident radiation should be absorbed by the iodide (in effect, 90% or greater), (b) the concentration



Table 7

Quantum Yields from the Photolysis of trans-[Ir(en)<sub>2</sub>X<sub>2</sub>]<sup>+</sup>

| Complex                                                           | Absorption Band | $\lambda_{nm}$ | $\phi(X^-)$ |
|-------------------------------------------------------------------|-----------------|----------------|-------------|
| <u>trans</u> -[Ir(en) <sub>2</sub> Cl <sub>2</sub> ] <sup>+</sup> | CTTM            | 254            | 0.080±0.005 |
|                                                                   | LF              | 345            | 0.070±0.005 |
| <u>trans</u> -[Ir(en) <sub>2</sub> Br <sub>2</sub> ] <sup>+</sup> | CTTM            | 254            | 0.070±0.005 |
|                                                                   | LF              | 364            | 0.040±0.005 |
| <u>trans</u> -[Ir(en) <sub>2</sub> I <sub>2</sub> ] <sup>+</sup>  | CTTM            | 254            | 0.65±0.02   |
|                                                                   | LF              | 398            | 0.22±0.02   |

of the complex must be such that essentially all of the photoelectrons generated in the primary act are scavenged by the complex, and (c) that there is sufficient complex to ensure linearity in yields (i.e., avoid rapid solute depletion).

In order to ascertain optimum conditions, various  $I^-$  to complex concentration ratios were tested. The optimum condition found was a  $I^-$  : complex ratio of 10:1 with  $[I^-]$  approximately  $10^{-2}$  M.

#### 4.2. Solutions Containing $[Rh(en)_2Cl_2]^+$ Complexes

##### 4.2.1. Aerated Conditions

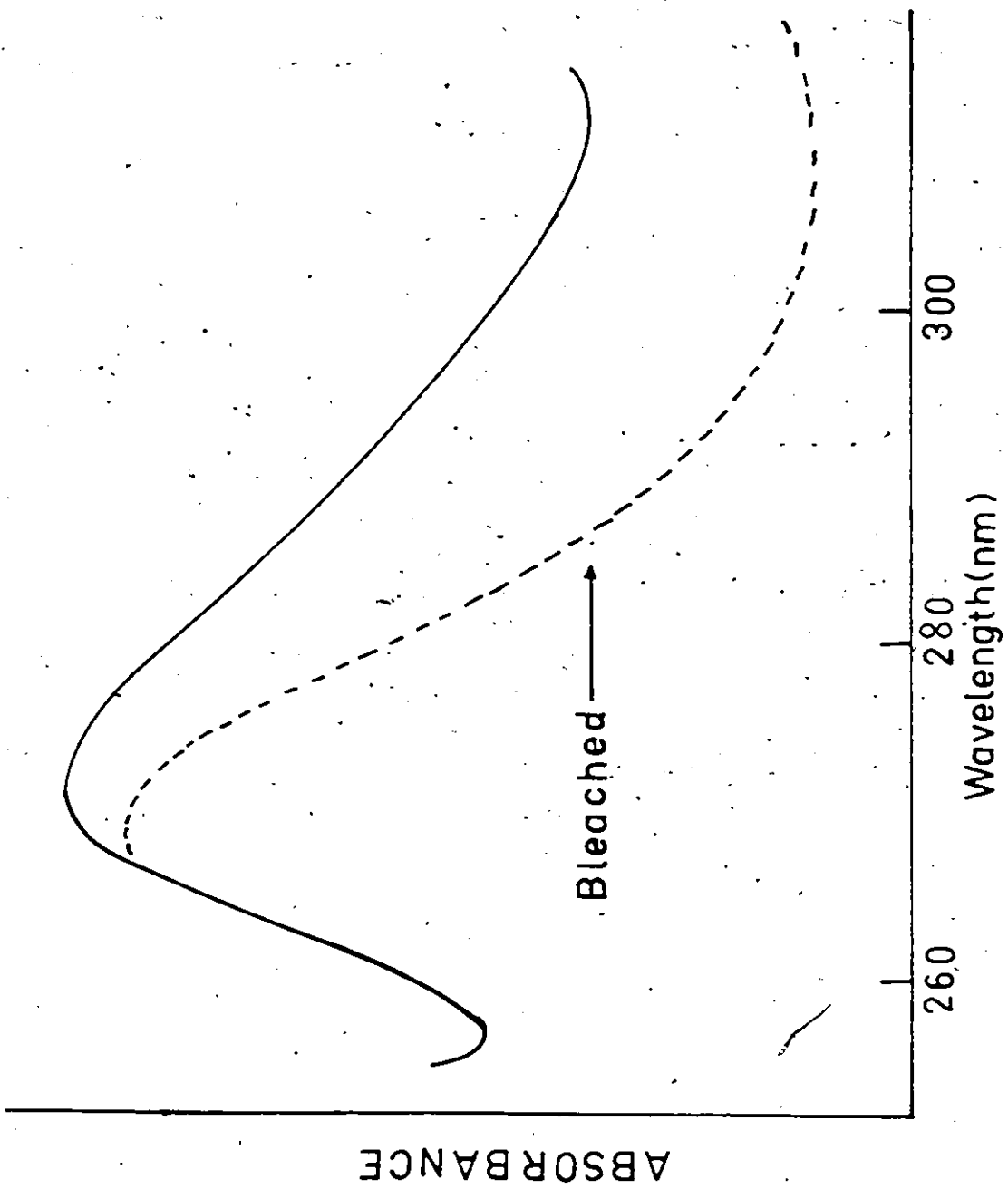
Photolysis products were monitored by differential spectrophotometry. A broad asymmetric band with a maximum at 285 nm was found to be common for all photolytic solutions. Since triiodide formation was suspected, known amounts of sodium thiosulfate were added to the irradiated samples and the spectrum recorded. The original product band was observed to change into a new band with a maximum at 270 nm (Figure 12). Of the possible compounds which could conceivably be formed<sup>1</sup>, only the trans-diiodo conforms to the spectral wavelength observed. Thus, the species

<sup>1</sup>The possibility of the band being due to trans- $[Rh(en)_2-ClI]^+$  absorption was discarded since the band maximum for this complex in that region occurs at 304 nm.

Figure 12

Figure 12. Electronic Spectrum of the Product from  
the Photolysis of Aqueous Iodide Solutions  
of trans-[Rh(en)<sub>2</sub>Cl<sub>2</sub>]<sup>+</sup> at 254 nm (aerated  
conditions).

4



giving rise to the permanent band at 270 nm was unambiguously assigned to trans-[Rh(en)<sub>2</sub>I<sub>2</sub>]<sup>+</sup> when either trans-[Rh(en)<sub>2</sub>Cl<sub>2</sub>]<sup>+</sup> or cis-[Rh(en)<sub>2</sub>Cl<sub>2</sub>]<sup>+</sup> was the complex. In addition, I<sub>3</sub><sup>-</sup> was recognized as the product inducing the asymmetry in the original photolyte spectrum. The results are summarized in Table 8.

#### 4.2.2. Deaerated Conditions

Deaeration of the solutions was achieved by vigorous purging for a minimum of 20 minutes with helium gas immediately prior to irradiation. As described directly above, for both the cis and trans complexes, the spectra of the original photolyte solutions showed a broad asymmetric band at 285 nm which shifted to 270 nm upon addition of sodium thiosulfate. Hence, the identical products were formed under the two conditions. The results are reported in Table 8.

#### 4.3. Solutions Containing [Rh(cyclam)Cl<sub>2</sub>]<sup>+</sup> Complexes

##### 4.3.1. Aerated Conditions

Addition of sodium thiosulfate to irradiated solutions containing either cis- or trans-[Rh(cyclam)Cl<sub>2</sub>]<sup>+</sup> resulted in a complete bleaching of the band at 285 nm (Figure 13). The pH of each system was measured before and after irradiation. Typical pH changes were as follows with inclusion of the bisethylenediamine complexes: trans-[Rh(en)<sub>2</sub>Cl<sub>2</sub>]<sup>+</sup>

Figure 13

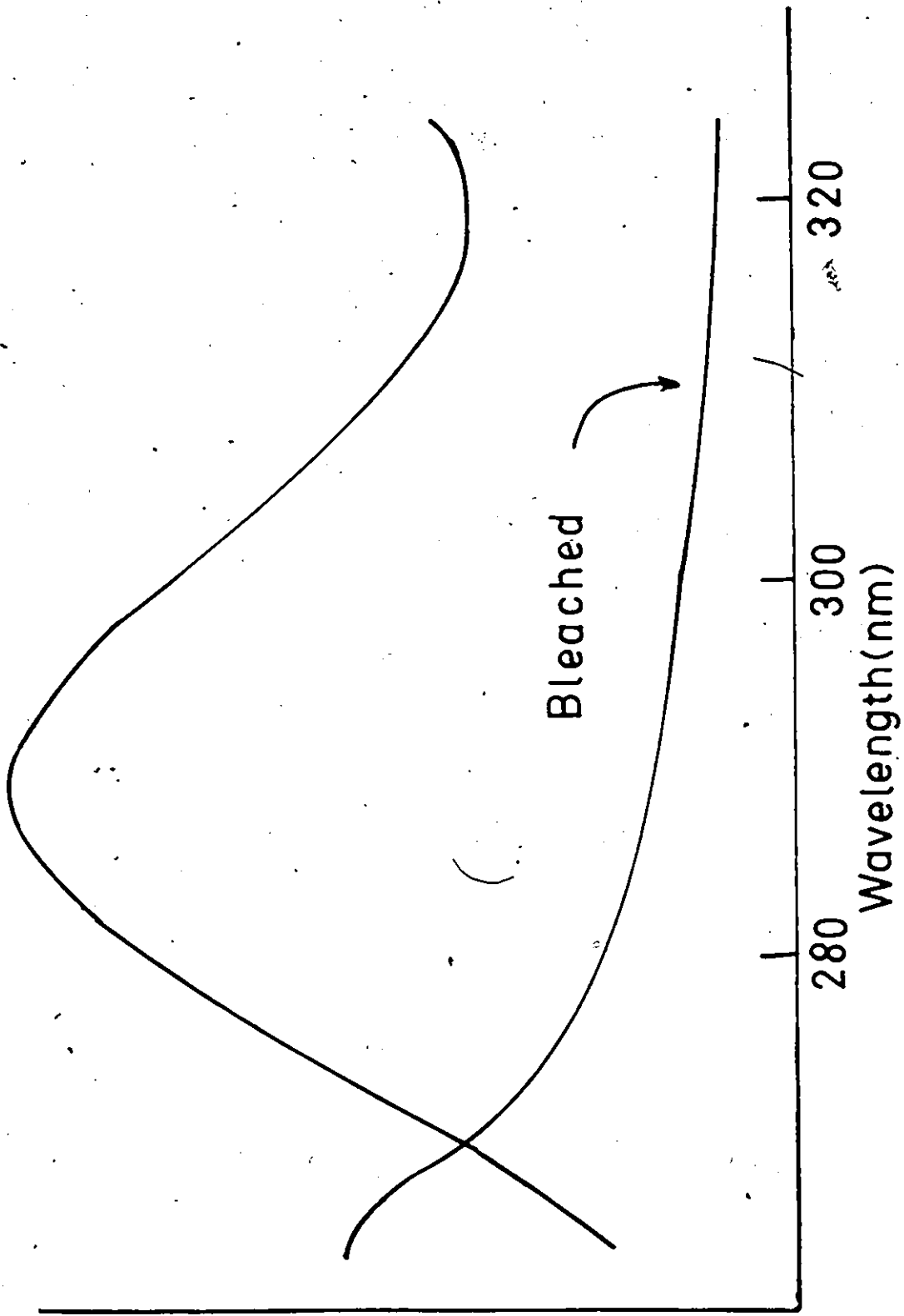
Figure 13. Electronic Spectrum of the Product from  
the Photolysis of Aqueous Iodide Solutions  
of cis-[Rh(cyclam)Cl<sub>2</sub>]<sup>+</sup> at 254 nm (aerated  
conditions).

20



5

ABSORBANCE



(4.40 → 4.60), cis-[Rh(en)<sub>2</sub>Cl<sub>2</sub>]<sup>+</sup> (4.15 → 4.35), cis-[Rh(cyclam)Cl<sub>2</sub>]<sup>+</sup> (4.90 → 5.90), and trans-[Rh(cyclam)Cl<sub>2</sub>]<sup>+</sup> (5.30 → 5.80). The trend of pH changes for the former are consistent with a simple halide exchange, whereas the notable increase in pH observed for the cyclam complexes indicates a substantial liberation of base. The only possible source of base would be the cyclam ligand system. To identify the free base, 10 cm<sup>3</sup> of a 50-50 mixture of ethanol and diethyl ether containing 10% NaHCO<sub>3</sub> was added to the photolyte solution. The organic layer was extracted and evaporated to dryness whereby a white precipitate was formed. This procedure was not found to liberate cyclam from an unirradiated solution. NMR and mass spectral analyses identified this precipitate as cyclam.

The absence of spectrophotometric evidence for any iodo-rhodium(III) complex indicated that the product rhodium species was one of the conjugate base forms of hexa-aquo-Rh(III). Due to the onset of thiosulfate absorption at approximately 250 nm, detection of this species was not possible but can be reasonably inferred.

Cyclam product yields were calculated by measuring hydrogen ion uptake by the free base. To calculate cyclam yields, solutions prior to irradiation were acidified with HCl to a pH of 3.0. Measurement of the hydrogen ion up-

Table 8

Quantum Yields from the Photolysis of Aqueous Iodide  
Solutions Containing Rh(III)-Amine Complexes

| Complex                                                           | Principal Product(s)<br>Formed                                   | $\phi$ (product)                                 |
|-------------------------------------------------------------------|------------------------------------------------------------------|--------------------------------------------------|
| <u>trans</u> -[Rh(en) <sub>2</sub> Cl <sub>2</sub> ] <sup>+</sup> | <u>trans</u> -[Rh(en) <sub>2</sub> I <sub>2</sub> ] <sup>+</sup> | 0.25±0.02 <sup>a</sup><br>0.22±0.02 <sup>b</sup> |
| <u>cis</u> -[Rh(en) <sub>2</sub> Cl <sub>2</sub> ] <sup>+</sup>   | <u>trans</u> -[Rh(en) <sub>2</sub> I <sub>2</sub> ] <sup>+</sup> | 0.25±0.02 <sup>a</sup><br>0.22±0.02 <sup>b</sup> |
| <u>cis</u> -[Rh(cyclam)Cl <sub>2</sub> ] <sup>+</sup>             | Rh(H <sub>2</sub> O) <sub>5</sub> (OH) <sup>2+</sup><br>cyclam   | —<br>0.22±0.02 <sup>b</sup>                      |
| <u>trans</u> -[Rh(cyclam)Cl <sub>2</sub> ] <sup>+</sup>           | Rh(H <sub>2</sub> O) <sub>5</sub> (OH) <sup>2+</sup><br>cyclam   | —<br>0.22±0.02 <sup>b</sup>                      |
| <u>trans</u> -[Rh(cyclam)I <sub>2</sub> ] <sup>+</sup>            | Rh(H <sub>2</sub> O) <sub>5</sub> (OH) <sup>2+</sup><br>cyclam   | —<br>0.22±0.02 <sup>b</sup>                      |
| <u>cis</u> -[Rh(cyclam)I <sub>2</sub> ] <sup>+</sup>              | Rh(H <sub>2</sub> O) <sub>5</sub> (OH) <sup>2+</sup><br>cyclam   | —<br>0.22±0.02                                   |

<sup>a</sup>Aerated conditions.

<sup>b</sup>Deaerated conditions.

take proved to be a sensitive and reproducible analytical technique. It should be noted that it was first necessary to determine the number of nitrogens of cyclam that would be protonated in this pH range. This was accomplished by adding known amounts of free cyclam to a solution<sup>1</sup> of  $10^{-3}$  M HCl and measuring the ratio of hydrogen ion uptake concentration to the concentration of added cyclam. This ratio was found to be 3:1. The quantitative results for the iodide photolyses are reported in Table 8.

#### 4.3.2. Deaerated Conditions

Deaeration of sample solutions was accomplished by the same procedure described in Section 4.2.2. Under these conditions, analogous results were obtained as those directly above. Cyclam product yields were quantitatively measured and are shown in Table 8.

#### 4.4. Solutions Containing $[\text{Rh}(\text{cyclam})\text{I}_2]^+$ Complexes

Irradiations of respective solutions of cis- $[\text{Rh}(\text{cyclam})\text{I}_2]^+$  and trans- $[\text{Rh}(\text{cyclam})\text{I}_2]^+$  with absorbing concentrations of  $\text{I}^-$  gave product solutions containing free cyclam with quantum yields identical to those reported for the dichloro complexes in Table 8. This experiment was significant in that it demonstrated that the electron was

<sup>1</sup>These blanks contained 10%  $\text{CH}_3\text{CN}$  so as to be equivalent to the photolytic medium.

indeed reacting with the rhodium(III)-amine complex.

#### 4.5. Solutions Containing $\text{Rh}(\text{NR}_3)_5\text{I}^{2+}$

In a similar study involving iodide photolysis with nonabsorbing concentrations of  $\text{Rh}(\text{NH}_3)_5(\text{H}_2\text{O})^{3+}$ , Endicott and Kelly reported that their yields were pH independent (13). Their results seemed anomalous in view of the apparent lack of pH dependence with the complexes studied in this work.

Since  $\text{Rh}(\text{NH}_3)_5\text{I}^{2+}$  is obviously a Brönsted acid and its particular initial state will be pH dependent, the analogous compound  $\text{Rh}(\text{NMe}_3)_5\text{I}^{2+}$  which is a non-Brönsted acid was also studied.

The pH range employed was 2-5 where  $\text{HClO}_4$  was used. All samples were deaerated prior to irradiation in accordance with the procedure outlined in Section 4.2.2. As described earlier, differential spectrophotometry was used to monitor product formation and any  $\text{I}_3^-$  formed was destroyed by the addition of  $\text{Na}_2\text{S}_2\text{O}_3$ . In all cases, a product band appeared at 270 nm thereby signifying the formation of trans- $[\text{Rh}(\text{NH}_3)_4\text{I}_2]^+$ . The results are summarized in Table 9. From this table it can be seen that no change in the quantum yield was found for both complexes in the pH range employed.

Table 9

Quantum Yields from the Photolysis of Aqueous Iodide  
Solutions Containing Rh(III)-Amine Complexes

| Complex                                  | pH  | $\phi(\text{trans-I}_2)$ |
|------------------------------------------|-----|--------------------------|
| $\text{Rh}(\text{NH}_3)_5\text{I}^{2+}$  | 2.0 | 0.23±0.02                |
|                                          | 3.0 | 0.23±0.02                |
|                                          | 4.8 | 0.23±0.02                |
| $\text{Rh}(\text{NMe}_3)_5\text{I}^{2+}$ | 2.0 | 0.23±0.02                |
|                                          | 3.0 | 0.23±0.02                |
|                                          | 5.0 | 0.23±0.02                |

#### 4.6. Solutions Containing Nonabsorbing Concentrations of Iodide in the Presence of Rh(III)-Amines

To ensure that the reactions with iodide were a direct consequence of the electron produced from iodide photolysis reacting with the rhodium(III)-amine complex, trans-[Rh(en)<sub>2</sub>Cl<sub>2</sub>]<sup>+</sup> was irradiated in the presence of non-absorbing amounts of I<sup>-</sup>. The absence of the characteristic 270 nm band of trans-[Rh(en)<sub>2</sub>I<sub>2</sub>]<sup>+</sup> in the spectrum of the irradiated sample established that disubstitution had not occurred.

#### 5. Temperature Dependence Studies

The effect of temperature on the photochemical processes was investigated using the molecules cis-[Rh(cyclam)-X<sub>2</sub>]<sup>+</sup> (X = Cl, Br) and trans-[Rh(cyclam)Br<sub>2</sub>]<sup>+</sup>. These complexes were chosen because of their greater thermal stability over their ethylenediamine and simple amine analogs.

Cis-[Rh(cyclam)Cl<sub>2</sub>]<sup>+</sup> was irradiated in both the CT (254 nm) and LF (400 nm) manifolds. For cis-[Rh(cyclam)-Br<sub>2</sub>]<sup>+</sup>, irradiations were conducted at 254 nm(CT) while for studies of trans-[Rh(cyclam)Br<sub>2</sub>]<sup>+</sup>, the first LF band (400 nm) was employed.

Immediately after photolysis, the sample was cooled in an ice bath to quench the potential thermal reactions.

Concurrent blank runs were made at each temperature in order to make corrections for the thermal dark reactions. Typical thermal blanks were of the order  $5.0 \times 10^{-6}$  M. Table 10 presents the quantum yields for each complex at the various temperatures.

#### 6. Solvent Dependence Studies

The photochemistry of selected Rh(III)- and Ir(III)-amines was studied in various mixture compositions of glycerol and water. To ensure that there were no significant shifts in the band maxima and intensities in the electronic spectra of the complexes utilized, absorption spectra of the complexes were run in the various mixed-solvent systems. These spectra were compared with the corresponding spectra in aqueous media. No differences were observed even in the CT region which is often solvent sensitive.

The identical excitation wavelengths chosen for standard condition photolyses were used. Kirk and Wong (53) have recently suggested that spectrophotometric measurements of the photohydrolysis product can often lead to erroneous interpretation of solvent viscosity effects. The analytical techniques previously described were employed to measure products. However, it was necessary to recalibrate the specific ion electrodes due to the introduction



Table 10

Quantum Yields for the Photoaquation of Various  
Rhodium (III)-Amines as a Function of Temperature

| Complex                                                 | $\lambda$ nm | Temp.°C | $\phi$ ( $X^{-}$ ) |
|---------------------------------------------------------|--------------|---------|--------------------|
| <u>cis</u> -[Rh(cyclam)Cl <sub>2</sub> ] <sup>+</sup>   | 254          | 24      | 0.45±0.02          |
|                                                         |              | 35      | 0.55±0.02          |
|                                                         |              | 38      | 0.61±0.02          |
|                                                         |              | 56      | 0.89±0.02          |
|                                                         | 400          | 36      | 0.36±0.02          |
|                                                         |              | 48      | 0.77±0.02          |
|                                                         |              | 62      | 0.95±0.02          |
| <u>cis</u> [Rh(cyclam)Br <sub>2</sub> ] <sup>+</sup>    | 254          | 26      | 0.22±0.02          |
|                                                         |              | 38      | 0.31±0.02          |
|                                                         |              | 44      | 0.39±0.02          |
|                                                         |              | 55      | 0.53±0.02          |
| <u>trans</u> -[Rh(cyclam)Br <sub>2</sub> ] <sup>+</sup> | 400          | 26      | 0.023±0.002        |
|                                                         |              | 35      | 0.031±0.002        |
|                                                         |              | 62      | 0.071±0.002        |

of glycerol into the systems.

The product yields were based on direct measurement of halide ion or amine release. Thus, the problems described by Kirk and Wong (53) are avoided and the effects observed can be considered to be real. The quantum yields of product as a function of the solvent system are presented in Tables 11 and 11A.  $\phi(\text{product})^{\circ}$  corresponds to quantum yields from aqueous media whereas  $\phi(\text{product})^{\text{S}}$  represents the quantum yields from the mixed-solvent systems.

Table II

Quantum Yields of Rh(III)- and Ir(III)-Amines as a Function of Medium

| Complex                                            | Wt %<br>glycerol | $\lambda_{\text{nm}}$ | $\phi(X^-)^{\circ}$ | $\phi(X^-)^{\text{S}}$ | $\phi(\text{amine})^{\circ}$ | $\phi(\text{amine})^{\text{S}}$ | $\phi(X^-)^{\circ} / \phi(X^-)^{\text{S}}$ | $\phi(\text{amine})^{\circ} / \phi(\text{amine})^{\text{S}}$ |
|----------------------------------------------------|------------------|-----------------------|---------------------|------------------------|------------------------------|---------------------------------|--------------------------------------------|--------------------------------------------------------------|
| Rh(NH <sub>3</sub> ) <sub>5</sub> Cl <sup>2+</sup> | 63               | 254                   | 0.11                | 0.11                   | —                            | —                               | 1.00                                       | —                                                            |
|                                                    | 63               | 254                   | 0.085               | 0.085                  | 0.03                         | 0.03                            | 1.00                                       | 1.00                                                         |
| Rh(NH <sub>3</sub> ) <sub>5</sub> Br <sup>2+</sup> | 63               | 254                   | 0.019               | 0.032                  | 0.027                        | 0.03                            | 1.63                                       | 1.00                                                         |
|                                                    | 63               | 360                   | 0.015               | 0.02                   | 0.14                         | 0.10                            | 1.33                                       | 0.71                                                         |
| Rh(NH <sub>3</sub> ) <sub>5</sub> I <sup>2+</sup>  | 25               | 254                   | —                   | —                      | 0.43                         | 0.43                            | —                                          | 1.00                                                         |
|                                                    | 63               | 254                   | —                   | —                      | 0.43                         | 0.43                            | —                                          | 1.00                                                         |
|                                                    | 25               | 420                   | —                   | —                      | 0.87                         | 0.62                            | —                                          | 0.71                                                         |
|                                                    | 63               | 420                   | —                   | —                      | 0.87                         | 0.55                            | —                                          | 0.63                                                         |
| Rh(NH <sub>3</sub> ) <sub>5</sub> I <sup>2+</sup>  | 25               | 254                   | —                   | —                      | 0.55                         | 0.47                            | —                                          | 0.85                                                         |
|                                                    | 63               | 254                   | —                   | —                      | 0.55                         | 0.34                            | —                                          | 0.62                                                         |

Table 11A

Quantum Yields of Rh(III)- and Ir(III)-Amines as a Function of Medium

| Complex                                                           | Wt. %<br>glycerol | $\lambda_{\text{nm}}$ | $\phi(X^-)^e$ | $\phi(X^-)^S$ | $\phi(\text{amine})^o$ | $\phi(\text{amine})^S$ | $\phi(X^-)^S/\phi(X^-)^o \cdot \phi(\text{amine})^S/\phi(\text{amine})^o$ |
|-------------------------------------------------------------------|-------------------|-----------------------|---------------|---------------|------------------------|------------------------|---------------------------------------------------------------------------|
| <u>cis</u> -[Rh(cyclam)Cl <sub>2</sub> ] <sup>+</sup>             | 36                | 254                   | 0.47          | 0.47          | —                      | —                      | 1.00                                                                      |
|                                                                   | 47                | 254                   | 0.47          | 0.41          | —                      | —                      | 0.87                                                                      |
|                                                                   | 57                | 254                   | 0.47          | 0.33          | —                      | —                      | 0.70                                                                      |
|                                                                   | 67                | 254                   | 0.47          | 0.21          | —                      | —                      | 0.45                                                                      |
|                                                                   | 76                | 254                   | 0.47          | 0.12          | —                      | —                      | 0.25                                                                      |
| <u>trans</u> -[Rh(cyclam)Cl <sub>2</sub> ] <sup>+</sup>           | 57                | 254                   | 0.035         | 0.077         | —                      | —                      | 2.20                                                                      |
| <u>trans</u> -[Ir(en) <sub>2</sub> Cl <sub>2</sub> ] <sup>+</sup> | 63                | 254                   | 0.08          | 0.10          | —                      | —                      | 1.00                                                                      |
| <u>trans</u> -[Ir(en) <sub>2</sub> I <sub>2</sub> ] <sup>+</sup>  | 25                | 254                   | 0.65          | 0.033         | —                      | —                      | 0.05                                                                      |
|                                                                   | 63                | 254                   | 0.65          | 0.0031        | —                      | —                      | 0.0046                                                                    |
|                                                                   | 25                | 398                   | 0.22          | 0.036         | —                      | —                      | 0.16                                                                      |
|                                                                   | 63                | 398                   | 0.22          | 0.038         | —                      | —                      | 0.17                                                                      |

## IV. DISCUSSION

### 1. General

The first section of this chapter will involve a discussion of the electronic properties influencing the photochemistry of the complexes studied in this thesis. The subsequent sections will be concerned with the results obtained from the mechanistic studies. A discussion of these systems will constitute the substance of the remainder of this chapter.

### 2. Photochemistry of Rh(III)-Amines Under Standard Conditions

Examination of Tables 2-5 reveal that, without exception, the axis of labilization is always the weak field axis and is in accordance with Adamson's first rule. Thus, it would seem that as the number of systems studied accumulates, this rule is approaching the proportions of a "Law".

The major challenge to any interpretative model lies in the study of mixed-ligand complexes. Assuming Adamson's first rule is obeyed, in prospect, there exist several possibilities for the pathway of photolabilization. First of all, exclusive labilization can occur whereby only one ligand on the unique axis is aquated and thus the reaction can be termed as photospecific. This seems to be the case

for the majority of systems studied. However, the complexes  $\text{Rh}(\text{NH}_3)_5\text{Br}^{2+}$  and  $\text{trans-}[\text{Rh}(\text{en})_2\text{ClI}]^+$ , for example, deny this as a true characteristic of the photochemistry of Rh(III)-amines. In the case where dual labilization is found, there exists the possibility of two excited states as proposed by Endicott (16). The primary criticism of this postulate is the identity of these states. From ligand field theory, the only state in this environment is the  $^3\text{E}$ . The nearest other states,  $^3\text{A}_2$  or  $^3\text{B}_2$ , do not provide an adequate explanation for the minor and major labilizations. The only possibility would be a splitting of the E state into two states such that each state would have unique ligand labilizing characteristics. However, the E state is not split by the presence of nonequivalent ligands along the z axis. Therefore, it is difficult to visualize just what these two states could be. The possibility that the primary photoactive state is the  $^3\text{E}$  and the so-called second state is an unidentified  $^3\text{CT}$  or  $^5\text{E}$ , cannot be immediately discounted; however, these possibilities seem rather unlikely since the same phenomenon of dual labilization also occurs in the CT region. Thus, it seems reasonable to seek an element common to both LF and CT excited states which would provide a basis for the observed dual labilization. Such a common element is immediately recognized in the MO treat-

ment because both  $CT^*$  and  $LF^*$  use the  $a_{1g}$  (MO). Hence this recommends Zink's treatment as a *modus operandi* for interpretative analysis whereby the distribution or partition of energy within a single excited state is responsible for the aquation of both ligands on the unique axis.

The application of Zink's model to systems such as  $Rh(NH_3)_5X^{2+}$  would predict the following: (a) the total labilization (represented by the sum of the quantum yields of aquation for ligands on the z axis) will decrease as the ligand field strength of the unique axis approaches that of the other axes (i.e., as  $Dt$  decreases) and (b) the quantum yield of aquation of the ammine will decrease and that of  $X^-$  will increase as the energy of the donor orbital of  $X^-$  decreases and approaches that of the ammine. Reference to Table 2 shows the total quantum yield of aquation to decrease in the order  $Rh(NH_3)_5I^{2+} > Rh(NH_3)_5Br^{2+} > Rh(NH_3)_5Cl^{2+}$  as predicted on the basis of the decreasing values of  $Dt$  which have been estimated by Zink (35b) to be  $789\text{ cm}^{-1}$ ,  $560\text{ cm}^{-1}$ , and  $457\text{ cm}^{-1}$  respectively. Prediction (b) is also fulfilled since the energies of the halide donor orbitals approach that of the ammine in the order  $I^- > Br^- > Cl^-$  (34a). By simply examining the products formed in this series, it is evident that the degree of antibonding of the Rh-N bond changes considerably for  $X = Cl$  to  $X = I$ . Thus,

it seems logical to presuppose that there would be a median effect for  $X = \text{Br}$  whereby the Rh-N bond would predominate in antibonding character but the Rh-Br bond would also possess a sufficient degree of antibonding to effect labilization of this ligand as a minor component. This is found to be the case for  $\text{Rh}(\text{NH}_3)_5\text{Br}^{2+}$  where  $\phi(\text{NH}_3) \gg \phi(\text{Br}^-)$ . Since the electronic spectra of  $\text{Rh}(\text{NMe}_3)_5\text{X}^{2+}$  are very similar to those of  $\text{Rh}(\text{NH}_3)_5\text{X}^{2+}$  (Table 1), it is anticipated and found, that the two series exhibit parallel photochemical trends. The dual labilization found from  $\text{Rh}(\text{NMe}_3)_5\text{Cl}^{2+}$  suggests that the energy difference of the  $\text{Cl}^-$  and  $\text{NMe}_3$  donor orbitals is greater than that of the corresponding  $\text{Cl}^-$  and  $\text{NH}_3$ . The small yield of  $\text{NMe}_3$  (0.03) found would indicate that the ligand field strength of  $\text{NMe}_3$  is not considerably greater than that for  $\text{NH}_3$  and would, in turn, explain the lack of band maxima shifts in the electronic spectra of the two series. Following from the above, in comparison to  $\text{Rh}(\text{NH}_3)_5\text{Br}^{2+}$ , it would be predicted that for  $\text{Rh}(\text{NMe}_3)_5\text{Br}^{2+}$  the yields of  $\text{Br}^-$  and  $\text{NMe}_3$  should slightly increase. Table 2 confirms this prediction. Figure 14 presents a qualitative MO diagram to illustrate the proposed energy levels for the two series.

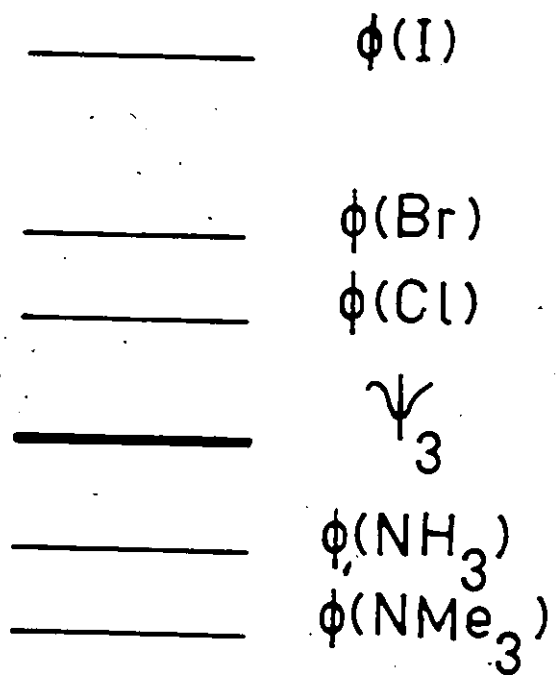
An apparent contradiction to this proposal is evident by comparing the quantum yields of amine for the iodo



Figure 14

D

Figure 14. Relative Energy Level Diagram for Trans  
Ligands of Mixed-Ligand Rh(III)- Amine  
Complexes.



complexes. Instead of the yield for  $\text{Rh}(\text{NMe}_3)_5\text{I}^{2+}$  increasing from irradiation in the LF region, it is found to decrease. An explanation for this may be suggested by the electronic absorption data in Table 1. From a comparison of the extinction coefficients, it appears that methylating the  $\text{Rh}(\text{NH}_3)_5\text{Cl}^{2+}$  complex produces further distortion from octahedral microsymmetry (i.e., larger extinction coefficients for  $\text{Rh}(\text{NMe}_3)_5\text{Cl}^{2+}$ ) while the methylated iodo complex more closely approaches  $O_h$  symmetry as evidenced by the smaller extinction coefficients. Methylation of the bromo complex does not produce any significant changes in the symmetry of the molecule. The only plausible means by which the iodo complex could achieve a higher symmetry would be steric compression caused by the bulkier methyl groups. A molecule which is sterically compressed would be expected to have a lower yield of product (lb) than a more distorted complex as in  $\text{Rh}(\text{NH}_3)_5\text{I}^{2+}$ . Thus, although the model is still operative for  $\text{Rh}(\text{NMe}_3)_5\text{I}^{2+}$ , a true indication must also consider the steric factors introduced by methylation.

The electronic spectra of the mixed-dihalo complexes (i.e. trans- $[\text{Rh}(\text{A}_4)\text{XY}]^+$ ) are very similar to the halopentaamines and thus, one would expect, following Zink's model, their photochemistries to be similar. Also, these

complexes provide a variation since both ligands on the unique axis are charged. For the chloriodo and bromiodo complexes, the model is upheld whereby chloride and bromide respectively, are the aquated ligands (Table 4). In addition, quantitative agreement is found for  $A = en^1$  since the yield of the principal aquated ligand is the approximate average of the quantum yields of the two parent dihalo complexes (Table 3). On the other hand, the cyclam complexes appear to be anomalous because yields from the mixed-dihalo complexes are larger than those of either parent molecule. However, there is strong suspicion that the structures of the mixed-dihalo complexes are more distorted in the ground state than the parent molecules and thus such a distortion could provide a greater stabilization in the excited state. Consequently, larger yields would be anticipated for these complexes.

Although the quantitative results for trans-[Rh(en)<sub>2</sub>-ClBr]<sup>+</sup> correlate well with the model, the qualitative prediction of Cl<sup>-</sup> as the principal ligand aquated is not observed. Close examination of Table 3 shows the quantum yields for trans-[Rh(A<sub>4</sub>)Cl<sub>2</sub>]<sup>+</sup> and trans-[Rh(A<sub>4</sub>)Br<sub>2</sub>]<sup>+</sup> (A = NH<sub>3</sub>, en) to be the same within experimental error and hence

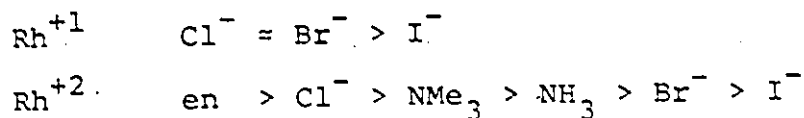
---

<sup>1</sup>Using the value  $\phi(I^-) = 0.86$  for trans-[Rh(en)<sub>2</sub>I<sub>2</sub>]<sup>+</sup> at 254 nm reported in this work.

is not in agreement with Zink's proposal that within a particular series  $[\text{Rh}(\text{A}_4)\text{I}_2]^+ > [\text{Rh}(\text{A}_4)\text{Br}_2]^+ > [\text{Rh}(\text{A}_4)\text{Cl}_2]^+$ . The same experimental yields strongly imply that the energies (VOIP's) of the  $\text{Cl}^-$  and  $\text{Br}^-$  donor orbitals are very similar. This would explain the identical yields for the dihalo complexes and also why  $\text{Br}^-$  is aquated in the chloro-bromo complex since a unique axis possessing two ligands of similar electronegativities and donor orbital energies would be expected to be indiscriminate with respect to labilization.

The trends exhibited by the mixed-ligand complexes reveal some interesting features. It appears that for those complexes with the unique axis containing ligands where the difference in donor orbital energies is large, (e.g. I-Rh- $\text{NH}_3$  or I-Rh-Cl), exclusive aquation occurs whereas if the energies are similar, (e.g. Cl-Rh- $\text{NH}_3$  or Cl-Rh-Br), there is preferential aquation. In addition, the charge on the metal is important for those complexes where preferential aquation occurs. For example, for  $\text{Rh}(\text{NH}_3)_5\text{Cl}^{2+}$ , the metal-ligand overlap population is greater for Rh-Cl and thus  $\text{Cl}^-$  is aquated whereas for trans- $[\text{Rh}(\text{en})_2\text{ClBr}]^+$ , the overlap population is greater for Rh-Br. Likewise, the same phenomenon is found by comparing  $\text{Rh}(\text{NH}_3)_5\text{Br}^{2+}$  and trans- $[\text{Rh}(\text{en})_2\text{ClBr}]^+$ . Based on experimental results such as those

described above, it is possible to construct two series to order the degree of metal-ligand overlap between Rh(III) and various ligands in the excited state.



It is noteworthy that for the  $\text{Rh}^{+2}$  series, the ligands with the least degree of metal-ligand overlap are  $\pi$ -donor ligands and ligands trans to these have the greatest quantum yields in a particular series. Although it is felt that  $\sigma$ -bonding effects on the unique axis in the excited state predominate over  $\pi$  effects, the series does lend support to Zink's proposal (34a) that  $\pi$  effects contribute to the relative quantum yields.

The wavelength dependence exhibited by the halopentamine series is rather peculiar and contrasts with that observed for the trans- $[\text{Rh}(\text{A}_4)\text{X}_2]^+$  series. For the former complexes, the general trend is that the quantum yields decrease with increasing excitation energy. Such a trend is rather strange since intuitively one might be lead to expect that increasing excitation energy would produce a more distorted excited state and hence higher product yields. Critical examination of the electronic spectra of  $\text{Rh}(\text{NMe}_3)_5^- \text{X}^{2+}$  (Figures 6,7,and 8) reveals considerable asymmetry

in the LF bands which is indicative of more than one band. In contrast, the CT bands are symmetrical. This anomaly is also observed in the other mixed-ligand series  $\text{Rh}(\text{NH}_3)_5\text{X}^{2+}$  and trans- $[\text{Rh}(\text{en})_2\text{XY}]^+$  but not in the spectra of the trans- $[\text{Rh}(\text{A}_4)\text{X}_2]^+$  complexes. Without a detailed assignment of the bands in this region of the spectra wavelength dependence trends will remain ambiguous. It is possible that the asymmetry (or apparent splitting) of the first LF band may be due to a low lying  $^3\text{CT}$ . Thus, 'pure' LF excitation would not be achieved unless only the leading edge of the first LF band was irradiated. If this were the case, the larger quantum yields observed from LF irradiations could be a consequence of population of more than one excited state. The most peculiar wavelength dependence is seen for the  $\text{Rh}(\text{NMe}_3)_5\text{Br}^{2+}$  complex where a significant drop in the product yields occur from 360 nm excitation whereas 254 nm and 420 nm irradiations produce the same product yields. Such behavior strengthens the proposal that simultaneous excitation of both CT and LF manifolds persists even into the nominally LF region. A more notable asymmetry is observed in the 420 nm region for  $\text{Rh}(\text{NH}_3)_5\text{I}^{2+}$  than  $\text{Rh}(\text{NMe}_3)_5\text{I}^{2+}$  and is borne out by the greater wavelength dependence for the former. Thus, until the extremely difficult task of elucidating the precise assign-



ments of the bands in the absorption spectra of these complexes is accomplished, it seems conceivable that the origin of the observed wavelength dependence will remain uncertain.

The series trans-[Rh(A<sub>4</sub>)Cl<sub>2</sub>]<sup>+</sup> (A = NH<sub>3</sub>, en, cyclam) (Table 3) whose electronic spectra are very similar shows a notable decrease in  $\phi(\text{Cl}^-)$  for the cyclam complex. As was previously mentioned, this has been attributed by other authors (26,28) as being due to the rigidity of the cyclam belt system which reduces stereomobility in the excited state and consequently decreases the yield of chloride. As was also discussed in the first chapter, distortional effects on the effective symmetry of the cis-[Rh(cyclam)X<sub>2</sub>]<sup>+</sup> complexes leads to an unpredictable photochemistry. Thus, X<sup>-</sup> rather than amine is photoaquated which is opposite to that observed for cis-[Rh(en)<sub>2</sub>Cl<sub>2</sub>]<sup>+</sup>. The cyclam complexes clearly demonstrate the necessity for the inclusion of mechanistic factors such as structural characteristics in a comprehensive model. Similarly, the magnitudes of the yields from the photolysis of Ir(III) complexes are not immediately explicable in terms of a purely electronic model, although as seen from Table 7, the photoreactions of the trans-[Ir(en)<sub>2</sub>X<sub>2</sub>]<sup>+</sup> series follow precisely the trends predicted by their Rh(III) analogs.

Although Zink's model correctly predicts which axis will be labilized from charge transfer excitation (34a), his assumption that the charge transfer mechanism will lead to increased labilization of the ligand which primarily provides the charge is not generally found to be the case for Rh(III) complexes studied in this work. For example, the most easily oxidized ligand in the trans-[Rh(en)<sub>2</sub>ClI]<sup>+</sup> complex is the iodo ligand. However, chloride is the ligand aquated. A reasonable prerequisite to interpreting the photochemistry in the CT region is an elementary distinction between a redox and an ionic substitution mechanism. For this reason, experiments were designed to potentially elucidate whether or not CT excitation led to redox processes in Rh(III) photochemistry.

### 3. Charge Transfer Photochemistry of Rh(III)-Amines

Charge transfer excitation is frequently portrayed in casual terms as an intramolecular redox process. Whereas it is recognized that such a description bears approximately the same relationship to reality as the identification of formal oxidation numbers to actual charge, nonetheless, photoactivation by excitation of charge transfer states does offer a serious possibility of initiation of redox processes. Since a comparison of the yield data in Tables

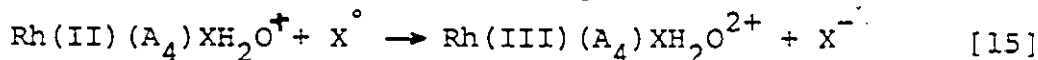
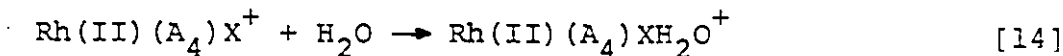
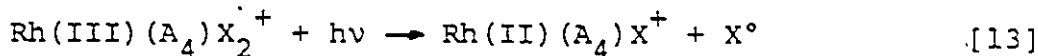
2-5 indicates a recognizable difference in the quantitative aspects resulting from CT and LF excitations, it seemed prudent to at least consider that this difference may reflect contributions of a redox process in the CT photochemistry. The likely prospects of a photoredox process would only seem probable for a charge-transfer-to-solvent (CTTS) (54) or  $\sigma \rightarrow \sigma^*$  transition. The former is equivalent to a solvent-assisted photoionization process whereas the latter constitutes a change of bond order of one and thus would correlate with a homolytic bond fission. The lower energy CT transitions (i.e.  $\pi^n \rightarrow \sigma^*$ ) would correspond to a nominal change of bond order which would cause a general destabilization within the molecule in which specificity must be determined by the distribution of repulsive energies of the excited state.

Rumfeldt and Sellan (28) have conjectured that the more facile reaction coordinate would involve a halide ion rather than a halogen as the leaving group since the former would not only be more sensitive to metal-ligand repulsion but would also experience the advantage of solvent stabilization. Thus, if this were the case, the CT and ligand field mechanisms should be virtually the same. They attributed the higher quantum yields from CT excitation to a higher charge density localized on the metal which would

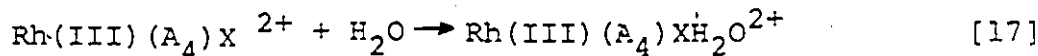
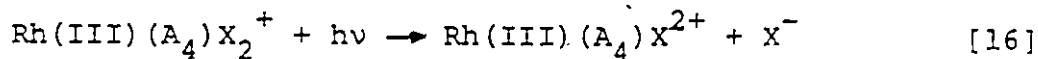
effect a greater metal-ligand repulsion (28).

However, although it seems unlikely that CT transitions initiate redox processes, this possibility cannot be immediately dismissed particularly in view of Endicott's reported observation (13) that u.v. excitation of  $\text{Rh}(\text{NH}_3)_5\text{I}^{2+}$  leads to oxidation of  $\text{I}^-$  and the formation of a transient  $\text{Rh}(\text{NH}_3)_4^{2+}$  species. Flash photolysis of  $\text{Rh}(\text{NH}_3)_5\text{I}^{2+}$  containing relatively nonabsorbing quantities of  $\text{I}^-$  was found to produce  $\text{I}_2^-$  and photodecomposition of the Rh(III) starting material to trans- $[\text{Rh}(\text{NH}_3)_4(\text{H}_2\text{O})\text{I}]^{2+}$ .

The three step mechanism shown below could account for the observed products without inclusion of any net overall oxidation or reduction.



Thus, it is evident that the net effect is precisely the same as a unimolecular ionic process.

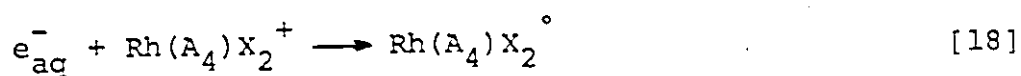


It should be noted that in the former mechanism the key dissociative step involves a neutral atom as opposed to an

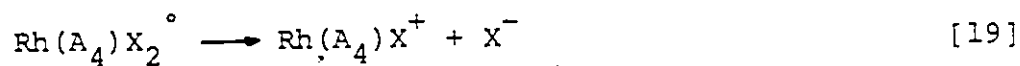
anion as the leaving group which could in all probability provide an easy explanation for the enhanced photosensitivity at shorter wavelengths.

To test the above hypothesis, a genuine redox process was initiated in the Rh(III)-amine systems to characterize any unique features such as product distribution and overall yield sensitivity. Then, by comparison of these results with the systems previously studied by direct photolysis at 254 nm, sensible conclusion with respect to a redox process may become possible.

The redox reaction used for comparison was the reduction of Rh(III) complexes by hydrated electrons generated by the photolysis of iodide (51). The initial step in the reaction sequence would be



The species,  $\text{Rh}(\text{A}_4)\text{X}_2^\circ$ , would be expected to undergo a rapid dissociation



thereby generating an intermediate or transient which would be common to that suggested by reaction [13]. This is depicted in Figure 15 where I is the species produced by the induced redox process, II being the starting species

for direct photolysis, and III being the presumed intermediate common to both mechanisms.

The existence of such a common intermediate was not found as evidenced by the lack of disubstituted products from direct photolysis. Such observations unambiguously indicate that the excited state species and subsequent product mechanistic pathways produced from CT excitation are different from those occurring in the  $I^-$  complex redox system. As a result, the obvious conclusion to be drawn from such studies is that the charge transfer excited state species must lack the essential thermodynamic and kinetic characteristics of a true  $d^7$  configuration.

It would appear that the foremost distinction other than the CT transitions being more intense, is the type of  $d^7$  configuration formed. Figure 16 reveals an essential configurational similarity between  $LF^*$ ,  $CT^*$ , and  $Rh(II)$ . It should be noted that for all configurations, the  $d_{z^2}$  is the acceptor orbital. Thus, a ligand field transition may be described as producing a pseudo  $d^7$  configuration with a hole within the  $d$  configuration, whereas a CT transition such as those seen for complexes in this study (i.e.  $\pi^n \rightarrow \sigma^*$ ) would again be a pseudo  $d^7$  with the hole in the  $\pi$ -nonbonding configuration. Such an analysis would provide an adequate basis for explaining the common element

Figure 15



Figure 15. Reaction Scheme for Direct Photolysis and  
Photolysis of Aqueous Iodide Solutions of  
trans-[Rh(en)<sub>2</sub>Cl<sub>2</sub>]<sup>+</sup> at 254 nm.



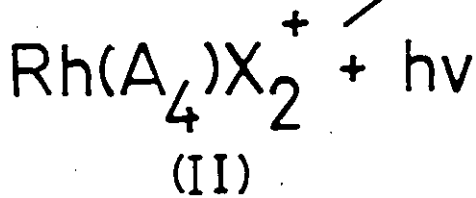
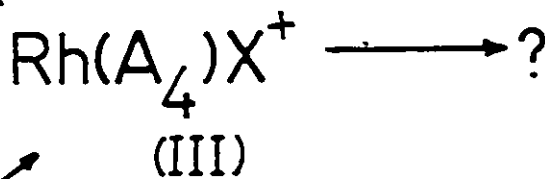
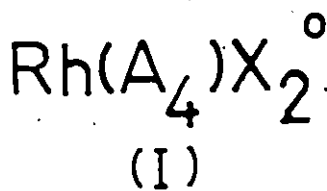
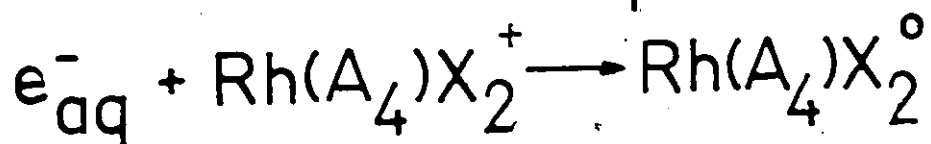
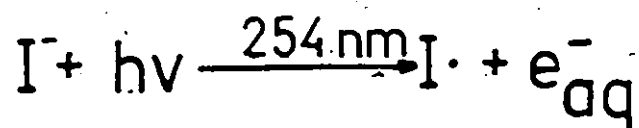
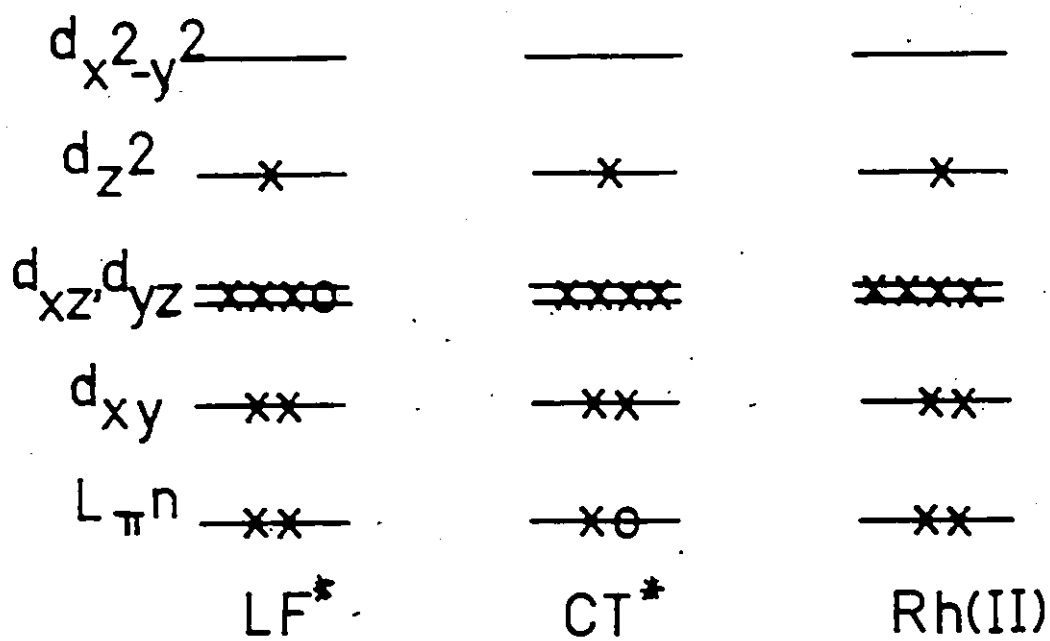


Figure 16

Figure 16. LF\*, CT\*, and Rh(II) d Electron Configurations.



between CT and LF illuminations with the enhanced yields from CT excitation being due to the intrinsically greater repulsive nature anticipated for the CT excited states.

This would seem to suggest the principle that the more closely the excited state resembles a true  $d^7$  configuration, the more substitution labile it becomes.

Although the experiments with the  $I^-$  : complex redox system were negative in the sense that they did not definitively prove the type of mechanism occurring from CT excitation, they did provide considerable insight into the reactivity and structure of the relatively unknown rhodium (II) monomeric species.

Contrasting views pertaining to coordination geometry have been reported in the literature for rhodium(II) intermediates (13,55,56). Kelly and Endicott (13) have suggested that rhodium(II) species are axially labile in two coordination positions analogous to axially distorted  $Co(II)-(N_4)X_2$  species (57) (where  $N_4$  = a cyclic tetraamine, porphyrin, etc.). They proposed that generation of tetraamine rhodium(II) was a necessary criterion for the intermediacy of rhodium(II). However, Basolo et al. (55) have indicated that pentaamminerhodium(II) species and azide radicals were among the products resulting from ultraviolet irradiations of  $Rh(NH_3)_5N_3^{2+}$  thereby inferring that rhodium(II)-

amine complexes behave more like  $\text{Co}(\text{CN})_5^{3-}$  which is five coordinate. Recently, Lilie and coworkers (56) have examined the pulse radiolytic reduction of  $\text{Rh}(\text{NH}_3)_5\text{Cl}^{2+}$ ,  $\text{Rh}(\text{NH}_3)_5(\text{H}_2\text{O})^{3+}$ , and trans- $[\text{Rh}(\text{NH}_3)_4\text{Br}_2]^+$  by the hydrated electron. The rate constant for reaction of the complexes with hydrated electrons was reported to be of the order of  $7 \times 10^{10} \text{ M}^{-1} \text{ sec}^{-1}$ . They found that the first two ligands of the product rhodium(II) complex are eliminated very fast ( $< 1 \mu\text{sec}$ ), and the first intermediate was identified as a highly labile  $\text{Rh}(\text{NH}_3)_4^{2+}$  species.

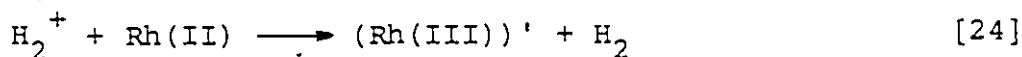
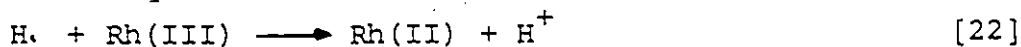
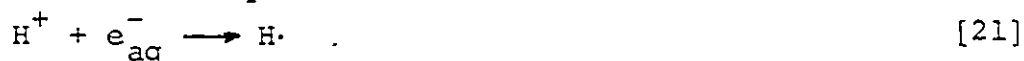
The only geometry which could suscite both cis to trans isomerization and disubstitution in the iodide photolysis with cis- $[\text{Rh}(\text{en})_2\text{Cl}_2]^+$  would be a four coordinate intermediate either of tetrahedral geometry or closely approximating it. It would appear that the only means by which a rhodium(II) species can reduce the high repulsiveness generated by the seventh electron is to rapidly de-coordinate to four and rearrange to a geometry that produces the greatest stabilization (i.e. tetrahedral). The cyclam complexes are a diagnostic test for this whereby the inability of cyclam to distort to the proximity of a tetrahedral geometry results in complete loss of the ligand system.<sup>1</sup>

<sup>1</sup>For cyclam complexes there exists a significant energy barrier for stereochemical change and requires the inversion of two nitrogens (39).

Such phenomena can be correlated to CT\* and LF\* excited states in the sense that they borrow the Rh(II) tendency to reduce repulsion by distortion in which a necessary prerequisite is stereomobility. This would suggest that stereomobility is an essential part of a reaction coordinate. For example, the quantum yields of the trans-[Rh(cyclam)X<sub>2</sub>]<sup>+</sup> complexes are very much less than those of the corresponding bisethylenediamine analogs. Whereas the bisethylenediamine ligands are flexible and can distort, the stereorigid cyclam belt system does not permit mobility. The structure of the cis-[Rh(cyclam)X<sub>2</sub>]<sup>+</sup> complexes in the ground state are in essence distorted and hence product yields are much greater than those from excitation of the trans-[Rh(cyclam)X<sub>2</sub>]<sup>+</sup> series.

The quantitative features of the experimental results showed that in each case the quantum yield of product formation, whether it was the trans-diiodo complex or cyclam liberation, was 0.22 ± 0.02. It is interesting to note that this value corresponds to the value of 0.23 obtained by Dainton (51a) for  $\phi(e_{aq}^-)$  from the photolysis of aqueous solutions of KI containing nitrous oxide. Thus, from these results it is concluded that the scavenging of electrons by the Rh(III) complex occurs with unit efficiency. The studies conducted in acid media confirm this conclusion.

However, these results contrast with those obtained by Kelly and Endicott (13) who found the presence of competitive scavenging between Rh(III) and  $H^+$  for the produced electron in the iodide photolysis of  $Rh(NH_3)_5(H_2O)^{3+}$ . They reported a linear  $\phi_{app}^{-1}$  versus  $[H^+]/[Rh(III)]$  (at constant  $[H^+]$ ) plot from which they calculated a primary yield corresponding to  $\phi(e_{aq}^-) = 0.26 \pm 0.03$ . As described earlier, reinvestigation of this phenomenon using  $Rh(NH_3)_5I^{2+}$  and  $Rh(NMe_3)_5I^{2+}$  showed the quantum yield of product to be constant in the pH range 2-5. Considering the possibility of competitive scavenging, the following mechanism could be devised



with reactions [20] and [21] being the type of competition as described by Endicott (13). Reaction [23] has been reported by Dainton and Buxton (51b) and introduces an additional competition neglected by Endicott. Since no decrease in the product yields were found in this work with concentrations of  $H^+$  as high as 100 times in excess of the rhodium complex,



the likelihood of any competitive scavenging between reactions [20] and [21] is minimal. It is possible that at very high  $[H^+]$  (greater than  $10^{-2}$  M) reaction [21] may become important. However, in the event of this occurring, competitive scavenging is more likely to be between reactions [22] and [23]. Such a proposal may account for the decrease in yields observed by Endicott (13) at high  $[H^+]$ . In any respect, the  $H^+$  concentrations ( $10^{-5}$  -  $10^{-2}$  M) utilized in this work show the Rh(III) metal centre to be a much more efficient scavenger for electrons.

#### 4. Effect of Temperature on the Photochemistry of Rh(III)-Amines

The substantial difference in quantum yields between otherwise similar complexes (e.g., cis- $[Rh(\text{cyclam})Cl_2]^+$  versus trans- $[Rh(\text{cyclam})Cl_2]^+$ ) could conceivably be due to differences in activation energies between the molecules. Experimentally, one means of obtaining this type of information is to investigate the temperature dependencies of a series of molecules. .

From Table 10, it can be seen that the photosensitivity of each complex was temperature dependent. The difficulty arises in selection of an equation and subsequent plot that is an appropriate representation of the data. As discussed in the first chapter, the temperature dependence of a com-

plex can be attributed to the photochemical rate constant ( $k_p$ ) and/or the nonradiative deactivation rate constant ( $k_n$ ). However, at the present stage of development, it is only realistically feasible to calculate an apparent activation energy that is a composite of a number of possible temperature dependent processes. Various authors have employed equations which encompass rate constants for both chemical reaction and nonradiative quenching. For example, Ford and Petersen (58,59) have studied the photolysis of  $\text{Rh}(\text{NH}_3)_6^{3+}$  as a function of temperature and used equation [7b] with the assumption that  $k_2/A \gg e^{-E_a/RT}$ . A plot of  $\ln \phi$  versus  $1/T$  displayed curvature which was attributed to be the result of the requirement of a temperature sensitive deactivation term besides the  $k_p$  term in the quantum yield expression.

$$\phi = \frac{k_p}{k_p + k_n} \quad [25]$$

Therefore, from the above and the fact that the photoaquation yields were sensitive to perdeuteration, these authors concluded that nonradiative deactivation was predominantly occurring via the weak coupling limit with some competitive strong coupling contributions. The most direct criticism that can be rendered here is that the fitting of experi-

mental data to a linear equation which results in a curve is obvious evidence that the equation employed is inappropriate. Subsequent rationalization for the misfit of data and equation is simply a matter of speculation. It would seem that a minimum prerequisite to interpretation would be a fit between the experimental and theoretical predictions (i.e., a linear plot with a linear equation).

In principle, the derivation of a "correct" equation is predicated to a knowledge of the reaction mechanism. In the absence of knowledge of the "correct" mechanism it is necessary to consider all possible processes which could contribute to the overall temperature dependence. The reactions listed below are intended to summarize these potential processes.



where  $k_n$  denotes the rate constant for nonradiative quenching,  $k_p$  the rate constant for progress along a reaction coordinate but not necessarily leading to reaction (e.g. solvent caged ion-pair),  $k_d$  represents the rate constant

for diffusive escape, and finally,  $k_r$  is the rate constant for recombination of the two fragments (i.e.  $X+Y$ ). Using this simple sequence, it can be easily shown that the appropriate Arrhenius-type equation would be

$$(\phi_{\text{app}})^{-1} = \left(1 + \frac{k_n}{k_p}\right) \left(1 + \frac{k_r}{k_d}\right) \quad [30]$$

For a derivation of this equation, the reader is referred to Appendix II. The mechanism outlined directly above is not intended to be an exclusive one but rather an exemplar of the complexity of an equation that includes a more detailed mechanistic scheme for product formation. It is evident that additional reactions would only exacerbate the situation.

Rather than adopting the ab initio approach, it would seem more fruitful to determine the fit of the data to various empirical equations. For example, plots of  $\log(\phi^{-1} - 1)$  versus  $1/T$  and  $\log(\phi_p/(1 - \phi_p))$  versus  $1/T$  were attempted whereby varying degrees of curvature were found. However, the best linear fit of the data was obtained by plotting  $(\log \phi_1 - \log \phi_2)$  versus  $(1/T_2 - 1/T_1)$  (equation[8]). Thus, from plots such as those illustrated in Figure (17), apparent activation energies can be calculated from the slopes. Table 12 summarizes the calculated values. Emphasis must

Figure 17

Figure 17. "Activation Energy" Plot of the Temperature  
Dependent Quantum Yield for Photoaquation  
of cis-[Rh(cyclam)Br<sub>2</sub>]<sup>+</sup> at 254 nm.

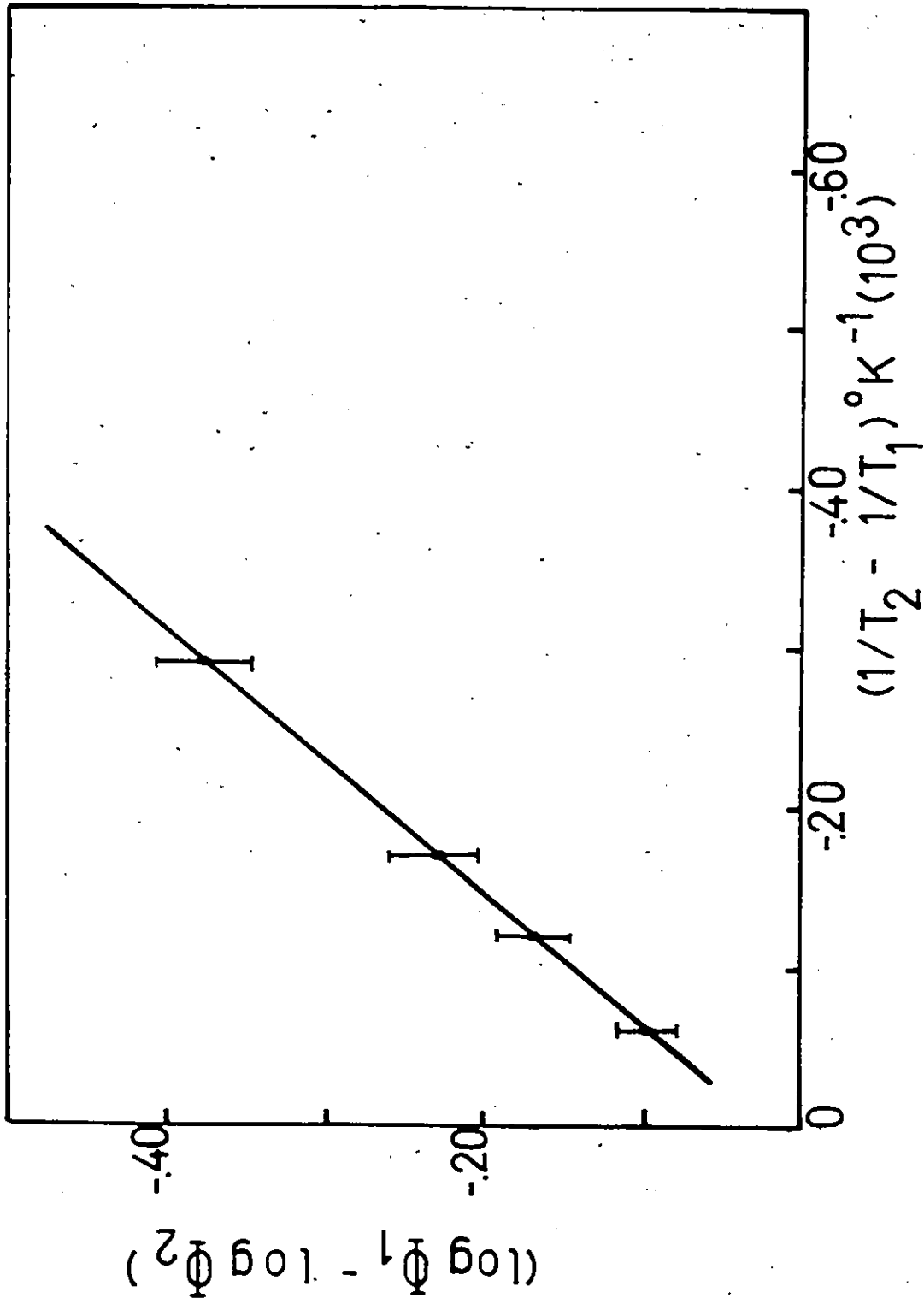


Table 12

Apparent Activation Energies for Some Rh(III)-Amines

| Complex                                                           | $\lambda_{\text{irr}}$ (nm) | $E_{\text{app}}$ | Ref. |
|-------------------------------------------------------------------|-----------------------------|------------------|------|
| <u>cis</u> -[Rh(cyclam)Cl <sub>2</sub> ] <sup>2+</sup>            | 254                         | 21 ± 4 kJ        | a    |
|                                                                   | 400                         | 17 ± 4 kJ        | a    |
| <u>cis</u> -[Rh(cyclam)Br <sub>2</sub> ] <sup>+</sup>             | 254                         | 21 ± 4 kJ        | a    |
| <u>trans</u> -[Rh(cyclam)Cl <sub>2</sub> ] <sup>+</sup>           | 401                         | 25 ± 8 kJ        | b    |
| <u>trans</u> -[Rh(cyclam)Br <sub>2</sub> ] <sup>+</sup>           | 400                         | 21 ± 4 kJ        | a    |
| <u>trans</u> -[Rh(en) <sub>2</sub> Cl <sub>2</sub> ] <sup>+</sup> | 407                         | 21 ± 4 kJ        | b    |

<sup>a</sup>This work.

<sup>b</sup>Reference 40.



be placed on the adjective "apparent" since plots such as that shown in Figure 17 are not based on a precise mechanism but are merely a convenient organizational representation of the data. The advantage of this, at least in an empirical way, is that it provides a method for direct comparison of the relative temperature effects of the different molecules.

In addition to lack of precise knowledge of a reaction mechanism, photochemical reactions such as those studied in this work have the compounded inherent difficulty in terms of temperature effects due to internal heating or "local hot spots" generated by the incident radiation. In the simplest of terms, all nonradiative quenching processes ultimately serve to convert the incident radiative energy into thermal energy. Consequently, from an experimental point of view, this creates a serious problem with respect to knowledge of the internal temperature of the photolytic system. Therefore, a phenomenon such as this, makes the interpretative analysis of any temperature dependence study somewhat suspect.

Despite the theoretical and experimental inadequacies, the similarity in apparent activation energies over such a diverse range of molecules cannot escape attention. The most immediate implication suggested by these results is

that the process or processes which give rise to the origin of the temperature dependence appear to be the same for all of the molecules. These data suggest the possibility that if diffusive escape was the common element, then one would anticipate that the apparent activation energies would closely approximate the pseudo activation energy for the temperature dependence of the self-diffusion coefficient of water. The value for the latter has been reported to be of the order of 20 kJ (40,60) and reference to Table 12 indicates that these values are unmistakably similar. As a result, the participation of diffusion processes in the overall mechanism seems reasonable. On the other hand, Petersen (58,59) and Endicott (14) have described what appears to be a contrasting mechanism. For the sake of exposition, it might be useful to describe two possible extremes. The first case, which represents the ideas put forth by Petersen and Endicott, depicts nonradiative deactivation processes in competition with bond dissociation. In such a scheme it would be presumed that any of the energy dissipation occurring via photochemical reaction would result in 100% product formation. If the nonradiative deactivation is strong coupling, then this process would be temperature dependent. Otherwise, only photochemical reaction is temper-

ature sensitive. The other extreme would involve a neglect of temperature dependent nonradiative deactivation processes and would assume 100% efficient bond dissociation with geminate recombination (quenching) in competition with diffusive escape (product formation). In reality, the most likely situation lies between these two extremes.

Endicott's conclusions from the study of the temperature and perdeuteration effects for the  $\text{Rh}(\text{NH}_3)_5\text{X}^{2+}$  series (14) are somewhat suspect. He found that while the quantum yields of product for  $\text{Rh}(\text{NH}_3)_5\text{Cl}^{2+}$  and  $\text{Rh}(\text{NH}_3)_5\text{I}^{2+}$  were insensitive to temperature, the quantum yield of  $\text{NH}_3$  aquation for  $\text{Rh}(\text{NH}_3)_5\text{Br}^{2+}$  doubled ( $0.18 \rightarrow 0.34$ ) whereas the bromide yield remained constant from photolysis at  $75^\circ\text{C}$ . Upon perdeuteration of the chloro and bromo complexes, only  $\text{Rh}(\text{NH}_3)_5\text{Cl}^{2+}$  showed any sensitivity whereby  $\phi(\text{Cl}^-)$  was enhanced by 33% ( $0.12 \rightarrow 0.16$ ). Therefore, from these results it was concluded that  $\text{Rh}(\text{NH}_3)_5\text{Cl}^{2+}$  may be undergoing some weak coupling (N-H) nonradiative deactivation with strong coupling (Rh-X) being the predominant mode. It was further suggested that greater deviation from octahedral environments of  $\text{Rh}(\text{NH}_3)_6^{3+}$  to  $\text{Rh}(\text{NH}_3)_5\text{Br}^{2+}$  and  $\text{Rh}(\text{NH}_3)_5\text{I}^{2+}$  apparently eliminates weak coupling as a competitive mode of deactivation. In prospect, it would seem that the limited temperature dependence data for  $\text{Rh}(\text{NH}_3)_5\text{Br}^{2+}$  only estab-

lishes that the molecule is temperature sensitive and provides no indication as to those parameters responsible for the dependence. In addition, it is highly probable that  $k_p$  will remain unchanged upon perdeuteration of the leaving group (i.e.  $\text{NH}_3$ ). Hence, in critical terms, the experimental techniques presently employed for isolating the type of nonradiative deactivation coupling mode are subject to uncertainty owing to the multitude of other mechanistic parameters which have an equal probability for temperature sensitivity. Although the possibility of temperature dependent nonradiative deactivation processes cannot be excluded, it is the opinion of this author that the mechanistic pathways for the photochemistry of Rh(III)-amines bear a closer proximity to a diffusion model. Not only can such a model provide an adequate explanation for the observed temperature dependencies observed in this work but it is also capable of rationalizing the experimentally observed effects such as stereomobility in the excited state as discussed in the preceding section and relative leaving group dependencies. As an example, consider the cis- and trans- $[\text{Rh}(\text{cyclam})\text{Cl}_2]^+$  complexes. When bond rupture occurs for the former, the five coordinate metallo fragment possesses a structure which is capable of distorting such that it protects the open orbital vacated by the chloride lea-

ving group. Consequently, the recombinative probability would be reduced and diffusive escape favoured. On the other hand, the geometry of the trans complex is such that the cyclam ligand system is essentially immobile and thus geminate recombination over diffusive escape would be highly favoured.

#### 5. Effect of pH on the Photochemistry of $\text{Rh}(\text{NR}_3)_5\text{X}^{2+}$

From a mechanistic point of view, it is of interest to study the dependence of pH upon a particular system. Although the main purpose for acidifying the solutions of the halopentaamine complexes prior to irradiation is to maintain the complexes in their acido form, the role of  $\text{H}^+$  could possibly be manifested in other areas of the reaction. Thermal studies have shown that even low concentrations of hydroxide ion can result in an acceleration of the release of halide ion and other labile ligands from amine complexes of Co(III) and Rh(III) (61). The acceleration in rates for Rh(III)-amines has been attributed to the formation of an amido group ( $\text{NH}_2^-$ ) which is a  $\pi$ -donating substituent. Such a group would place more negative charge on the metal thereby increasing the ease of dissociation of other groups. A dissociative mechanism is facilitated which should occur much more effectively for a cis substituent than for a trans.

Thus, it seemed reasonable to ascertain whether or not this kinetic phenomenon was operative in the photochemistry of  $\text{Rh}(\text{NH}_3)_5\text{X}^{2+}$ .

As the results demonstrate, photolysis in the pH range 4.0-5.75 of  $\text{Rh}(\text{NH}_3)_5\text{Cl}^{2+}$ , which is a strong Brønsted acid, produced yields of chloride that were greater by a factor of 2 than those observed in a medium of pH 3.0. Consequently, it would appear that some factor of activation and/or stabilization was responsible for the higher yields. To establish the validity of this,  $\text{Rh}(\text{NMe}_3)_5\text{Cl}^{2+}$ , which is a non-Brønsted acid, was photolysed at natural pH (5.0) and from Table 6 it can be seen that the yield of chloride was the same as that found at pH 3.0. The yield of amine at pH 5.0 can only be considered apparent since two competing factors are occurring: (a) the formation of the more acidic aquo product complex and (b) the liberation of base (i.e.  $\text{NMe}_3$ ). Thus, a true pH difference measurement was not possible. In any event, it is significant that the yield of chloride was constant thereby indicating that the phenomenon occurring at higher pH for  $\text{Rh}(\text{NH}_3)_5\text{Cl}^{2+}$  was not present for the methylated complex. There exists the possibility of two forms of activation and/or stabilization on the chloro ligand by the amido group, namely, cis or trans. The identical yields of chloride from the photolyses of

$\text{Rh}(\text{NH}_3)_5\text{Cl}^{2+}$  and trans- $[\text{Rh}(\text{NH}_3)_4\text{Cl}_2]^+$  at pH values higher than 3.0 would suggest it to be cis. It is noteworthy that the mechanistic effect of higher pH from thermal studies of  $\text{Rh}(\text{NH}_3)_5\text{Cl}^{2+}$  has been proposed to form an amido group that activates the ligand trans to it (i.e. Cl) (61). However, under photochemical conditions, the energy is already present from excitation to cause bond dissociation. Thus, it would appear that the amido group is acting as a stabilizer through  $\pi$ -bonding to the vacant metal orbital after dissociation of the Rh-Cl bond. This would in turn reduce the probability of recombination of the metallo fragment and chloride. Since an amido group trans to the chloro cannot  $\pi$ -bond efficiently without rearranging, an amido cis to the chloro is more likely. Such a rationalization reinforces the viability of a diffusion model being operative in Rh(III)-amine photochemistry whereby increased structural stability of the metallo fragment results in more facile diffusive escape of the leaving group.

The results for the  $\text{Rh}(\text{NH}_3)_5\text{I}^{2+}$  indicate that when an amine is the leaving group, hydrogen ion acts as a scavenger to inhibit recombination by protonating its only available coordination site. This is evidenced by the decrease in amine yields at higher pH. Hence, these results are also in agreement with a diffusion model and demonstrate the

importance of a stable leaving group for successful diffusive escape.

It is interesting to note that in each case the yields were independent of pH for values greater than 3.0. Such an observation suggests that  $[\text{OH}^-]$  is not critical and is only necessary to be in sufficient quantity to form the amido group.

#### 6. Solvent Effects on the Photochemistry of Rh(III)-Amines

Reference to Tables 11 and 11A clearly indicate that the net photoreactivity of these complexes does indeed exhibit a solvent sensitivity. The observed phenomena could be the result from any combination of the following: (a) increased cage effects brought about by increasing viscosity, (b) the variation of the composition of the primary solvation sphere, (c) the effectiveness of the components as nucleophiles, (d) the steric constraints on substitution, and (e) the influence of solvent structure including hydrogen bonding.

To commence any discussion of functions of solvents in reactions solvation must be discussed. From coordination chemistry, solvation shells may be classified as (a) the primary coordination sphere (the nearest neighbours of a solute central atom), (b) the second coordination sphere,



and (c) the bulk solvent. In the case of simple mono-atomic ions, the primary solvation shell is the equivalent to a ligand field whereas for transition metal complexes, the ligands coordinated to the metal center can be considered as the primary coordination sphere. Hence, the primary solvation sphere is one of high order imposed by the influence of the solute on nearby solvent molecules whereas the bulk solvent is unaltered by the presence of the solute (62). The secondary coordination sphere is a disordered compromise region which is influenced comparably by the forces exerted by the solute which produce the primary coordination sphere (c.s.) and the solvent-solvent forces which produce the bulk solvent (62). When water is the solvent, it has been found that there is a constant exchange of water molecules among the solvation sheaths (63).

The effect of ions on the viscosity of the solvent is directly related to their effect on the translational motion of the solvent molecules (63). Multicharged or small singly-charged ions (e.g.  $Mg^{2+}$ ,  $Ca^{2+}$ ,  $Li^{+}$ ) increase viscosity (i.e. structure makers) whereas large singly-charged ions (e.g.  $K^{+}$ ,  $Cs^{+}$ ,  $I^{-}$ ) decrease viscosity (structure breakers).

"Cage" is a loose term denoting those solvent molecules

which surround a radical pair that are nearest neighbours and thus any molecule in a liquid is always in a solvent cage (64). The cage has only one important property, that of temporarily preventing the separation by diffusion of a pair of radicals. Solvent water molecules are perhaps the most efficient scavengers of radicals produced in a reaction since in an aqueous medium they are a charter member of the cage.

Addition of large amounts of some other solvent can lead to drastic changes in the structure, dielectric constant and other solvent properties, and introduces uncertainties concerning the relative distribution of the two types of solvent molecules between the second c.s. and the bulk solvent (65). Glycerol was chosen as the second component for the mixed-solvent system used in this work for the following reasons: (a) with as much as 76% weight of glycerol in the system, the bulk dielectric constant of the solvent mixture is 60 as compared to 78 for a pure aqueous system (66) (i.e., bulk dielectric constant not appreciably altered from that of water), (b) the glycerol is capable of hydrogen bonding thereby not disrupting the solvent structure as much as a component unable to hydrogen bond, and (c) it is a poor coordinating agent and thus would not introduce any competitive solvolysis into the system.

It is interesting to observe that for the chloro complexes, with the exceptions of cis- and trans-[Rh(cyclam)-Cl<sub>2</sub>]<sup>+</sup>, the quantum yields of chloride (and amine for Rh(NMe<sub>3</sub>)<sub>5</sub>-Cl<sup>2+</sup>) are independent of solvent composition up to at least 63% weight of glycerol. These results indicate that the initial aqueous solvent cavity apparently remains unaltered up to 63% weight glycerol. From solvation studies of ions in mixed-aqueous solutions it has been found that compositions of about 20-30% and 75-90% weight of an organic component in an aqueous medium are critical regions with respect to the overall structure of the solvent system (63). For compositions of 20-30% it has been proposed that this is the range whereby the outermost water solvent layer of the ion is being replaced by the organic component whereas 75-90% weight of organic component begins to replace the innermost layers. Consequently, it is conceivable that at higher concentrations of glycerol solvent effects would be observed. Unfortunately, this was not possible to determine experimentally because of the insolubility of the complexes in high glycerol concentrations.

The decrease in  $\phi(\text{Cl}^-)$  for cis-[Rh(cyclam)Cl<sub>2</sub>]<sup>+</sup> at concentrations as low as 47% weight of glycerol suggests that this molecule, due to the alkyl groups in the cyclam system, is a poorer structure maker than the pentaamine or

bisethylenediamine complexes. Hence, one would anticipate that smaller concentrations of glycerol would more effectively penetrate the innermost solvation layers of the cationic complex thereby inhibiting solvation and diffusion of the two fragments. The proposal of a structure breaking influence by the cyclam on the aqueous solvent system can be viewed in the light of the ligand system having essentially four coordinating nitrogens with four spectator hydrocarbon bridges. This hydrocarbon content can be thought of as tantamount to the relatively high concentrations of organic solvent referred to previously (64).

Perhaps the results found for trans-[Rh(cyclam)Cl<sub>2</sub>]<sup>+</sup> more closely approximate a solvent cage effect but in a different sense as is generally predicted. The increase in the yield of chloride in the mixed-solvent system implies that photoreaction is more facile in a less structured solvent system and thus in a pure aqueous medium the molecule is in a more confining solvent cage which favours recombination over diffusive separation.

The solvent effects on the photochemistries of Rh(NH<sub>3</sub>)<sub>5</sub><sup>+</sup> and trans-[Ir(en)<sub>2</sub>I<sub>2</sub>]<sup>+</sup> are particularly interesting because the effects differ from LF excitation to CT excitation. Apart from all other considerations, this distinction between the two is indicative of a lack of internal

conversion between the two manifolds of states or otherwise the solvent effects would be identical in both cases. The drastic decrease in  $\phi(I^-)$  observed from both CT and LF illuminations of trans- $[\text{Ir}(\text{en})_2\text{I}_2]^+$  is strongly indicative of a poorly structured immediate solvent environment of the complex which would be highly amenable to recombinative processes due to the inability of the solvent to effectively solvolyse either fragment. Such a phenomenon must not be characteristic of iridium(III) complexes in general, since the same behavior should be observed for the analogous dichloro complex. Thus, the presence of the iodo ligands must be a critical factor. In an aqueous medium, the conditions of solvation for the diiodo complex must be such that diffusive escape is highly favoured as evidenced by the high quantum yield of iodide at 254 nm irradiation ( $0.65 \pm 0.02$ ). The gradual decrease in amine yields from LF irradiation of  $\text{Rh}(\text{NH}_3)_5\text{I}^{2+}$  and CT excitation of  $\text{Rh}(\text{NMe}_3)_5\text{I}^{2+}$  are suggestive of these complexes being less structure making than the corresponding chloro complexes in the excited state and consequently, concentrations of glycerol as low as 25% weight produce profound effects on the solvent structure.

The lack of solvent dependence on the amine yield from CT excitation of  $\text{Rh}(\text{NH}_3)_5\text{I}^{2+}$  is also observed for the

corresponding bromo complex. As with the iodo complex, LF irradiation of  $\text{Rh}(\text{NH}_3)_5\text{Br}^{2+}$  in the glycerol-water mixture causes a decrease in the yield of amine aquation. Thus, for these two molecules it would appear that solute-solvent interactions are different for LF and CT excited states whereby for the latter type of excited state, the glycerol at even 63% weight has not effectively penetrated the inner coordination spheres. The increases in  $\text{Br}^-$  yields for  $\text{Rh}(\text{NH}_3)_5\text{Br}^{2+}$  indicate that the structure making tendency of this complex is poorer for the mixed-solvent system and hence promotes diffusive escape of bromide. The apparent lack of a temperature dependence for  $\phi(\text{Br}^-)$  reported by Endicott (14) seems inconsistent with the solvent effects and thus should be the subject of further investigation.

EPILOGUE

Perhaps the molecules studied in this work that best demonstrate the present stage of development of the photochemistry of Rh(III)-amines is the  $\text{Rh}(\text{NMe}_3)_5\text{X}^{2+}$  series. For example, from previous models, chloride is predicted and found to be the principal ligand aquated from photolysis of  $\text{Rh}(\text{NMe}_3)_5\text{Cl}^{2+}$ . However, the unanticipated  $\text{NMe}_3$  liberation could only be retrospectively rationalized. From the wavelength dependence trend observed for ammine aquation from  $\text{Rh}(\text{NH}_3)_5\text{I}^{2+}$  one would have justifiably predicted that the same trend would be exhibited by the corresponding methylated complex. Not finding this to be the case further indicates the limited predictive powers of existing models. These complexes were synthesized in the latter stages of this work and had their photochemistries not been a subject of study, one might have been led to believe that the photochemistry of Rh(III)-amines had emerged from an infancy of the unknown to a maturity of high predictability. As disappointing as this might appear, there is a very positive side and that is the exciting challenge that complexes of this sort present to the inorganic photochemist. Several variations of these molecules await to be synthesized and studied to obtain yet a clearer understanding of the intri-

cacies involved. As the number of such studies increases, more detailed trends will be established which will no doubt prompt the retirement of several existing theories and models and initiate the formulation of new models that are based on a more extensive range of experimental evidence.

Perhaps these thoughts can be best likened to the New Year whereby we "ring out the old and bring in the new" with no regrets of the past and only expectations of the future as we begin a new era with previous experience.



APPENDIX I

Table of Approximate Acid Dissociation Constants<sup>a</sup>

| Complex                                                           | $K_a^b$                 |
|-------------------------------------------------------------------|-------------------------|
| <u>trans</u> -[Rh(en) <sub>2</sub> Cl <sub>2</sub> ] <sup>+</sup> | 4.6 x 10 <sup>-5</sup>  |
| <u>trans</u> -[Rh(en) <sub>2</sub> Br <sub>2</sub> ] <sup>+</sup> | 2.8 x 10 <sup>-5</sup>  |
| <u>trans</u> -[Rh(en) <sub>2</sub> I <sub>2</sub> ] <sup>+</sup>  | 3.2 x 10 <sup>-6</sup>  |
| <u>trans</u> -[Rh(cyclam)I <sub>2</sub> ] <sup>+</sup>            | 3.6 x 10 <sup>-10</sup> |
| <u>cis</u> -[Rh(en) <sub>2</sub> Cl <sub>2</sub> ] <sup>+</sup>   | 4.9 x 10 <sup>-5</sup>  |
| <u>cis</u> -[Rh(cyclam)I <sub>2</sub> ] <sup>+</sup>              | 4.3 x 10 <sup>-10</sup> |
| <u>trans</u> -[Rh(en) <sub>2</sub> ClBr] <sup>+</sup>             | 3.6 x 10 <sup>-11</sup> |
| <u>trans</u> -[Rh(en) <sub>2</sub> BrI] <sup>+</sup>              | 3.4 x 10 <sup>-9</sup>  |
| <u>trans</u> -[Rh(en) <sub>2</sub> ClI] <sup>+</sup>              | 1.6 x 10 <sup>-9</sup>  |
| <u>trans</u> -[Rh(cyclam)ClBr] <sup>+</sup>                       | 1.5 x 10 <sup>-11</sup> |
| <u>trans</u> -[Rh(cyclam)BrI] <sup>+</sup>                        | 1.9 x 10 <sup>-10</sup> |
| <u>trans</u> -[Rh(cyclam)ClI] <sup>+</sup>                        | 9.1 x 10 <sup>-10</sup> |

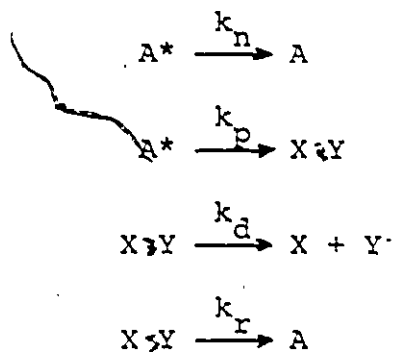
<sup>a</sup> Calculated from the equation:  $K_a = \frac{[\text{Conjugate base}] \cdot [\text{H}^+]}{[\text{Complex}]}$

where for simplicity it is assumed that [conjugate base] = [H<sup>+</sup>] = -antilog[pH] and [complex] =  $\frac{[\text{complex}]_{\text{initial}}}{1 - [\text{conjugate base}]}$ .

<sup>b</sup> Reference 40.

APPENDIX II

Derivation of Arrhenius-Type Equation [30]



$$\phi_{X \rightleftharpoons Y} = \phi_{A^*} \frac{k_n [A^*]}{k_p [A^*] + k_n [A^*]}$$

$$\phi(p) = \phi_{X \rightleftharpoons Y} \frac{k_d [X \rightleftharpoons Y]}{k_d [X \rightleftharpoons Y] + k_r [X \rightleftharpoons Y]}$$

$$\phi(p) = \phi_{A^*} \frac{k_n}{k_p + k_n} \times \frac{k_d}{k_d + k_r}$$

Assuming  $\phi_{A^*} = 1$ ,

$$(\phi(p))^{-1} = \left(1 + \frac{k_n}{k_p}\right) \left(1 + \frac{k_r}{k_d}\right)$$

Note:  $(\phi(p))^{-1}$  is  $(\phi_{app})^{-1}$  as shown in equation [30].

## REFERENCES

- (1) (a) L. S. Forster and G. P. Porter, "Concepts of Inorganic Photochemistry", A. W. Adamson and P. D. Fleischauer, Eds., Wiley-Interscience, New York, 1975, Chapters 1-2; (b) P. C. Ford, R. E. Hintze, and J. D. Petersen, ibid., pages 215-216.
- (2) W. L. Waltz and R. G. Sutherland, Chem. Soc. Rev., 1, 241 (1972).
- (3) V. Balzani and V. Carassiti, "Photochemistry of Coordination Compounds", Academic Press, Inc., London, 1970, Chapters 2-3.
- (4) J. H. van Vleck, J. Phys. Chem., 41, 67 (1937).
- (5) B. N. Figgis, "Introduction to Ligand Fields", Wiley-Interscience, New York, 1966, Chapter 9.
- (6) T. M. Dunn, "Modern Coordination Chemistry", J. Lewis and R. G. Wilkins, Eds., Interscience Publishers, Inc., New York, 1960, Chapter 4.
- (7) R. Englman and J. Jortner, Mol. Phys., 18, 145 (1970).
- (8) W. M. Gelbart, K. F. Freed, and S. A. Rice, J. Chem. Phys., 52, 2460 (1970).
- (9) G. W. Robinson and R. P. Frosch, J. Chem. Phys., 37, 1962 (1962); 38, 1187 (1963).
- (10) A. W. Adamson, J. Phys. Chem., 71, 798 (1967).

- (11) M. F. Manfrin, L. Moggi, and V. Balzani, Inorg. Chem., 10, 207 (1971).
- (12) L. Moggi, Gazz. Chim. Ital., 97, 1089 (1967).
- (13) T. L. Kelly and J. F. Endicott, J. Amer. Chem. Soc., 94, 1797 (1972).
- (14) T. L. Kelly and J. F. Endicott, J. Phys. Chem., 76, 1937 (1972).
- (15) T. L. Kelly and J. F. Endicott, Chem. Comm., 1061 (1971).
- (16) T. L. Kelly and J. F. Endicott, J. Amer. Chem. Soc., 94, 278 (1972).
- (17) T. L. Kelly and J. F. Endicott, J. Amer. Chem. Soc., 92, 5733 (1970).
- (18) T. R. Thomas and G. A. Crosby, J. Mol. Spectrosc., 38, 118 (1971).
- (19) T. R. Thomas, R. J. Watts, and G. A. Crosby, J. Chem. Phys., 59, 2123 (1973).
- (20) J. N. Demas and G. A. Crosby, J. Amer. Chem. Soc., 94, 7262 (1970).
- (21) P. C. Ford, J. D. Petersen, and R. E. Hintze, Coord. Chem. Rev., 14, 67 (1974).
- (22) P. C. Ford, J. D. Petersen, and R. J. Watts, J. Amer. Chem. Soc., 98, 3188 (1976).
- (23) J. A. Osborn, R. D. Gillard, and G. Wilkinson, J. Chem. Soc., 3168 (1964).

- (24) R. D. Foust and P. C. Ford, Inorg. Chem., 11, 899 (1972).
- (25) P. C. Ford and J. D. Petersen, Inorg. Chem., 14, 1404 (1975).
- (26) C. Kutal and A. W. Adamson, Inorg. Chem., 12, 1454 (1973).
- (27) M. M. Muir and W. L. Huang, Inorg. Chem., 12, 1831 (1973).
- (28) J. Sellan and R. Rumfeldt, Can. J. Chem., 54, 519 (1976).
- (29) J. Sellan and R. Rumfeldt, Can. J. Chem., 54, 1061 (1976).
- (30) R. A. Bauer and F. Basolo, Inorg. Chem., 8, 2231 (1967).
- (31) R. A. Bauer and F. Basolo, J. Amer. Chem. Soc., 90, 2437 (1968).
- (32) M. M. Muir and W. L. Huang, Inorg. Chem., 12, 1930 (1973).
- (33) (a) J. I. Zink, J. Amer. Chem. Soc., 94, 8039 (1972);  
(b) Mol. Photochem., 5, 151 (1973).
- (34) (a) J. I. Zink, Inorg. Chem., 12, 1018 (1973); (b) J. I. Zink, Inorg. Chem., 12, 1957 (1973).
- (35) (a) J. I. Zink, J. Amer. Chem. Soc., 96, 464 (1974);  
(b) M. J. Incorvia and J. I. Zink, Inorg. Chem., 13, 2489 (1974).
- (36) P. C. Ford, Inorg. Chem., 14, 1441 (1975).

- (37) P. Scheridan and A. W. Adamson, Inorg. Chem., 13, 2482 (1974).
- (38) S. R. Koprach and E. J. Bounsall, Can. J. Chem., 48, 1481 (1970).
- (39) S. R. Koprach, Ph.D. Dissertation, Univ. of Windsor, 1970.
- (40) J. Sellan, Ph.D. Dissertation, Univ. of Windsor, 1974.
- (41) S. A. Johnson and F. Basolo, Inorg. Chem., 1, 925 (1962).
- (42) H. L. Bott and A. J. Poe, J. Chem. Soc., 5931 (1965)
- (43) E. J. Bounsall and A. J. Poe, J. Chem. Soc. (A), 286 (1966).
- (44) R. A. Bauer and F. Basolo, Inorg. Chem., 8, 2233 (1969).
- (45) Reference 41.
- (46) G. U. Bushnell, G. L. Lalor, and E. A. Moelwyn-Hughes, J. Chem. Soc. (A), 717 (1966).
- (47) C. Hatchard and C. Parker, Proc. Roy. Soc. A235, 518 (1956).
- (48) E. E. Wegner and A. W. Adamson, J. Chem. Soc., 88, 394 (1966).
- (49) B. L. Ingram, Analytical Chem., 42, 1825 (1971).
- (50) C. K. Jørgensen, Chim. Acta Scand., 10, 500 (1956).
- (51) (a) F. S. Dainton and S. R. Logan, Proc. Roy. Soc., A287, 281 (1965); (b) F. S. Dainton and G. V. Buxton, ibid., 427 (1965).
- (52) J. G. Calvert and J. N. Pitts, Jr., "Photochemistry",

- J. Wiley and Sons, Inc., New York, 1966, page 184.
- (53) A. D. Kirk and C. F. C. Wong, Can. J. Chem., 54, 3794 (1976).
- (54) M. C. R. Symons and M. Smith, Trans. Faraday Soc., 54, 338, 346 (1958).
- (55) J. Reed, H. D. Gafney and F. Basolo, J. Amer. Chem. Soc., 96, 1363 (1974).
- (56) J. Lilie, M. G. Simic, and J. F. Endicott, Inorg. Chem., 14, 2129 (1975).
- (57) (a) M. D. Liteplo and J. F. Endicott, Inorg. Chem., 10, 1420 (1971); (b) T. S. Roche and J. F. Endicott, J. Amer. Chem. Soc., 94, 866 (1972); (c) T. S. Roche and J. F. Endicott, Inorg. Chem., 13, 1575 (1974); (d) S. D. Malone and J. F. Endicott, J. Phys. Chem., 76, 2223 (1972).
- (58) J. D. Petersen, Ph.D. Dissertation, Univ. of California, 1975.
- (59) J. D. Petersen and P. C. Ford, J. Phys. Chem., 78, 1144 (1974).
- (60) S. R. Logan, J. Phys. Chem., 73, 277 (1969).
- (61) F. Basolo and R. G. Pearson, "Mechanisms of Inorganic Reactions", J. Wiley and Sons, Inc., New York, 1958, Chapter 3.
- (62) C. H. Langford and J. P. K. Tong, Acc. Chem. Res., 10,

258 (1977).

- (63) E. S. Amis and J. F. Hinton, "Solvent Effects on Chemical Phenomena", Academic Press, New York, 1973, Chapters 2-3.
- (64) J. P. Lorand, Prog. Inorg. Chem., 17, 207 (1972).
- (65) T. W. Swaddle, Coord. Chem. Rev., 14, 217 (1974).
- (66) F. Scandola, M. A. Scandola, and C. Bartocci, J. Amer. Chem. Soc., 97, 4757 (1975).



VITA AUCTORIS

Born: May 21, 1953, Saint John, New Brunswick

University Education:

1971-1974: Acadia University, Wolfville, Nova  
Scotia

1974: Received BSc.

Awards and Scholarships:

1973: Gerald T. Eaton Scholarship in Engineering

1974: University Bronze Medal in Chemistry

1974: Chemical Institute of Canada Merit Award

1975-1978: National Research Council of Canada  
Postgraduate Scholarship

1977: Ontario Graduate Scholarship (Declined)

1978: National Research Council of Canada Post-  
doctoral Fellowship (Declined)

Publications: The Reactions of Atomic Oxygen with Methanol  
and Ethanol, Can. J. Chem., 54, 984 (1976).

Professional Society: Chemical Institute of Canada

Marital Status: Husband, Brian Clarence Trudell